PB 198 816

RESEARCH GRANTS

AEROSOL MEASUREMENTS IN LOS ANGELES SMOG

VOLUME I

Reproduced by
NATIONAL TECHNICAL
INFORMATION SERVICE
Springfield, Va. 22151

U. S. ENVIRONMENTAL PROTECTION AGENCY

153

PB 198 816

BIBLIOGRAPHIC DATA SHEET

1. Report No. APTD-0630

2.

3. Recipient's Accession No.

4. Title and Subtitle
Aerosol Measurements in Los Angeles Smog Volume I

5. Report Date
February 1971

6.

7. Author(s)
K. T. Whitby (Principal Investigator)

8. Performing Organization Rept. No.

9. Performing Organization Name and Address
Particle Technology Laboratory
Mechanical Engineering Department
University of Minnesota
Minneapolis, Minnesota

10. Project/Task/Work Unit No.

11. Contract/Grant No.

12. Sponsoring Organization Name and Address
U. S. Environmental Protection Agency
Air Pollution Control Office
Research Triangle Park, North Carolina 27709

13. Type of Report & Period Covered

14.

15. Supplementary Notes
[illegible]

16. Abstracts

A collaborative research study on the physical and chemical properties of Los Angeles smog aerosol by a group of investigators. One of the prime goals of this study was to carry out a comprehensive, collaborative, effort, using a sufficient variety of chemical and aerosol measurement techniques on the same aerosol at the same place at the same time, so that a significant improvement in the correlations between various measurements could be made. The experiments were divided into the following main categories: 1. Measurement of the number versus size spectra measurements using the automated Minnesota Aerosol Analyzing System. 2. Sampling of the aerosol by lundgren impactor for mass and chemical composition versus size distribution 3. Continuous gas analyzers, 4. Turbidimetric measurements, 5. Miscellaneous experiments including: cloud condensation and ice nuclei, samples for electron microscope and single particle chemicalanalysis, humidity effects, smog making in a bag, smog coagulation in a bag and particle beam experiments.

17. Key Words and Document Analysis. 17a. Descriptors

Aersols
Smog
Chemical analysis
Measurement
Particle size
Particle size distribution
Turbidity
Nephelometers
Condensation Nuclei
Gas sampling

17b. Identifiers/Open-Ended Terms

Air pollution (Measurement) Los Angeles

17c. COSATI Field/Group 7/D, 13/B

18. Availability Statement
Unlimited

19. Security Class (This Report)
UNCLASSIFIED

20. Security Class (This Page)
UNCLASSIFIED

21. No. of Pages
151 153

22. Price
3.00 .95

C

AEROSOL MEASUREMENTS
IN LOS ANGELES SMOG

VOLUME I

Particle Technology Laboratory
Mechanical Engineering Department
University of Minnesota

Details of illustrations in
this document may be better
studied on microfiche

U.S. ENVIRONMENTAL PROTECTION AGENCY
Air Pollution Control Office
Research Triangle Park, North Carolina
February 1971

The APTD (Air Pollution Technical Data) series of reports is issued by the Air Pollution Control Office to report technical data of interest to a limited readership. Copies of APTD reports are available free of charge to APCO staff members, current contractors and grantees, and nonprofit organizations - as supplies permit - from the Office of Technical Information and Publications, Air Pollution Control Office, U. S. Environmental Protection Agency, Research Triangle Park, North Carolina 27709.

This report was furnished to the Air Pollution Control Office of the U. S. Environmental Protection Agency by the Particle Technology Laboratory, Mechanical Engineering Department, University of Minnesota in fulfillment of NAPCA Research Grant No. AP-00839-01. The contents of the report are reproduced herein as-received from the contractor. The opinions, findings, and conclusions expressed are those of the authors and not necessarily those of the Air Pollution Control Office of the U. S. Environmental Protection Agency.

Air Pollution Control Office Publication No. APTD-0630

Particle Laboratory Publication No. 141

Description of the Experiment

AEROSOL MEASUREMENTS IN LOS ANGELES SMOG
APCO Research Grant No. AP-00839-01

I. Introduction - K.T. Whitby and B.Y.H. Liu

II. Background Information on the Site and Meteorological Experiments - G.M. Hidy and S.K. Friedlander, with contributions from W. Green

III. University of Minnesota Size Spectra and Miscellaneous Experiments - R. Husar, N. Barsic, M. Tomaides, B.Y.H. Liu and K.T. Whitby

IV. Determination of Particulate Composition, Mass Concentration and Size Distribution Using the Lundgren Impactor - D.A. Lundgren

V. University of Washington Aerosol Turbidity Experiments Using Integrating Nephelometers - R.J. Charlson and N.C. Ahlquist

VI. Measurement of O_3, NO, NO_2, SO_2 and PAN Using Continuous Gas Analyzers - P. Mueller, K. Smith and Y. Tokiwa

Report submitted by K.T. Whitby - Principal Investigator

University of Minnesota
Department of Mechanical Engineering
Particle Technology Laboratory
Minneapolis, Minnesota 55455

November, 1970

FOREWORD

This is the first detailed report describing the experiments conducted during a collaborative study of smog aerosols in Los Angeles during the summer of 1969. What was originally conceived as a relatively small experiment to measure aerosol size distributions using the MAAS and to make some chemical analysis of collected particulates, grew by the addition of investigators and experimentors to a relatively large project that taxed the resources of several of the groups involved. However, the outstanding cooperation from everyone, all done on an informal basis, made the project a success.

Since this project may well serve as a prototype for further collaborative research on aerosols, it is worthwhile to make a few candid observations about why most of the work went well, and only a few things did not.

First, the informal collaborative arrangements used probably succeeded because all of the key investigators knew each other well and were willing to commit themselves and their resources without a lot of time consuming red tape. A less well acquainted group would probably need more time and perhaps more organizational formalities to make things go smoothly.

Secondly, this project proved that first string equipment and personnel is essential if good data is to be obtained and the work is to get done close to schedule. It also proved the wisdom of thoroughly exercising the equipment in the home laboratory, using the same people who will operate it during the collaborative study. With only a couple of minor exceptions, no new and untried instruments or procedures yielded much useful data.

Thirdly, several weeks of preparation time is desirable before the main collaborative experiments are to be run. In addition to the inevitable instrument recalibrations required for sophisticated instrumentation after shipment, there are always unexpected "bugs" which occur. For example, a crash program to construct an inlet bug screen had to be instituted when Lundgren found that small gnats were ruining his impactor runs.

And then there was the night a whole days worth of data tapes were lost when a janitor inadvertently emptied a wastebasket that had been pressed into service as a punched tape receptacle when all the boxes provided for this purpose had been used up.

Although the detailed data analysis has just begun, it is now safe to conclude that the project has been successful in obtaining some very valuable coordinated data. We expect that it will be several years before we have exhausted the possible applications of the data.

This project, which Friedlander has called the "Great Smog Caper", has been most enjoyable. I am most indebted and grateful to the many participants for their contributions to what has been a great experience.

Ken Whitby

I - INTRODUCTION

by
K.T. Whitby and B.Y.H. Liu

History of the Project

This collaborative research study on the physical and chemical properties of Los Angeles smog aerosol by the group of investigators listed in Table I-1 developed out of discussions between Friedlander, Mueller, and Whitby several years ago. These investigators came to the conclusion that further insights into the mechanisms of formation and the behavior of smog and of smog aerosols could probably best be developed by a collaborative study carried out by a group of investigators, each well equipped with apparatus and competent in his own area. Until now, most of our understanding of behavior of polluted urban atmospheres has been derived from separate studies by different investigators studying the aerosol in different places at different times, and often using different techniques. While this disjointed approach has yielded information about the general behavior of polluted atmospheres, it has not been too successful in revealing the more complex relationships between the aerosol and the gas phase reactions. Thus one of the prime goals of this study was to carry out a comprehensive, collaborative effort, using a sufficient variety of chemical and aerosol measurement techniques on the same aerosol at the same place at the same time, so that a significant improvement in the correlations between various measurements could be made.

Los Angeles was chosen for this study for several reasons. First, Friedlander and Hidy at the California Institute of Technology and Peter Mueller, Head of the California Air and Industrial Hygiene Laboratory, at Berkeley, California, were located in the state of California and could utilize their resources for a study located there. A second factor was that Los Angeles smog is an unusual and severe pollution problem. The California Institute of Technology in Pasadena was chosen as the site because of the availability of excellent laboratory in the Keck Environmental Sciences Building and the excellent support that could be provided by Dr. Friedlander's group. Although Pasadena does not represent the center of the smog area, it is subjected to incursions of heavy smog, and therefore a variety of smog conditions can be encountered in a reasonably short time in the summer.

Dale Lundgren was asked to participate because of his experience in using his impactor for mass distribution measurements and classification by size for chemical analysis. The simultaneous measurements of the number distributions using the Minnesota Aerosol Analyzing System (MAAS) and of the mass distribution using Lundgren's impactor provided a unique opportunity to compare these two techniques.

The participation of Charlson and Ahlquist from the University of Washington made it possible to further investigate the relationship between light scattering and aerosol mass and also for the first time made it possible to compare the theoretical scattering calculated from the size distributions with the measured values.

In addition to the principal investigators, the many other participants in the project are listed in Table I-2 along with the experiments in which they participated.

Although the project was originally conceived by Whitby, Friedlander, and Mueller, Liu actually provided most of the supervision in Los Angeles during the project, and Charlson, Hidy, and Lundgren made important contributions by providing their expertise in their respective areas. Furthermore, the project could never have succeeded without the contributions of many graduate students and technicians who worked on the project. Outstanding among these are the work of Mr. R. Husar, Mr. N. Barsic, and Mrs. R. Husar, from the University of Minnesota, and Y. Tokiwa and K. Smith from the California Department of Public Health.

Objectives

Perhaps the most important objective of this study was to provide space, time and technique coordinated data which could provide new insights into the mechanisms of formation and the behavior of smog. These data can be expected to provide new correlations between various instruments for the continuous measurement of smog.

In addition to the above general objectives, the various investigators have stated their interest in using the data to study the applications listed in Table I-3.

Experiment Schedule

The major portion of the instrumentation was shipped to Pasadena at the end of July, 1969. The first two weeks of August were used for setup and checkout. Actual data collection with the complete system began on August 19 and ended on September 8 with a power supply failure in one of the major instruments. Because 363 complete size spectra had been measured by then under a variety of smog conditions, the primary size spectra experiments were discontinued and secondary experiments such as smog making and classification were performed until September 19, at which time the project was ended and most of the equipment returned. A few of the gas analyzers were operated into October.

The dates and time of the major experiments are shown in Figure I-1.

Summary Description of the Project

Although the following sections of this report give detailed descriptions of the various experiments, the brief description given below is provided to give an overview of the project.

The experiments may be divided into five main categories as follows:

1. Measurement of the number versus size spectra measurements over the size range from 0.003 to 6 µm using the automated Minnesota Aerosol Analyzing System.
2. Sampling of the aerosol by Lundgren impactor for mass and chemical composition versus size distribution.
3. Continuous gas analyzers
4. Turbidimetric measurements
5. Miscellaneous experiments including:
   a) cloud condensation nuclei and ice nuclei
   b) samples for electron microscope and single particle chemical analysis
   c) humidity effects
   d) smog making in a bag
   e) smog coagulation in a bag
   f) particle beam experiments

The experiments, the techniques used and the investigators involved are given in Table I-2.

Sampling Site

Except for the meteorological instruments and the smog making experiments, which were operated on the building roof, all of the apparatus was located in a large air conditioned laboratory in the basement of the Keck Environmental Sciences Building at the California Institute of Technology in Pasadena, California.

Sampling System

The basement location of the laboratory necessitated that the aerosol be transported from the sampling line inlet 6.7 m above the roof down through a vertical, 20.5 m long by 7 cm internal diameter PVC pipe to the aerosol distribution piping in the basement. Important details of the piping system are shown in Figure I-2.

Flow velocities and tubing sizes for each instrument were chosen so that the losses of the aerosol or gas being measured were small. Actual losses of ozone and condensation nuclei, the two components for which it was suspected there would be the greatest losses, were actually measured and found to be on the order of 10%.

The impactors and total mass samplers were located at the bottom of the vertical line to minimize losses of large particles. The high smog aerosol concentrations necessitated diluting the aerosol by a factor of 12 for the condensation nuclei counter and by a factor of 100 for the optical counter. All other instruments measured undiluted aerosol.

Minnesota Aerosol Analyzing System (MAAS)

The MAAS consists of five parts: 1. The aerosol distribution and dilution system described above and shown in Figure 1, 2. An optical particle counter, 3. A condensation nuclei counter, 4. The Whitby Aerosol Analyzer (WAA), and 5. A data acquisition system (DAS) which controls the whole system and records the data. A schematic of the system with the DAS channel assignments is shown in Figure I-3. This system is capable of completely automatic "in situ" measurement of the aerosol number spectra from 0.003 to 6 µm diameter with very good accuracy. A detailed discussion of the accuracy and the calibration procedures used is given in section III.

The optical particle counter (OPC) consists of a Royco model 220 sensor with a modified, passive sheath air inlet system and a Royco model 170-1 pulse converter. As operated in Los Angeles, the OPC has a sampling air flow of 470 cm^3/min, a sizing range of 0.4 to 6 µm linearly spread over 57 channels, a resolution of better than 10% and a maximum allowable aerosol inlet concentration of about 50/cm^3.

From Figure I-3, it will be noted that the OPC is connected so that upon command from the DAS, it will make a measurement cycle, record the data and then wait for the next command. This permits time correlation of its data with the other instruments being read and controlled by the DAS. Since all data from the DAS and from the OPC is available on punched tape, computer processing of the data is easy. The minimum time for a measurement cycle is 4 minutes.

The condensation nuclei counter (CNC) is a standard automatic General Electric counter operated at an under-pressure expansion of 8 inches of Hg. vacuum. It was equipped with a fixed ratio 12 to 1 capillary diluter to keep the indication within the linear range of the counter. The counter output was recorded both with the DAS and a strip chart recorder.

The Whitby Aerosol Analyzer (WAA) is an automated commercial version, manufactured by Thermo Systems, Inc., of St. Paul, Minnesota, of the instrument described by Whitby and Clark (1966). This instrument has feedback controlled high voltage power supplies which permit automatic operation in conjunction with a Dymec DAS.

Some characteristics of the WAA used in Los Angeles are as follows: minimum scan time = 4 min., sizing range 0.0075 - 0.6 µm, aerosol flow rate = 11.5 l/min., charger volume = 1.7 l, and mobility resolution = 15%.

Sampling for Mass and Chemical Distribution

During all of the major intensive sampling periods the aerosol was sampled by Lundgren impactors and the filter sampler to obtain the aerosol mass distribution and to obtain size classified samples for chemical analysis for the elements and ions shown in Table I-2, line 3.

The aerosol was sampled for mass and chemical size distribution with two Lundgren impactors (Lundgren, 1969). Most of the samples were of 12 hour duration, with some of 4 hours, at a sampling rate between 60 and 85 l/min. At 70 l/min. the cut sizes are 18, 5.6, 1.9, and 0.6 µm. Samples were collected on a 1 mil Teflon film for weighing and subsequent chemical analysis.

Total mass samples were collected simultaneously, at the same flow rate as the impactor, onto 90 mm diameter Teflon filters.

These experiments are described in detail in Section IV.

After the conclusion of the main experiments, the WAA was also operated in the classification mode to classify the aerosol in the 0.01 - 0.5 µm range into 4 fractions for mass and chemical analysis. Because this was the first attempt at using the WAA for mass distribution analysis using a Teflon coated collector electrode, only a few good data have been obtained. The usefulness of these samples for chemical analysis must await processing of the samples.

Continuous Gas Analysis

An Atlas Electric Devices NO, NO_2, SO_2, O_3, a Beckman O_3, and a Mast O_3 continuous recording gas analyzer provided by the California AIHL, Berkeley, were operated for the entire project period. In addition, an experimental Chemiluminescence O_3 analyzer provided by J. Hodgeson, R.K. Stevens and Andy O'Keeffe of the Division of Chemical and Physical Research and Development of NAPCA, Durham, North Carolina, and an experimental peroxyacetyl nitrate (PAN) analyzer provided by the Statewide Air Pollution Center, Riverside, California, were operated part of the time.

Data from these analyzers was recorded both on strip charts and on punched tape by the DAS, to permit obtaining both instantaneous readings and hourly averages.

These experiments are described in detail in Section VI.

Atmospheric Turbidity Measurements

1. Description

The University of Washington experiment, conducted byProfessor Robert J. Charlson and Mr. Norman C. Ahlquist, consisted mainly of light scattering measurements made with three integrating nephelometers. (Ahlquist and Charlson, 1968-1969.) Dew point and instrument temperature were also recorded. The instruments were:

1) A four channel instrument operating in four very narrow wavelength bands located at 360, 436, 546, and 675 nm.

2) A broad-band device covering the wavelength range from 420 to 550 nm.

3) A device with a medium wavelength band located at 550 nm approximating the response of the human eye.

2. Purpose

The initial purpose of this portion of the experiment was to gather data on the light scattering properties of real Los Angeles smog. These data necessarily must be compared and correlated with the measurements by the other groups in order to put the results into proper perspective. The goals of the experiments fall into three classes:

1) experiments with three nephelometers and one hygrometer alone:
   a) correlation of broad-band and narrow-band light scattering coefficient with wavelength dependence as a parameter. Los Angeles provides a sufficiently variable aerosol for such a study.
   b) relation of light scattering coefficient to humidity
   c) relation of light scattering to visibility, utilizing weather bureau data for visibility
2) experiments relating nephelometer and hygrometer to that from other experimenters
   a) relationship of wavelength dependence of light scattering (angstrom exponent, α) to size distribution (Junge exponent, β)
   b) mass concentration-light scattering correlation with α as parameter
   c) extinction due to light scattering compared to that by nitrogen dioxide
   d) correlation of light scattering with gaseous pollutants
3) experiments or interpretations which will arise as a result of the observations

These experiments are described in detail in Section V.

Miscellaneous Experiments

The considerable number of miscellaneous experiments conducted are listed in Table I-2.

Cloud and Ice Nuclei measurements were made since this project offered an excellent opportunity to correlate them with the great variety of chemical and physical measurements being made on the aerosol.

Electron microscope samples were taken both to see what the particles looked like and for possible single particle electron microprobe analysis by the AIHL.

Solar radiation measurements by pyroheliometer; wind velocity, direction and turbulence; and temperatures at the sampling line inlet and the instruments inlet were measured to provide necessary supportive data.

A few rough experiments were made in which the aerosol was humidified by passage through a chamber containing water, to find out how hydroscopic the aerosol was.

Some smog coagulation experiments were performed by rapidly filling a $56m^3$ polyethylene balloon with a blower and then measuring the size spectra for times up to 5 hours as the smog in the closed bag coagulated. The measured size spectra are being compared with those predicted by various theories and with the observed day and night aerosols.

A number of smog making experiments were performed in which about 15 m^3 of ultra filtered smog was pumped into the balloon and the condensation nuclei count measured with the G.E. counter while the bag sat in bright sunlight on the roof. After the initial experiments in the large bag showed a large and variable smog making potential at different times of the day, a smaller automatic apparatus was constructed and operated continuously to see how the "smog making potential" of the air fluctuated during the day.

Douglas Advanced Research Laboratory also made some atmospheric probes in the vicinity with a LIDAR apparatus to see how these measurements would correlate with the turbidimetric and aerosol spectra data.

Data Analysis and Publication Plans

Since the primary purpose of this report is to provide a detailed description of the experiment as a background for interpreting the data, it includes only such data as is necessary to illustrate the procedures. As of the date of this report, all but a small part of the data on the chemical analysis of the particulate samples has been reduced, and distributed to the investigators. Analysis of the data is well along and papers are being written for presentation as a group at the American Chemical Society's Kendall award symposium in April, 1971.

One project review meeting of all of the principal investigators was held on February 28, 1970 at the University of Minnesota, and another is scheduled for November 30, 1970 at Berkeley.

Final plans for distribution of the data to other than the participants have not been finalized. Currently, the University of Minnesota's size spectra data, the meteorological data and most of the gas analyzer data is available as a computer printout and on a magnetic tape. Charlson nephelometer data and hourly averages of the gas analysis data are available on punched card decks. Lundgren's data is in table form. The chemical analyses of the particulate samples are still in process but should be finished by the end of 1970.

Some thought has been given to providing all of this data on microfiche for those who would like to have the complete data for further analysis. The large amount of good data of a type that has never been obtained before that has resulted from this project will undoubtedly mean that it will require several years for complete analysis and publication of the results.

Sample Computer Printout

Figure I-4 is a sample of the 363 pages of computer printout of the data obtained by and results computed from the data recorded by the data acquisition system.

Table I - 1

Investigators, Participants, and Their Addresses

University of Minnesota, Minneapolis, Minnesota

Mr. Nick Barsic
125 Mechanical Engng. Bldg.
University of Minnesota
Minneapolis, Minnesota 55455

Mr. Rudolf Husar
125 Mechanical Engng. Bldg.
University of Minnesota
Minneapolis, Minnesota 55455

Mrs. Rudolf Husar
139 Chemistry Building
University of Minnesota
Minneapolis, Minnesota 55455

Dr. Benjamin Liu
125 Mechanical Engng. Bldg.
University of Minnesota
Minneapolis, Minnesota 55455

Dr. Ken Whitby
125 Mechanical Engng. Bldg.
University of Minnesota
Minneapolis, Minnesota 55455

California Institute of Technology, Pasadena, California

Dr. Barton Dahneke
Institut fur Aerobiologie
der Fraunhofer-Gesellschaft
5949 Grafschaft
uber Schmallenberg (Sauerland)
West Germany

Dr. S.K. Friedlander
W.M. Keck Lab of Envirn. Hlth. Engng.
California Institute of Technology
Pasadena, California 91109

Dr. George Hidy
Science Center
Aerospace & Systems Group
North American Rockwell Corp.
1049 Camino Dos Rios
Thousand Oaks, California 91360

Mr. W.A. Moser
Life Sciences Department
Autometics Division
North American Rockwell Corporation
Anaheim, California

Dr. Josef Pich
W.M. Keck Lab of Envirn. Hlth. Engng.
California Institute of Technology
Pasadena, California 91109

J.H. Seinfeld
W.M. Keck Lab of Envirn. Hlth. Engng.
California Institute of Technology
Pasadena, California 91109

California Air and Industrial Hygiene Lab, Berkeley, California

Dr. Peter Mueller
Air and Industrial Hygiene Lab
California State Department of Public Hlth.
2151 Berkeley Way
Berkeley, California 94704

K. Smith
Air and Industrial Hygiene Lab
California State Department of Public Health
2151 Berkeley Way
Berkeley, California 94704

Y. Tokiwa
Air and Industrial Hygiene Lab
California State Dept. of Public Health
2151 Berkeley Way
Berkeley, California 94704

University of Washington, Seattle, Washington

Mr. N.C. Ahlquist
University of Washington
Room 305, More Hall
Civil Engineering Dept.
Seattle, Washington 98105

Dr. Robert Charlson
University of Washington
Room 305, More Hall
Civil Engineering Dept.
Seattle, Washington 98105

Environmental Research Corporation, St. Paul, Minnesota

Mr. Dale Lundgren
Environmental Research Corp.
3725 North Dunlap Street
St. Paul, Minnesota 55112

Meteorology Research, Inc., Altadena, California

Mr. W. Green, Paul MacCready, et.al.
Meteorology Research, Inc.
Altadena, California

Dr. Underwood
Meteorology Research, Inc.
Altadena, California

Douglas Advanced Research Laboratory, Huntington Beach, California

Dr. Freeman Hall, Research Scientist
Douglas Advanced Research Labs
5251 Bolsa Avenue
Huntington Beach, California 92647

Table I - 2
Summary of Experiments, Instruments, and Investigators

Experiments	Instruments or Technique	Investigators
1. (a) Size spectra 0.003-6 μm by number (b) Mass distribution below 0.5 μm	(a) General Electric Nuclei Counter (b) Whitby Electric Aerosol Analyzer (c) Modified Royco 220 sensor + Hewlett-Packard multi channel analyzer (d) Dymec 25 channel data acquisition system	Whitby Liu Husar Barsic
2. Sampling of particulates for mass distribution and chemical analysis	(a) Lundgren impactors (b) 75 mm Teflon filters	Lundgren Mrs. Husar
3. Chemical analysis of particulates	Analysis for Pb, Fe, V, Zn, Si, Na, Mg, C(Non $CO_3)^=$, NO_3^-, $SO_4^=$, Cl^-, and Bromine	Mueller Tokiwa K. Smith
4. Continuous gas analysis for NO, NO_2, SO_2, O_3, PAN, and H.C. (acetylene index?)	NO: Atlas Electric Devices, NO sensor NO_2: Atlas Electric Devices, NO_2 sensor SO_2: Atlas Electric Devices, SO_2 sensor O_3: Atlas Electric Devices, O_3 sensor O_3: Mast Development Co., #724-11 O_3: Chemiluminescence - AIHL PAN: Statewide Air Pollution Center, Riverside, Cal. H.C.: Calif. Air & Ind. Hygiene Lab., Berkeley, Cal.	Mueller Tokiwa K. Smith Mrs. Husar
5. Turbidity measurements	(a) Charlson-Ahlquist integrating nephelometer (b) Charlson-Ahlquist four wavelength integrating nephelometer	Charlson Ahlquist Barsic
6. Cloud Condensation Nuclei	Meteorology Research Incorporated (MRI) Diffusion cloud chamber	MRI-Underwood Hidy

Table I - 2, continued

Experiments	Instruments or Technique	Investigators
7. Ice nuclei	MRI Filter method	MRI-Underwood
8. Electron microscopy (a) Electrical precipitation (b) Particle beam	(a) Thermo Systems electrical sampler - evaluation AIHL & U. of M. (b) Cal. Tech. apparatus	Mueller Whitby Dahneke Friedlander
9. Meteorological measurements (a) solar radiation (b) wind velocity, direction and turbulence (c) temperature & humidity (d) smog forecasts	(a) pyroheliometer (b) MRI wind instrument (c) Thermocouples Hygrometer & dew point (d) from Los Angeles	Hidy Barsic Husar
10. Effect of humidity on aerosol size distribution	Aerosol spectrometers (1) with humidification and dehumidification	Husar Liu
11. Coagulation of smog in a 56 m^3 polyethylene bag	Aerosol spectrometers (1) - measurement as function of time	Husar Liu Friedlander
12. Smog making experiments	G.E. Nuclei Counter, 56 m^3 polyethylene bag, pyrex chamber and sunlight	Husar Liu Friedlander
13. LIDAR probing of atmospheric aerosols	Douglas Advanced Research Lab., LIDAR	Hall

Table I - 3

Proposed Applications of the Experimental Results

1.	Comparison of experimental measurements of size spectrum with theory	(Pich (Husar (Liu (Friedlander (Whitby
2.	Relationship between aerosol and gas phase a. What fraction of aerosol originates in gas? b. Is condensation process homogeneous or heterogeneous?	(Friedlander (Mueller (Whitby
3.	Development of models for photochemical smog formation in urban basins for both particle and gas phases, eventual application to standards setting	(Friedlander (Seinfeld
4.	Relationship between turbidity measurements and mass concentration models	(Charlson
5.	Inadvertent weather modification	(Hidy
6.	Comparative performance of oxidant analyzers	(Mueller
7.	Effect of humidity on size distribution	(Husar (Liu-Whitby
8.	Correlation of size spectrum with - gas concentrations - aerosol chemistry - mass concentration and distribution - electrom micrographs	Univ. of Minn. with other investigators

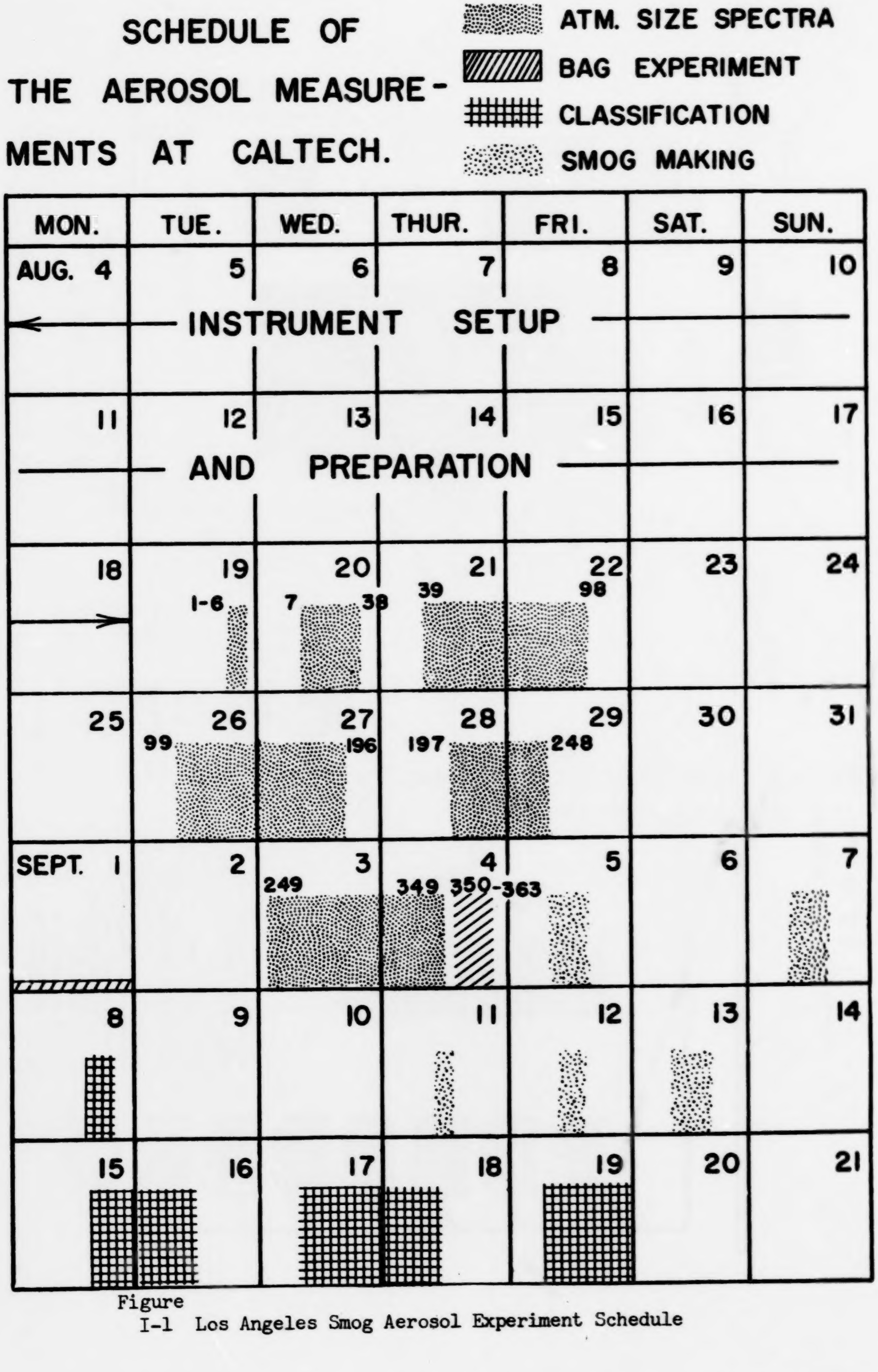

Figure I-1 Los Angeles Smog Aerosol Experiment Schedule

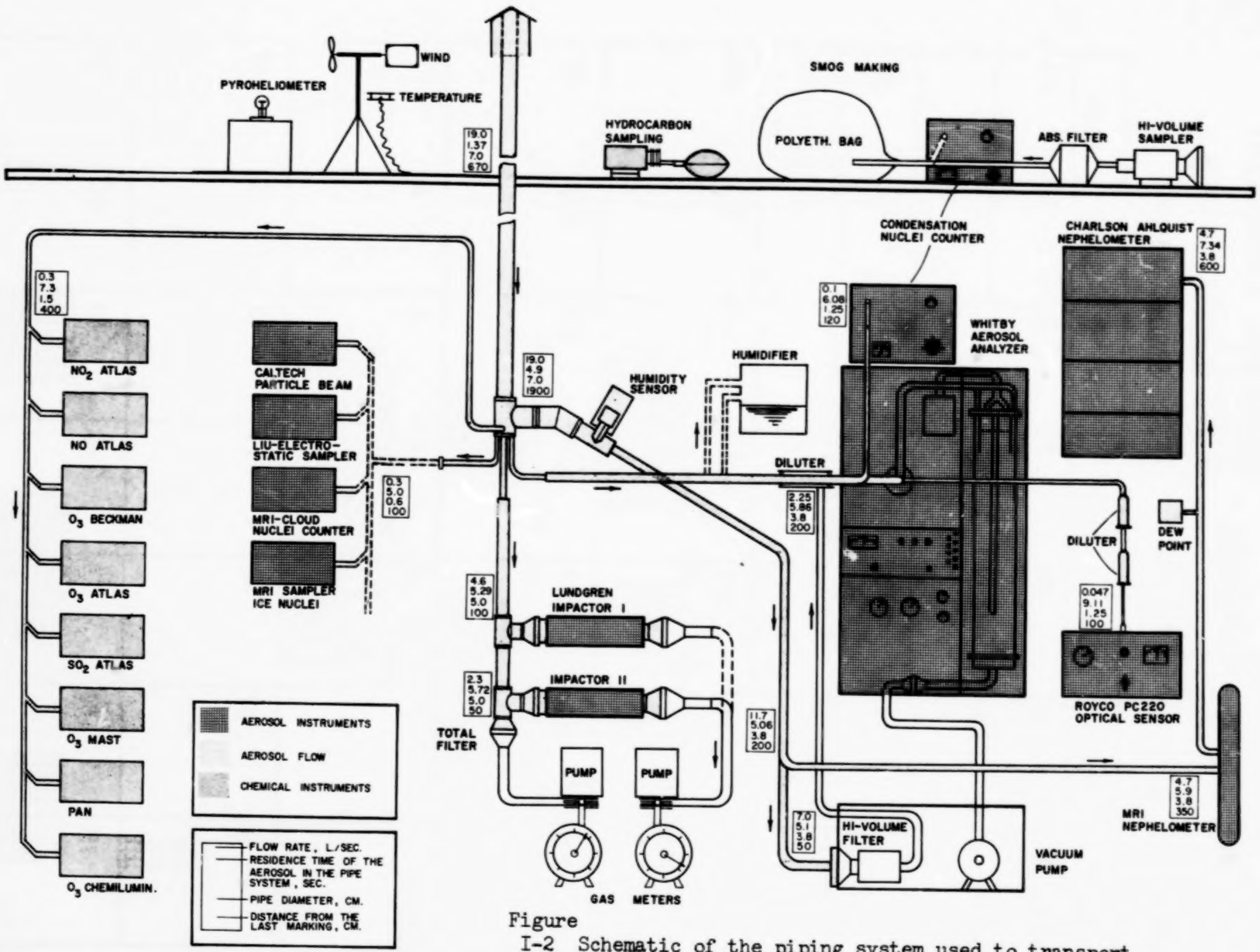
PYROHELIOMETER
WIND
TEMPERATURE
19.0
1.37
7.0
670
HYDROCARBON SAMPLING
SMOG MAKING
POLYETH. BAG
ABS. FILTER
HI-VOLUME SAMPLER
CONDENSATION NUCLEI COUNTER
CHARLSON AHLQUIST NEPHELOMETER
4.7
7.34
3.8
600
0.1
6.08
1.25
120
WHITBY AEROSOL ANALYZER
0.3
7.3
1.5
400
NO$_2$ ATLAS
NO ATLAS
O$_3$ BECKMAN
O$_3$ ATLAS
SO$_2$ ATLAS
O$_3$ MAST
PAN
O$_3$ CHEMILUMIN.
CALTECH PARTICLE BEAM
LIU-ELECTRO-STATIC SAMPLER
MRI-CLOUD NUCLEI COUNTER
MRI SAMPLER ICE NUCLEI
0.3
5.0
0.6
100
19.0
4.9
7.0
1900
HUMIDITY SENSOR
HUMIDIFIER
DILUTER
2.25
5.86
3.8
200
DILUTER
DEW POINT
0.047
9.11
1.25
100
ROYCO PC220 OPTICAL SENSOR
4.6
5.29
5.0
100
LUNDGREN IMPACTOR I
IMPACTOR II
2.3
5.72
5.0
50
TOTAL FILTER
11.7
5.06
3.8
200
PUMP
PUMP
GAS METERS
7.0
5.1
3.8
50
HI-VOLUME FILTER
VACUUM PUMP
4.7
5.9
3.8
350
MRI NEPHELOMETER
AEROSOL INSTRUMENTS
AEROSOL FLOW
CHEMICAL INSTRUMENTS
FLOW RATE, L./SEC.
RESIDENCE TIME OF THE AEROSOL IN THE PIPE SYSTEM, SEC.
PIPE DIAMETER, CM.
DISTANCE FROM THE LAST MARKING, CM.

Figure
I-2 Schematic of the piping system used to transport aerosol to the various experiments

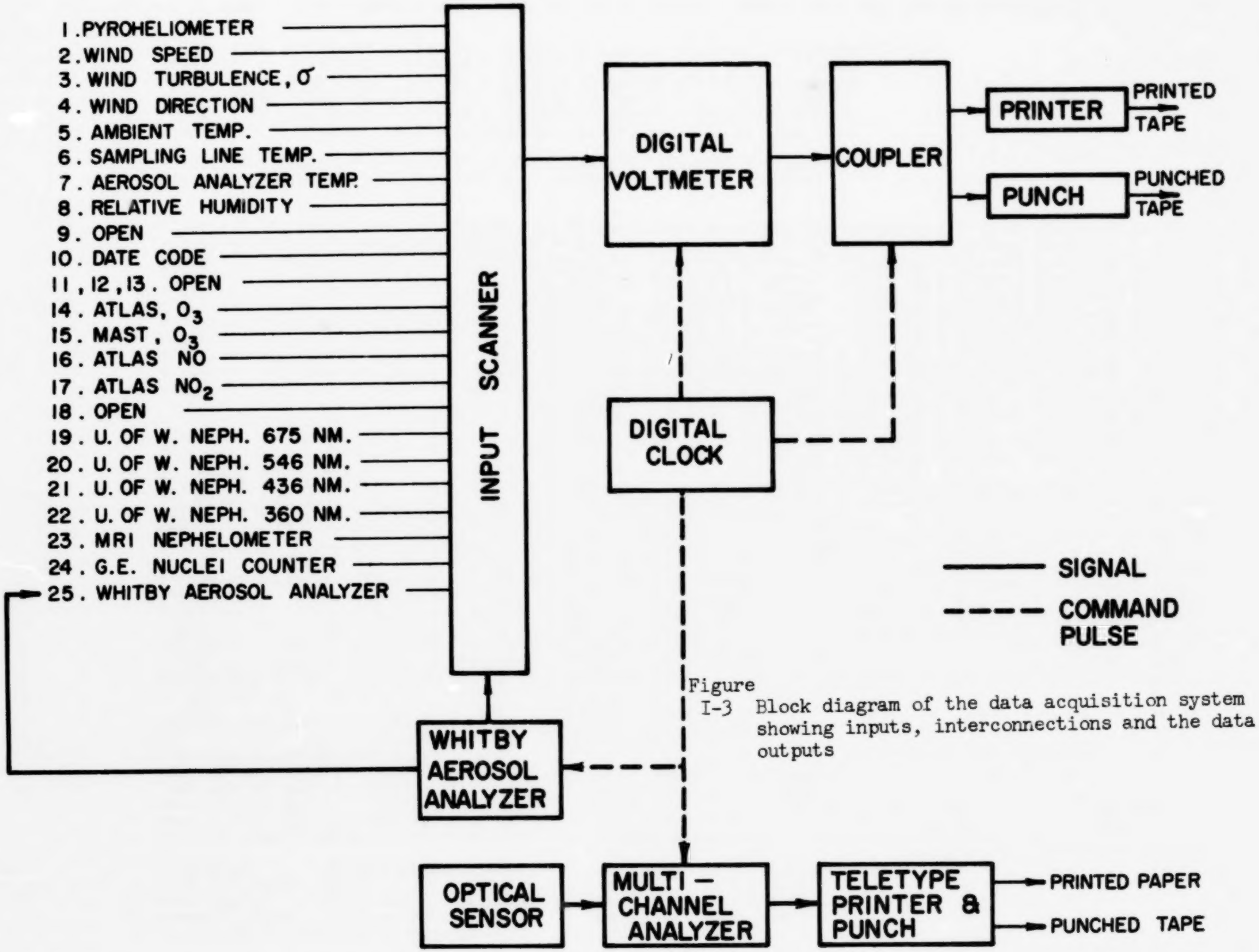
1. PYROHELIOMETER
2. WIND SPEED
3. WIND TURBULENCE, σ
4. WIND DIRECTION
5. AMBIENT TEMP.
6. SAMPLING LINE TEMP.
7. AEROSOL ANALYZER TEMP.
8. RELATIVE HUMIDITY
9. OPEN
10. DATE CODE
11, 12, 13. OPEN
14. ATLAS, O3
15. MAST, O3
16. ATLAS NO
17. ATLAS NO2
18. OPEN
19. U. OF W. NEPH. 675 NM.
20. U. OF W. NEPH. 546 NM.
21. U. OF W. NEPH. 436 NM.
22. U. OF W. NEPH. 360 NM.
23. MRI NEPHELOMETER
24. G.E. NUCLEI COUNTER
25. WHITBY AEROSOL ANALYZER
INPUT SCANNER
DIGITAL VOLTMETER
COUPLER
PRINTER
PRINTED TAPE
PUNCH
PUNCHED TAPE
DIGITAL CLOCK
SIGNAL
COMMAND PULSE
WHITBY AEROSOL ANALYZER
OPTICAL SENSOR
MULTI-CHANNEL ANALYZER
TELETYPE PRINTER & PUNCH
PRINTED PAPER
PUNCHED TAPE

Figure I-3 Block diagram of the data acquisition system showing inputs, interconnections and the data outputs

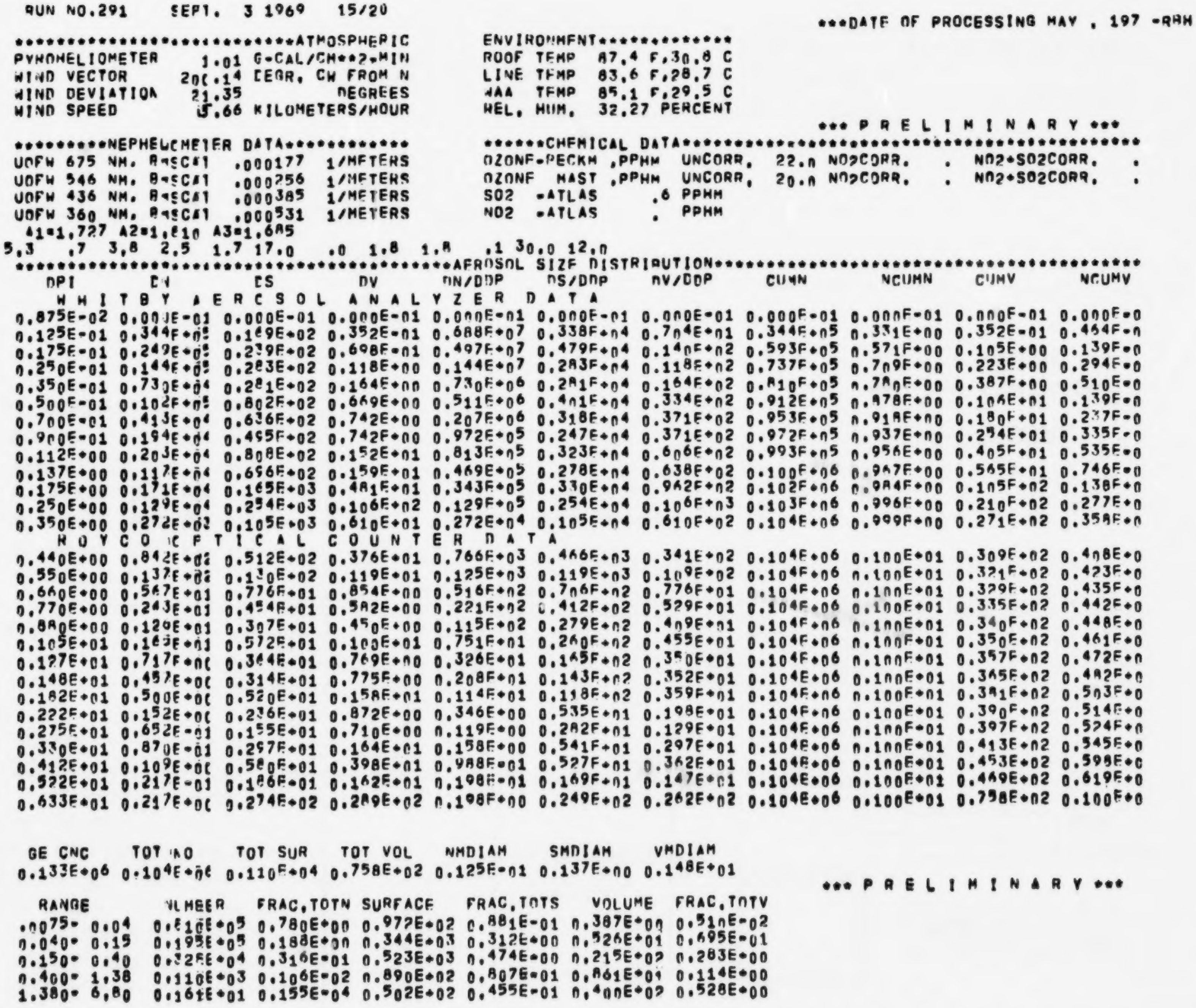

```
 RUN NO.291    SEPT.  3 1969   15/20
                                                                              ***DATE OF PROCESSING MAY , 197 -RHH
 ****************************ATMOSPHERIC       ENVIRONMENT*************
 PYRHELIOMETER       1.01 G-CAL/CM**2-MIN      ROOF TEMP  87.4 F,30.8 C
 WIND VECTOR       200.14 DEGR, CW FROM N      LINE TEMP  83.6 F,28.7 C
 WIND DEVIATION     21.35          DEGREES     HAA  TEMP  85.1 F,29.5 C
 WIND SPEED          5.66 KILOMETERS/HOUR      REL, HUM,  32.27 PERCENT
                                                                         *** P R E L I M I N A R Y ***
 **********NEPHELOMETER DATA*************      ******CHEMICAL DATA*******************************************
 UDFW 675 NM, B-SCAT  .000177  1/METERS        OZONE-BECKM ,PPHM  UNCORR,  22.0 NO2CORR.    .  NO2+SO2CORR,   .
 UDFW 546 NM, B-SCAT  .000256  1/METERS        OZONE  MAST ,PPHM  UNCORR,  20.0 NO2CORR.    .  NO2+SO2CORR,   .
 UDFW 436 NM, B-SCAT  .000385  1/METERS        SO2   -ATLAS      .6 PPHM
 UDFW 360 NM, B-SCAT  .000531  1/METERS        NO2   -ATLAS      .  PPHM
  A1=1,727 A2=1,810 A3=1,685
5,3   ,7  3,8  2,5  1.7 17.0   .0  1.8  1.8   .1 30.0 12.0
 *******************************************AEROSOL SIZE DISTRIBUTION*******************************************
   DPI        CN         CS         DV       DN/DDP     DS/DDP     DV/DDP      CUMN       NCUMN      CUMV      NCUMV
     W H I T B Y  A E R O S O L  A N A L Y Z E R  D A T A
 0.875E-02 0.000E-01 0.000E-01 0.000E-01 0.000E-01 0.000E-01 0.000E-01 0.000E-01 0.000E-01 0.000E-01 0.000E-0
 0.125E-01 0.344E+05 0.169E+02 0.352E-01 0.688E+07 0.338E+04 0.704E+01 0.344E+05 0.331E+00 0.352E-01 0.464E-0
 0.175E-01 0.249E+05 0.239E+02 0.698E-01 0.497E+07 0.479E+04 0.140E+02 0.593E+05 0.571E+00 0.105E+00 0.139E-0
 0.250E-01 0.144E+05 0.283E+02 0.118E+00 0.144E+07 0.283E+04 0.118E+02 0.737E+05 0.709E+00 0.223E+00 0.294E-0
 0.350E-01 0.730E+04 0.281E+02 0.164E+00 0.730E+06 0.281E+04 0.164E+02 0.810E+05 0.780E+00 0.387E+00 0.510E-0
 0.500E-01 0.102E+05 0.802E+02 0.669E+00 0.511E+06 0.401E+04 0.334E+02 0.912E+05 0.878E+00 0.106E+01 0.139E-0
 0.700E-01 0.413E+04 0.636E+02 0.742E+00 0.207E+06 0.318E+04 0.371E+02 0.953E+05 0.918E+00 0.180E+01 0.237E-0
 0.900E-01 0.194E+04 0.495E+02 0.742E+00 0.972E+05 0.247E+04 0.371E+02 0.972E+05 0.937E+00 0.254E+01 0.335E-0
 0.112E+00 0.203E+04 0.808E+02 0.152E+01 0.813E+05 0.323E+04 0.606E+02 0.993E+05 0.956E+00 0.405E+01 0.535E-0
 0.137E+00 0.117E+04 0.696E+02 0.159E+01 0.469E+05 0.278E+04 0.638E+02 0.100E+06 0.967E+00 0.565E+01 0.746E-0
 0.175E+00 0.171E+04 0.165E+03 0.481E+01 0.343E+05 0.330E+04 0.962E+02 0.102E+06 0.984E+00 0.105E+02 0.138E+0
 0.250E+00 0.129E+04 0.254E+03 0.106E+02 0.129E+05 0.254E+04 0.106E+03 0.103E+06 0.996E+00 0.210E+02 0.277E+0
 0.350E+00 0.272E+03 0.105E+03 0.610E+01 0.272E+04 0.105E+04 0.610E+02 0.104E+06 0.999E+00 0.271E+02 0.358E+0
     R O Y C O  O P T I C A L  C O U N T E R  D A T A
 0.440E+00 0.842E+02 0.512E+02 0.376E+01 0.766E+03 0.466E+03 0.341E+02 0.104E+06 0.100E+01 0.309E+02 0.408E+0
 0.550E+00 0.137E+02 0.130E+02 0.119E+01 0.125E+03 0.119E+03 0.109E+02 0.104E+06 0.100E+01 0.321E+02 0.423E+0
 0.660E+00 0.567E+01 0.776E+01 0.854E+00 0.516E+02 0.706E+02 0.776E+01 0.104E+06 0.100E+01 0.329E+02 0.435E+0
 0.770E+00 0.243E+01 0.454E+01 0.582E+00 0.221E+02 0.412E+02 0.529E+01 0.104E+06 0.100E+01 0.335E+02 0.442E+0
 0.880E+00 0.129E+01 0.307E+01 0.450E+00 0.115E+02 0.279E+02 0.409E+01 0.104E+06 0.100E+01 0.340E+02 0.448E+0
 0.105E+01 0.163E+01 0.572E+01 0.100E+01 0.751E+01 0.260E+02 0.455E+01 0.104E+06 0.100E+01 0.350E+02 0.461E+0
 0.127E+01 0.717E+00 0.364E+01 0.769E+00 0.326E+01 0.165E+02 0.350E+01 0.104E+06 0.100E+01 0.357E+02 0.472E+0
 0.148E+01 0.457E+00 0.314E+01 0.775E+00 0.208E+01 0.143E+02 0.352E+01 0.104E+06 0.100E+01 0.365E+02 0.482E+0
 0.182E+01 0.500E+00 0.520E+01 0.158E+01 0.114E+01 0.118E+02 0.359E+01 0.104E+06 0.100E+01 0.381E+02 0.503E+0
 0.222E+01 0.152E+00 0.236E+01 0.872E+00 0.346E+00 0.535E+01 0.198E+01 0.104E+06 0.100E+01 0.390E+02 0.514E+0
 0.275E+01 0.652E-01 0.155E+01 0.710E+00 0.119E+00 0.282E+01 0.129E+01 0.104E+06 0.100E+01 0.397E+02 0.524E+0
 0.330E+01 0.870E-01 0.297E+01 0.164E+01 0.158E+00 0.541E+01 0.297E+01 0.104E+06 0.100E+01 0.413E+02 0.545E+0
 0.412E+01 0.109E+00 0.580E+01 0.398E+01 0.988E-01 0.527E+01 0.362E+01 0.104E+06 0.100E+01 0.453E+02 0.598E+0
 0.522E+01 0.217E-01 0.186E+01 0.162E+01 0.198E-01 0.169E+01 0.147E+01 0.104E+06 0.100E+01 0.469E+02 0.619E+0
 0.633E+01 0.217E+00 0.274E+02 0.289E+02 0.198E+00 0.249E+02 0.262E+02 0.104E+06 0.100E+01 0.758E+02 0.100E+0


  GE CNC     TOT NO     TOT SUR    TOT VOL    NMDIAM     SMDIAM     VMDIAM
 0.133E+06 0.104E+06 0.110E+04 0.758E+02 0.125E-01 0.137E+00 0.148E+01
                                                                         *** P R E L I M I N A R Y ***
  RANGE          NUMBER    FRAC,TOTN SURFACE   FRAC,TOTS   VOLUME   FRAC,TOTV
 .0075- 0.04   0.810E+05 0.780E+00 0.972E+02 0.881E-01 0.387E+00 0.510E-02
 0.040- 0.15   0.195E+05 0.188E+00 0.344E+03 0.312E+00 0.526E+01 0.695E-01
 0.150- 0.40   0.328E+04 0.316E-01 0.523E+03 0.474E+00 0.215E+02 0.283E+00
 0.400- 1.38   0.110E+03 0.106E-02 0.890E+02 0.807E-01 0.861E+01 0.114E+00
 1.380- 6.80   0.161E+01 0.155E-04 0.502E+02 0.455E-01 0.400E+02 0.528E+00
```

Fig. I-4. Sample data printout illustrating typical data and results calculated from the data.

SECTION II

BACKGROUND INFORMATION ON SITE AND METEOROLOGICAL EXPERIMENTS

Pasadena Smog Experiment

August - October, 1969

by

G.M. Hidy and S.K. Friedlander
with contributions from
W. Green

1. Introduction

This portion of the description deals with three aspects of the experimental program. First, the general character of the observational site is outlined, covering an inventory of sources, and the meso-scale meteorology of the Los Angeles basin. In the second part, more details are given about the physical site in Pasadena. Finally, a brief summary of the meteorological instrumentation and support for the program is presented.

2. Inventory of Sources Around Pasadena

The general statistics concerning the nature of the pollution sources in the Los Angeles basin are given in Table II-1. The magnitude of the emissions from major sources are indicated in Table II-2. From these data one can readily see that motor vehicles make up the bulk of the sources of gaseous and particulate pollutants except for sulfur dioxide. However, stationary sources of various kinds also contribute a substantial fraction of material to the Los Angeles atmosphere. Pollutant sources have been broken down in further categories in Ref. (1).

Like most of the urban area in the Los Angeles basin, Pasadena is interlaced and surrounded by high speed highways, so that this community receives a dose of automobile exhaust from local sources each day. Unfortunately, it also is susceptible to pollutants sweeping in via the winds from densely populated areas to the south and west, as will be shown later.

The geography of the Los Angeles basin with major highways is sketched in Fig. II-1. Fuller _et al._(1) break down the typical stationary sources in this region into the following categories: (a) chemical processing equipment, (b) boilers and heaters, (c) paint bake ovens, (d) incinerating equipment, (e) melting equipment, (f) concrete plants, (g) petroleum processing plants, (h) rendering equipment, and (i) power plants. Except for the last source, all are concentrated mainly in the zone south of Pasadena from Inglewood to Whittier to the coast at Long Beach. There are major sources of electrical power just to the south and to the west in Pasadena and Glendale, accounting for about 10% of the total rated output in the basin. At the present time, the various sources listed above produce a variety of pollutants. The power plants, however, release mainly nitrogen oxides to the atmosphere.

Table II-1

GENERAL STATISTICS
for 1968-1969 (Ref. 1)

ITEM	QUANTITY
Population	7,300,000
Los Angeles County Land Area	4,083 Sq. Miles
Los Angeles Basin Land Area	1,250 Sq. Miles
Solvents Used (Emitted)	1,000,000 Lbs./Day
Refinery Crude Throughput	731,000 Bbls./Day
Fuels Burned During Rule 62 Period(a)	
Oil Containing More Than 0.5% Sulfur	193,200 Gals./Day(c)
Oil Containing 0.5% or Less Sulfur	59,430 Gals./Day
Natural Gas	1,894,400 MCF/Day
Refinery Make Gas	272,400 MCF/Day
Fuels Burned During Rule 62.1 Period(b)	
Oil Containing More Than 0.5% Sulfur	487,400 Gals./Day(c)
Oil Containing 0.5% or Less Sulfur	2,828,100 Gals./Day
Natural Gas	2,128,200 MCF/Day
Refinery Make Gas	277,200 MCF/Day
Gasoline-Powered Vehicle Registration	3,950,000
Gasoline Consumed	8,000,000 Gals./Day
Diesel-Powered Vehicle Registration	14,500
Diesel Fuel Consumed by Motor Vehicles	150,000 Gals./Day
Jet-Powered Aircrafe Flights/Day	1,505
Jet Fuel Consumed (Within L. A. County)	330,000 Gals./Day
Piston-Driven Aircraft Flights/Day	9,650
Helicopter Flights/Day	590
Aviation Gasoline Consumed (Within L. A. County)	110,000 Gals./Day

(a) Rule 62 period is from April 15 through November 15

(b) Rule 62.1 period is from November 16 through April 14.

(c) Burned under variance granted by Hearing Board.

Table II-2

EMISSIONS[a]

Based on Data for 1968-1969 (Ref. 1)
Contaminants, in Tons Per Day, from Major Sources
Within Los Angeles County

MAJOR SOURCE	ORGANIC GASES REACTIVITY			PARTICULATES	NO_x	SO_2	CO	TOTAL
	HIGH	LOW	TOTAL					
Motor Vehicles	1255	475	1730	45	645	30	9470	11920
Org. Solvent Usage	100	400	500	17	-	1	-	520
Petroleum	55	165	220	4	45	55	30	355
Aircraft	45	45	90	12	15	3	190	310
Combustion of Fuels	-	9	9	15	235	40	1	300
Chemical	-	-	-	-	-	90	-	90
Other	-	3	3	16	11	3	4	35
TOTAL (Rounded)	1455	1095	2550	110	950	225	9695	13530

[a] For Rule 62, that period of the year from April 15 through November 15, generally characterized by warm weather when the supplies of natural gas and low-sulfur fuel oil for utilities are great enough to prevent the use of high sulfur fuels.

Typical contaminant concentration levels in the area around Pasadena (West San Gabriel Valley) for the summer months are listed in Table II-3. In terms of other regions of the Los Angeles Basin, these values suggest that ozone concentrations are relatively high while the other pollutants listed are moderate to low compared with the more urban areas to the west and south.

3. The Meteorology of the Los Angeles Basin

Several general studies have been made of the meteorology of the Southern California region. Excellent summaries of measurements prior to the late 1950's are given by the Air Pollution Foundation.(2,3) More recent data are available from the Weather Bureau.(4) In general, the meteorology near the ground in the Los Angeles basin is dominated by the influence of the neighboring ocean and the peculiarities of the local topography.

The broad scale features that characterize Los Angeles weather are (a) the Pacific high pressure zone which dominates the synoptic scale atmospheric motion from early spring until early fall, (b) the continental high pressure region over the deserts and high plains to the east and north which is present much of the period from fall through winter, and (c) the winter passage of cyclonic storms originating to the north, south, and west over the Pacific.

The conditions which seriously restrict the dispersion of material in the planetary boundary layer develop most frequently in the summer months and in early fall when the Pacific high induces a subsidence inversion over the Basin. The resulting elevated inversion together with the blocking of the surrounding mountains forms a box-like trap for pollutants discharged into the atmosphere. Periods where a subsidence inversion exists are accompanied by a strong on-shore sea breeze during the day and diminished winds at night. Sometimes, the wind reverses direction at night to blow off-shore as a result of nocturnal radiation cooling and down slope drainage.

Outbreaks of air from intense high pressure areas over the deserts to the east create the Santa Ana condition, often observed during the fall. This condition is marked by strong dry winds sweeping across the Basin from the northeast, pushing the contaminants out to sea. As the Santa Ana winds diminish, however, shallow inversions sometimes form by radiative cooling during the night which can hinder dispersion of pollutants emitted at the earth's surface. This class of inversion tends to dissipate quickly during the day in contrast to the elevated subsidence inversions associated with the Pacific high.

In late fall and winter the passage of cyclones creates conditions of deep mixing near the ground giving rise to favorable dispersion conditions.

Generally then, the diffusion meteorology of the Los Angeles basin is identified with meso-scale (ten to a hundred of km.) horizontal ebbing and flowing of air limited to a rather shallow surface layer. The depth of this

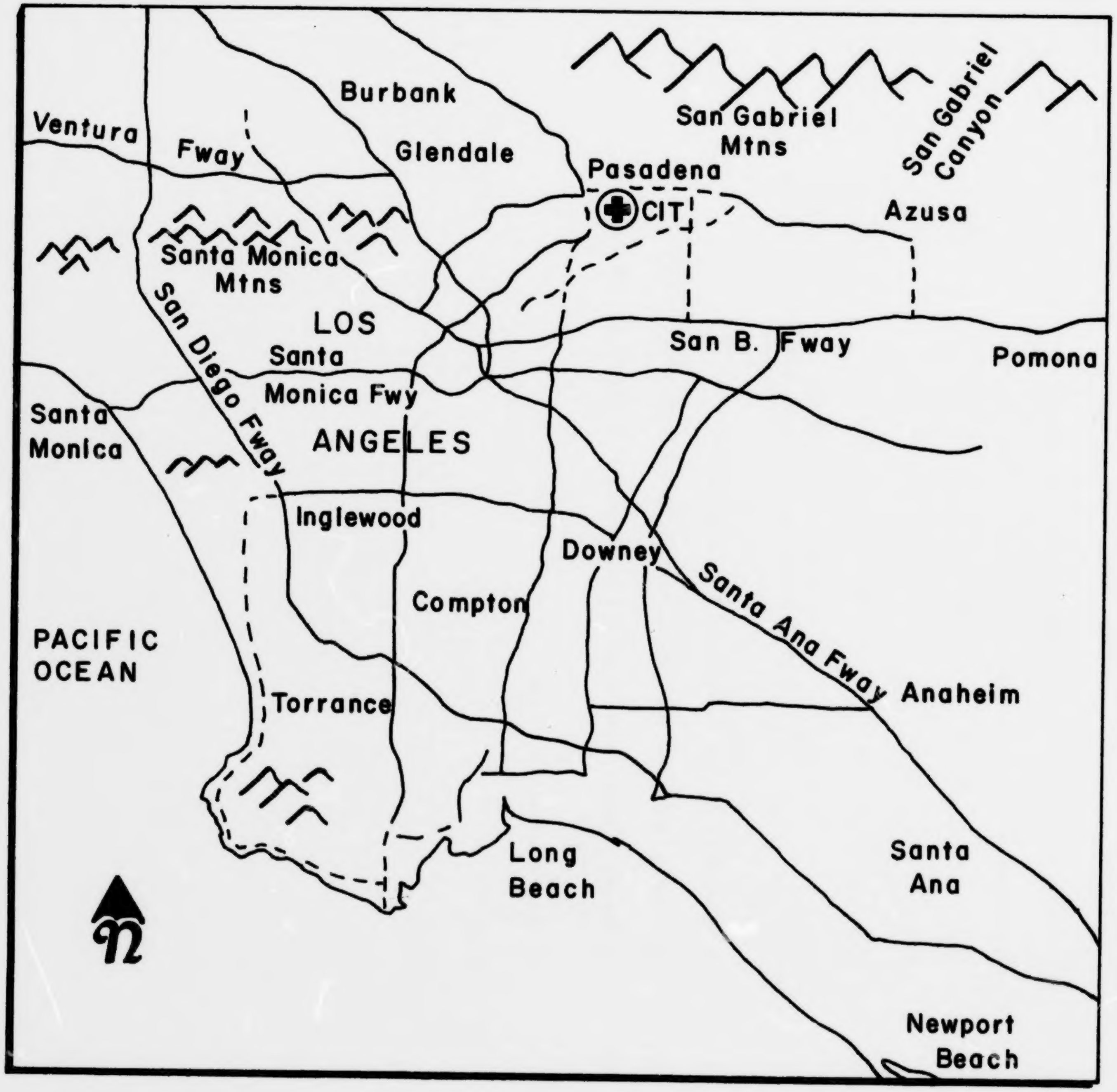
Ventura
Fway
Burbank
Glendale
San Gabriel
Mtns
San Gabriel
Canyon
Pasadena
CIT
Azusa
Santa Monica
Mtns
LOS
Santa
Monica Fwy
ANGELES
San B. Fway
Pomona
Santa
Monica
San Diego Fway
Inglewood
Downey
Compton
Santa Ana Fway
PACIFIC
OCEAN
Torrance
Anaheim
Long
Beach
Santa
Ana
Newport
Beach
n

Figure II-1 A map of the Los Angeles area showing major highways and communities around Pasadena.

Table II-3

Typical Air Pollution Concentrations
in the West San Gabriel Valley
for 1968-69 (in ppm)
(From Ref. 1)

	a	b	c	d
O_3	0.18	0.09	0.04	0.02
NO_x	0.76	0.50	0.29	0.17
CO	37	19	11	6
SO_2	0.12	0.07	0.06	0.02

a Average of the 4 highest daily maxima.

b Average of the 4 highest consecutive 8-hour periods

c Mean hourly average of 4 highest days based on 24-hour average.

d Mean hourly average.

mixing region under the inversion base at any particular time defines the volume of air available for handling the pollutant emissions. The altitude of the inversion base varies, but averages about 600 meters over Los Angeles.

For this experiment in air pollution, the period of late summer and early fall was chosen because this is the period of most frequent days for serious pollution. During this period the weather is associated largely with the Pacific high, and typical streamlines for surface air flow during the day look like those in Fig. II-2. Here the sea breeze penetrates the basin from the west pushing the pollutants emitted in the industrial zones northeastward over Pasadena. At night, average wind patterns, as drawn in Fig. II-3, show a reversal in flow out to sea bringing polluted air from the east back over Pasadena before being swept out toward sea.

Since there is often limited flushing of air in the marine layer as it ebbs out to sea, pollution may accumulate from day to day in the "tidal" flowing air mass. Therefore, air passing over Los Angeles may experience a buildup in pollutants over several days because of the persistence of the diurnal ebb and flow wind patterns. Some evidence for this sort of buildup is given by Pack and Angell.(5) Such conditions make the normal trapping of pollutants in the marine layer worse and may be involved in inordinately severe pollution episodes. In any case, we can expect that the pollution over Pasadena will be a complicated mixture from many sources, probably dominated by motor vehicle emissions.

4. Representativeness of Sample

Because of limited resources, it was possible to conduct the sampling program only at one location. Pasadena is not centrally located in the Los Angeles Basin. Based on the prevailing winds expected during the sampling period, pollution should come into the sampling point from the west-south sector. Because there are few major stationary sources within a 5 mile radius of Pasadena, it is expected that the samples taken will represent a very complicated mixture of material coming from concentrated stationary and mobile sources over about a 20 mile or more radius to the Pacific Ocean. The measured material will have aged varying degrees in the atmosphere before reaching Pasadena, and will be mixed to a varying extent with material emitted locally, primarily from power plants to the west, and motor vehicle traffic near the site. Samples also may contain a spurious component resulting from dust emissions associated with building construction adjacent to the Keck laboratories.

Aside from the possible contamination of building dusts, it is expected that the samples taken in Pasadena should satisfactorily represent at least the northeast sector of the Los Angeles Basin. Whether or not the results will be characteristics of the polluted atmosphere to the south and west in the Basin must remain an open question until new sampling is conducted over a broader area.

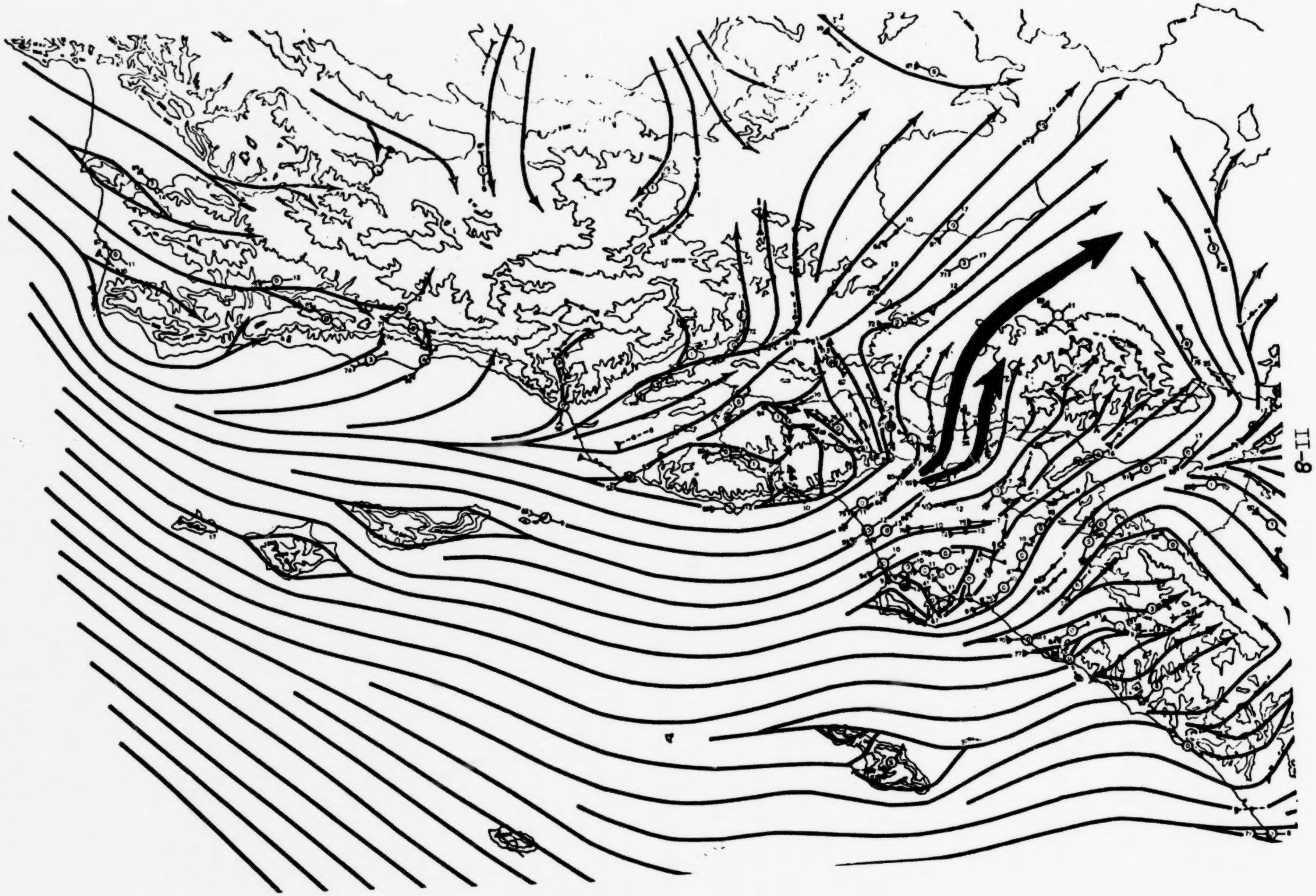

Figure II-2 Streamline chart for July, 1200-1800 PST
From USWB Tech. Paper 54, (1965)

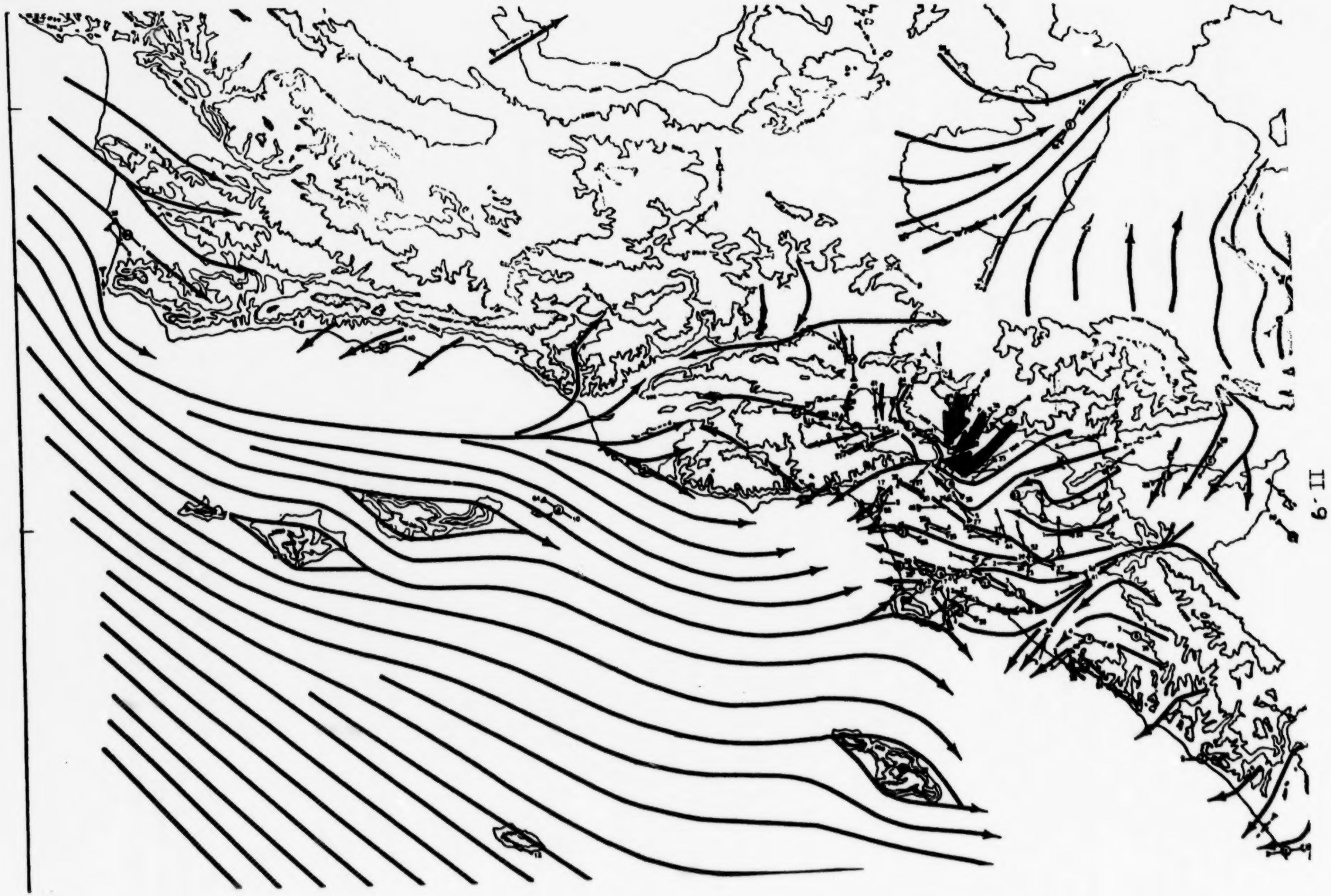

Figure II-3 Streamline chart for July, 0000-0500 PST

From USWB Tech. Paper 54, (1965)

In addition to the possibility of inhomogeneity of samples horizontally, it is anticipated that the material collected will not be entirely representative of the vertical distribution of aerosols in the Basin. It is known from other work that the number, size and mass distribution will change with height in urban and non-urban areas. However, it is not known to what extent the chemical composition changes with height.

The samples taken at Pasadena are not likely to be representative of the annual average character of the Los Angeles aerosol. Routine sampling at other periods of the year, particularly during winter, indicate marked seasonal differences in aerosol concentration in Pasadena. It is expected that similar differences should exist in the chemical composition of the aerosol.

At this time, we can only consider the samples taken in this study reasonably characteristic of a mixture of partially aged and newly formed aerosol in a northeast, quasi-suburban regime of the Los Angeles Basin during the months of more intense smog formation.

5. Characteristics of the Observational Site

The various instruments were placed either on the roof or the basement of the Keck Laboratories of California Institute of Technology. The building is three stories, 36 feet 6 inches high with a parapet 41 inches high on the roof. The anemometers were located on the roof to the west 16 feet above the roof. The PVC sampling tube, 2-7/8 inches O.D. was raised 22 feet above the roof on the west side. The total length of the tube to the diluters in the basement laboratory was 67 feet.

The long sampling tube may provide a deposition surface for particles and gases. For fully developed turbulent pipe flow, and a perfectly absorbing pipe wall, the fractional removal can be calculated from the expression

$$\ln \frac{c_1}{c_2} = 4\left(\frac{k}{V}\right)\left(\frac{L}{d}\right)$$

where c_1 and c_2 are concentrations of particles or gases entering and leaving the pipe, respectively, k the mass transfer coefficient, V the gas velocity, L the length of pipe, and d the pipe diameter. For gas diffusion, the Reynolds analogy can be used to estimate k:

$$\frac{k}{V} = \frac{f}{2}$$

where f is the coefficient of friction for the pipe flow. If, for example, the Reynolds number is 10,000, 99% of the pollutant gas will be removed over a 60-foot length of 2-1/2" pipe. Thus gas concentrations at the top and bottom of the sampling tube must be carefully checked because of the potentially high removal efficiency if the pipe wall is perfectly absorbing. The results of these tests are described in the section on gas sampling (Mueller).

In the case of aerosol deposition, the Reynolds analogy is no longer applicable because of the very small values of the particle diffusion coefficient. Instead it is necessary to use an expression for the mass transfer rate which includes a term for the Schmidt number, N_{Sc}, the ratio of the kinematic viscosity of the air to the particle diffusion coefficient, D. If, for example, the equation of Metzner and Friend$^{(6)}$ is used

$$\frac{k}{V} = 0.049\left(\frac{f}{2}\right)^{\frac{1}{2}} N_{Sc}{}^{-2/3}$$

for particles 0.01 μ in diameter ($D=5.24 \times 10^{-5}$ cm^2/sec), less than 2% are removed over a 60-foot length. A smaller percentage of the larger particles will be removed because the diffusion coefficient decreases with increasing particle diameter. Thus particle loss by diffusion would not be expected to be a serious problem.

Surrounding the Keck building are other multi-story buildings of the Institute and a parking lot. Farther away is a residential area ringing the entire Institute for a radius of approximately one mile. During the observational period, a new building was being constructed next to Keck. The layout of the Institute is sketched in Fig. II-4.

In a neighboring park, about one mile from Keck, the Los Angeles APCD has a monitoring station measuring continuously winds, temperature, oxidants, and particulates.

6. Summary of Instrumentation for Meteorological Observations

During the observational period of the experiment, limited meteorological data were obtained either by direct measurement, or from local sources such as the LA APCD or the weather bureau.

Direct Observations. Most of the direct observations were made from the roof of Keck Laboratories. They include the parameters listed in Table II-4. The output from instruments could be considered a bare minimum for monitoring local changes in atmospheric dynamics during the experiment. The mean wind and direction gives a good estimate of the steadiness and direction of air flow near the ground in the region near the sampling site. It may be extrapolated very roughly to suggest the direction and trajectory of air parcels entering the area from distances farther than a few hundred meters. Any such extrapolation should be made with great caution, however, because of the highly broken urban "surface" surrounding Keck Laboratories. Any such rough surface can contribute to spurious, non-representative wind patterns at heights less than the characteristic height of the roughness elements. In a similar way, the

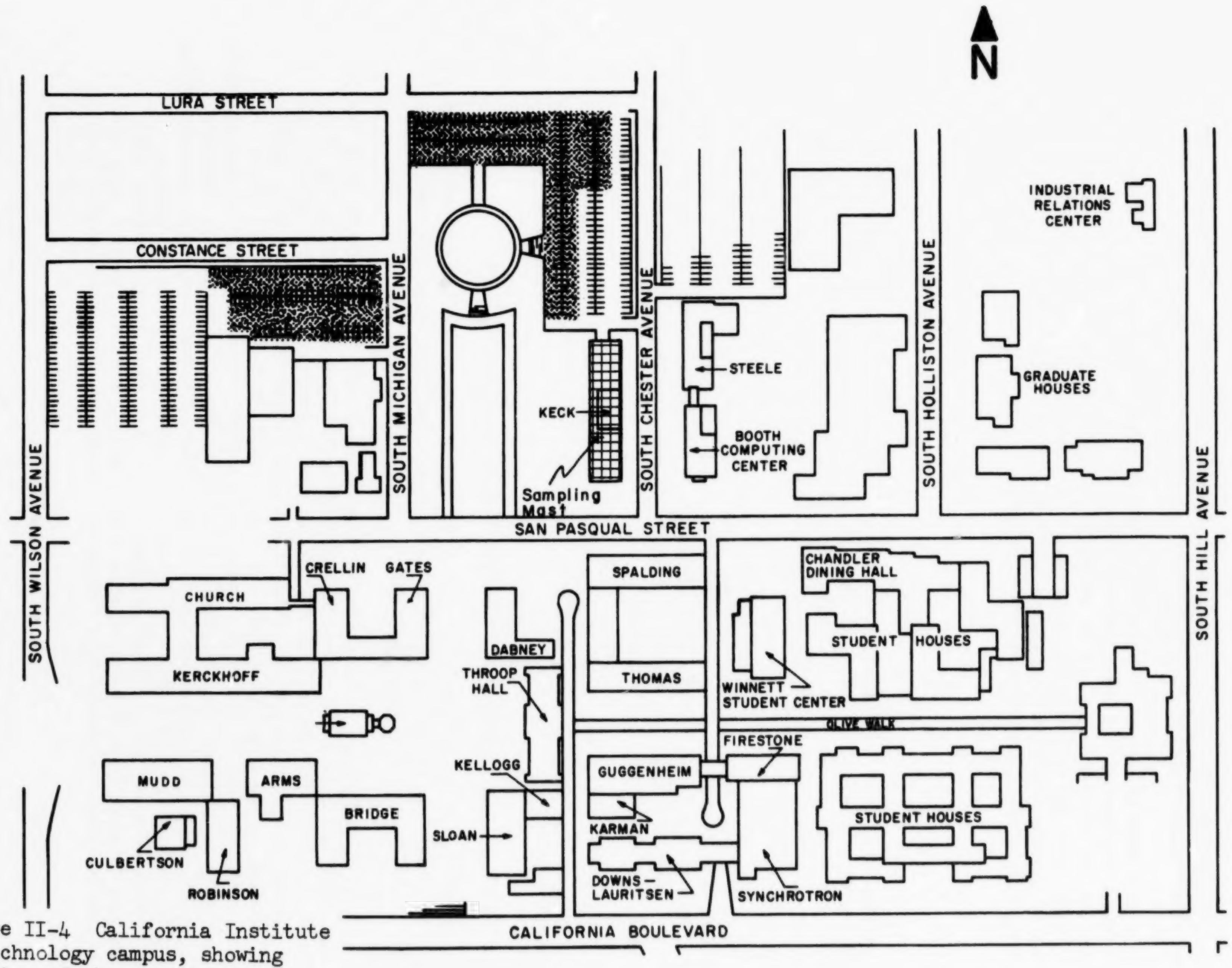
N
LURA STREET
CONSTANCE STREET
SOUTH WILSON AVENUE
SOUTH MICHIGAN AVENUE
SOUTH CHESTER AVENUE
SOUTH HOLLISTON AVENUE
SOUTH HILL AVENUE
SAN PASQUAL STREET
CALIFORNIA BOULEVARD
INDUSTRIAL RELATIONS CENTER
GRADUATE HOUSES
STEELE
BOOTH COMPUTING CENTER
KECK
Sampling Mast
CRELLIN
GATES
CHURCH
KERCHKHOFF
DABNEY
THROOP HALL
KELLOGG
SLOAN
SPALDING
THOMAS
CHANDLER DINING HALL
STUDENT HOUSES
WINNETT STUDENT CENTER
OLIVE WALK
FIRESTONE
GUGGENHEIM
KARMAN
DOWNS-LAURITSEN
SYNCHROTRON
STUDENT HOUSES
MUDD
ARMS
BRIDGE
CULBERTSON
ROBINSON

Figure II-4 California Institute of Technology campus, showing location of the sampling mast on the Keck Laboratory

Table II-4

Meteorological Instrumentation at Keck Laboratories

	Parameter	Instrument or Method	Sampling Rate	Period	Instrument Reference
1)	Mean Wind (Magnitude & direction)	Meteorology Research, Inc.	1 avg/hr (strip chart) 1 inst. /20 min tape punch	continuous	(7)
2)	Standard Deviation of Wind Direction	Meteorology Research, Inc.	same as above	continuous	(7)
3)	Temperature		1/20 min punch tape	continuous to Sept. 20	-
4)	Humidity		1/20 min punch tape	continuous to Sept. 20	-
5)	Net Radiation		1/20 min punch tape	continuous to Sept. 20	(8), (12)
6)	Aitken Nuclei	G.E. Continuous Counter	1/20 min punch tape or strip chart	intermittent operation with MAAS, and in October	(9)
7)	Cloud Condensation Nuclei	MRI diffusion counter		intermittent operation with MAAS, and in October	(10)
8)	Ice Nuclei	MRI Ice Nuclei Sampler	2 lit/min for 5 min	intermittent operation with MAAS, and in October	(14)

standard deviation of the wind direction will give a crude measure only of the dispersion capability of the atmosphere. Fluctuations, for example, can arise from a number of processes like eddy shedding from the parapet of the building which will be non-representative of the air boundary layer away from the building.

Both temperature and humidity were measured to characterize the thermodynamic state of the air mass in the Basin that was associated with local wind patterns. Care was taken to shield the thermometer mounted on the roof so that temperature observations should be reliable to within 1°C or less. Humidity was measured as relative humidity at the lower end of the sampling tube just upstream of the Minnesota Aerosol Analyzing System (MAAS). Therefore, care should be taken to correct the measured value to the outdoor temperature for any interpretation of the data requiring identification of atmospheric conditions.

The net solar radiation reaching the roof top was measured with an Epply pyroheliometer. This device is a standard one and should give reasonably accurate data for the total radiation received. For further discussion see, for example, Ref. (11). However, it gives no data for radiation received as a function of wavelength, which may be of use in detailed interpretation of the photochemistry involved in smog formation.

Aitken nuclei counts have only indirect bearing on meteorological phenomena. Nevertheless, these counts provide a measurement which appears to have some correlation with visibility and total aerosol loading. The monitoring with the G.E. Continuous Counter provided an independent estimate of the smog present and its variation, as well as being an integral part of the MAAS. The device's limitations are discussed elsewhere and will not be outlined further here.

Perhaps more relevant to the meteorology than Aitken nuclei are the condensation nuclei activated at low supersaturations of less than 1%. These "cloud" condensation nuclei associated with air pollution are of considerable interest now with respect to inadvertent weather modification and particularly, warm rain modification.

The production of ice nuclei from air pollution and particularly from automobile exhaust has been realized (Schaefer, 1968).(12) Although these nuclei may not appear to alter the formation of clouds and warm rain over the Los Angeles Basin, they may be very important to the physics of supercooled clouds downwind of Los Angeles. Rain and snow in the mountains ringing the basin and the activity of rain-producing clouds as far east as the Great Plains may be affected by these pollution particles (Hidy et al).(13)

To measure the "cloud" condensation nuclei a manually operated MRI Twomey-type diffusion chamber was used. Although the instrument is analogous to a Rich counter in operation, the MRI-Twomey device relies on supersaturation of diffusing water vapor between two moist plates at two different temperatures rather than expansion. Because of the curvature of the vapor pressure vs. temperature curve for water vapor, a small supersaturation, generally less than 1%, is achieved as a result of the differential transport of heat and water vapor between the two plates.

The MRI cloud condensation nuclei counter used in this study was of standard design, using visual detection of 30° forward scattered light from droplets formed in the supersaturation zone. After setting the temperature of the two moist plates to maintain a supersaturation at 0.3% to 0.7%, the observer uses a hand pump to flush the entry lines and chamber with fresh air. The chamber is closed, and after the sensitive region quiets down, the operator then counts visually the number of droplets visible in the zone of supersaturation. Several samples of air are counted for nuclei content in sequence. This constitutes one sample. A run required several to give a reasonable average value of nuclei counts.

The MRI-Twomey counter yields counts which agree qualitatively with the range observed in several different areas with characteristic air masses. However, the device is an experimental unit. As a result of manual operation of the device and an element of observer error, any correlation between cloud condensation nuclei and other aerosol measurements in this study will be qualitative only. More quantitative comparisons should be made, of course, in future experiments with newer improved instruments as they become available.

Because of difficulties with the cloud condensation nuclei counter, data over only two extended periods, August 21 and August 26, were obtained. Since the ice nuclei samples were of lesser interest, these were taken only on the same dates as the cloud condensation nuclei.

Ice nuclei were sampled by collecting the aerosol on a millipore filter and placing the filters in a specially designed diffusion chamber. After a period of time at a fixed temperature below 0°C, water saturation, crystals which have been grown in the chamber are counted on the filter surface. Sampling for ice nuclei was carried out using a millipore filter in a vacuum line for 5 minutes at a flow rate of 2 lit/min. This method has the advantage over all other ice nuclei counters in that the activation temperature and supersaturation can be controlled precisely.

Meteorological Data from Local Sources. In addition to the meteorological observation attempted at the Keck Laboratories, several parameters were recorded from local sources during the experiment. These are summarized in Table II-5.

The first two items were monitored largely to check the consistency with actual occurrences of these "interpretations" of available data by the local agencies. The items, 3 - 5, on which the LA APCD smog forecast is partly

Table II-5

Meteorological Parameters Available from Local Sources

Parameter	Period	Source
1) Forecast	once per day	USWB
2) Smog Forecast	once per day	LA-APCD
3) Oxidant Level	once per day	LA-APCD
4) Inversion Base	once per day	LA-APCD
5) Visibility	once per day	LA-APCD
6) Radiosonde (Temp., dew pt., surface winds up to 2000 meters altitude)	twice per day	USWB
7) Lidar sounding of inversion base	August 26, 28	Freeman Hall (McDonnell-Douglas)

based were of interest for comparison with daily observations, as well as giving an index of what sort of episodes to expect in scheduling longer duration operations of the aerosol counters.

In the Los Angeles area radiosonde soundings are taken twice daily from Los Angeles International Airport. These soundings give temperature and dewpoint as a function of altitude, with only surface winds. For the purposes of this study, only such data for the surface and up to altitudes just above the inversion base have been included since these are most relevant to our smog measurements.

Although the radiosonde observations provide a useful guide to the atmospheric structure on a meso-scale, they will not be entirely representative of local activity in Pasadena. Therefore, interpretation of the observations at Keck in terms of the mations of air over the Los Angeles Basin necessarily will be somewhat limited.

In parallel with our experiments, Dr. Hall and Dr. Ediger operated lidar sounding device at the lower reaches of San Gabriel Canyon. Dr. Freeman has found that the lidar can be used to trace the air motion near the San Gabriel Mountains by watching changes in back scattering from suspended particles. In addition he can deduce quantitative values of visibility from the lidar return which will be compared with nephelometer measurements and with direct measurements of size spectra using MAAS. Even though the lidar measurements were made only in late August, they nevertheless will be useful as supplemental, supporting data for main thrust of the experiment.

Acknowledgements

The following people were involved in this portion of the project and their efforts are acknowledged.

1. Paul MacCready (MRI)
2. William Green (MRI)
3. Walter Underwood (MRI)
4. T. Lockhardt (MRI)
5. Abdul Alkezweeny (MRI)
6. Len Doberne (CIT)
7. Freeman Hall (McDonnell Douglas)
8. Andy Moser (Autonetics-North American Rockwell)

Part of this portion of the project was supported by PHS Grant AP-00680-02.

REFERENCES

1. Fuller, L.J., R.L. Chass, and R.G. Lunche, Profile of Air Pollution Control in Los Angeles, Air Pollution Control District, Los Angeles County, (1969).

2. Neiburger, M. and J. Edinger, "Summary Report on the Meteorology of the Los Angeles Basin with Particular Respect to the Smog Problem", T.R. #1, Air Pollution Foundation, Los Angeles (1954).

3. Neiburger, M., N.A. Renzetti, and R. Tice, "Wind Trajectory Studies of the Movement of Polluted Air in the Los Angeles Basin", T.R. #7, Air Pollution Foundation, Los Angeles (1956).

4. U.S. Weather Bureau Tech. Paper #54, (1965).

5. Pack, D.H. and J.K. Angell, Monthly Weather Rev., 91, (1963).

6. Metzer, A.B. and W.L. Friend, Can. J. Chem. Eng., 36, 235 (1958).

7. Meteorology Research Inc., Manual: Wind Diffusion Recording System Model 2040, IM-112.

8. The Epply Laboratory, Bulletin No. 2.

9. General Electric Co., Instruction Manual - Condensation Nuclei Counter, GEI # 45069, Feb. 1967.

10. Fletcher, N.H., Physics of Rainclouds, Cambridge Univ. Press, 1962.

11. Kondratyev, K., Radiation in the Atmosphere, Academic Press, N.Y., Chap. 2 (1969).

12. Schaefer, V.T., "New evidence of inadvertant modification of the atmosphere", in Proc., of the 1st Natl. Conf. on Weather Modification, Albany, N.Y., April-May 1968, p. 163-172.

13. Hidy, G., R. Bleck, I. Blifford, P. Brown, G. Langer, JP. Lodge, Jr., J. Rosinski, and J. Shedlovsky, "Observations of Some Dynamical Properties of Aerosols over N.E. Colorado", NCAR TN.49.National Center for Atmospheric Research, Boulder, Colorado (1969).

14. Alkezweeney, A., "Ice nuclei measurement by millipore filter technique", Research Rept. No. 111, MRI Annual Report FY 1969, Ariz. Wx Mod Res. AOG to U.S. Bur. Rec., Denver, Colo., Contract # 14-06-D-6581.

SECTION III

MINNESOTA AEROSOL ANALYZING SYSTEM

1) Introduction - K.T. Whitby
2) Pump system, diluters, plumbing - M. Tomaides & R. Husar
3) Data Acquisition System - N. Barsic
4) Condensation Nculei Counter - N. Barsic & K.T. Whitby
5) Whitby Aerosol Analyzer - R. Husar & K.T. Whitby
6) Optical Particle Counter - B.Y.H. Liu

1. Introduction

The Minnesota Aerosol Analyzing System (MAAS) is probably the most complex set of apparatus that has ever been assembled to date for the in situ size distribution analysis of aerosols. Although our laboratory had been developing this system for a number of years, the system that was used in Los Angeles was new enough in many respects so that it took the best efforts of everyone in our laboratory to get it all working and to get it calibrated in time for the project. Because this system is unique and because it may well serve as the prototype for similar systems in the future, we have described it and its characteristics in considerable detail in this section.

We have discussed the calibration of all of the instruments in considerable detail and the calibration of the Whitby Aerosol Analyzer in particular detail because a knowledge of its performance and limitations is essential to several conclusions which will come out of this study. Although a fairly detailed calibration of the WAA had been made before the project, the calibration presented here was performed by R. Husar as part of his Ph.D. thesis after the project.

Although the accuracy of each instrument is discussed in detail in each part of this section, a summary and a few comments are given here.

a) Condensation Nuclei Counter

As used in L.A., the CNC reads 1.75 times the number read by the WAA. The latter is considered to be closer to the correct absolute number concentration. Because of losses in the connecting tubing and diluter, the smallest size sensed by the CNC is estimated to be 0.0035 μm.

b) Whitby Aerosol Analyzer

The maximum usable sizing range of the WAA is from 0.005 μm to 1.0 μm. However, in the L.A. study the instrument was used only over the range from 0.0075 to 0.4 μm. Estimated accuracy for calculating the number concentrations are as follows: 0.0075 μm ± 200%, 0.01 μm ± 100%, 0.04 μm ± 20% and for $D_p > .1$ μm ± 10%.

c) Optical Particle Counter

As operated in L.A., the OPC was used to count particles in the size range from 0.33 to over 6.8 μm. However, for reasons which are explained in part 6, only the count data from 0.4 to 6.8 μm was used. The last channel on the multichannel analyzer counted all particles larger than 6.8 µm. The instrument was calibrated against polystyrene latex so that the particle sizes will be correct only for aerosol particles having a refractive index of 1.6. The data indicates that the smog aerosols have considerable water associated with them so it is probable that the true refractive index of the smog aerosols was less than 1.6, perhaps as small as 1.4. If the true refractive index were 1.4, then the true particle size would be as much as 30% larger than that indicated. This would correspond to an underestimation by a factor of 2 of the number of particles in the optical range. It has therefore been estimated that the maximum error in the measured number concentration is about a factor of 2 and that the maximum error in size measurement is about 30%.

It should be noted that in the size range where the WAA and OPC overlap, the agreement between the dv/dD_p vs D_p curves calculated from the number data are ordinarily within a factor of two. This excellent agreement suggests that the absolute error in the particle concentration by number at a particle size of about 0.4 µm must be less than about ± 50%.

In view of the fact that the number concentration of the aerosol was found to vary from time to time by one to two orders of magnitude over most of the size range, it is considered that the MAAS accuracy and resolution was quite adequate to detect all significant changes in the aerosol over the size range from 0.0035 to 6.8 µm.

2. Pump system, diluters, plumbing

A schematic diagram of the piping system for the aerosol supply is shown in Figure I-2. Further information, besides the piping and instrumentation arrangement is contained in the rectangular boxes placed in the vicinity of distinct points of the system. The four numbers in each box correspond to the following specific information of the particular piping section: the flow rate in liters/second; the residence time of the aerosol from the time it entered the top of the main supply pipe to the point under consideration; the inside diameter of the pipe in cm; and the distance from the last marked distinct point of the piping system in cm.

The main purpose for giving the detailed specification of the flow rates, pipe diameters and distances, is to permit an estimation of the aerosol losses in the piping system. Although the system was designed to minimize aerosol and gas losses of O_3 and condensation nuclei, the loss was also checked experimentally as described later.

The smoggy air entered the piping system through a sampling cap placed on the top of the main sampling pipe, 6.7 meters above the roof of the three story building.

The cap itself included a screen (40 mesh) which had the purpose of preventing the entrance of small insects into the piping system because soon after the first experiments started, it was found that insects were transported along with the gaseous and particulate matter, deep into the system. Each insect, of course, was a potential cause of plugging and erratic readings. As a matter of fact, several of the initial impactor classification runs were ruined because of plugging of the impactor jets.

At the end of the main supply pipe, the aerosol was distributed through a manifold with five isokinetic probes to the various instruments.

The instruments located on the left of the main sampling pipe in Fig. I-2 are those for the monitoring of the chemical contaminants and several infrequently used aerosol instruments. The instruments for the aerosol size distribution measurements are on the right of the main supply pipe, consisting of the Whitby Aerosol Analyzer, the sensor unit of the Royco optical counter, two Lundgren impactors, GE nuclei counter, the Charlson-Ahlquist nephelometer, and the Meteorological Research Institute nephelometer. A flow rate of 7 l/sec through the main sampling stack was maintained by the high volume sampler blower. This air was discharged into the room after filtration. The high velocity through the sampling stack minimized the loss of O_3 and condensation nuclei. Tests made by comparing the O_3 concentration at the stack inlet with those measured by the instruments in place in the laboratory gave readings that were within about 10% of each other. This was within the estimated experimental error.

A similar comparison of the condensation nuclei readings at the stack inlet with those of the counter in its normal location in the laboratory gave an average penetration of 85%. This was considered to be near the experimental error. Since most of the losses would be of the smallest particles (e.g. those below 0.01 µm) the losses of particles in the WAA range are negligible.

No direct measurements of the losses of large particles in the system were accomplished. It had been hoped that comparisons of the results from the Noll impactor might provide an estimate of the accuracy of the MAAS on large particles. However, no useful data was obtained with the Noll impactor. Preliminary examinations of the data suggest that most of the time there were few particles above about 5 µ in the atmosphere at the sampling stack inlet location. For this and other reasons which will be discussed in more detail when the data is described in subsequent reports and papers, it is believed that the MAAS has provided an accurate measure of the particle concentration up to its upper limit of measurement of 6.8 µ.

All instruments for the gas analysis (see left hand side of the diagram, Fig. I-2) were supplied by the smoggy air through glass piping with rubber couplings. Glass was chosen for this purpose because of low adsorption activity of its surface for the gaseous contaminants.

The four instruments, the California Institute of Technology Particle Beam, the Liu Electrostatic Sampler, the Meteorological Research Institute (MRI) cloud nuclei counter, and the MRI ice nuclei sampler, were connected to the distribution manifold only temporarily with flexible plastic tubes of 1 cm in diameter.

In order to minimize the loss of large particles, the two Lundgren impactors were placed underneath the manifold as shown in Fig. I-2. The connection between the manifold and the impactors was made out of PVC pipe, 5 cm in diameter. Two impactors were used so that one could be prepared while the other was in use.

The wide range humidity sensor (Hygrodynamics, Inc.) and one of the temperature sensors (copper-constantan thermocouple) were installed at the end of the large T-branch of the manifold, as shown in Fig. I-2. This location was chosen because of the comparatively high flow rate at that point, and because of convenience of installation. The humidity sensor itself was placed in a bypass, the flow being generated by the stagnation pressure of a Pitot-tube arrangement, as shown in Fig. I-2. The time constant of this humidity sensing arrangement was checked out by rapidly switching the flow from outside air to room air and found to be on the order of one minute.

The end of the manifold where the humidity sensor and thermocouple were installed had a 2.0 meter long flexible connection of 3.8 cm I.D. to the high volume sampler.

Just before the high volume sampler, a branch of the flexible 3.8 cm diameter tube was conducted to the MRI nephelometer and then to the Charlson-Ahlquist nephelometer. The suction for both of the instruments was provided by a fan in the Charlson-Ahlquist instruments, so the MRI nephelometer was in line rather than on a separate branch, with an independent suction source. This arrangement was found to be necessary because the fan of the MRI nephelometer was not strong enough to pump air against the $\approx$ 2 cm of w.g. negative pressure that existed in the piping system. The negative pressure was mainly due to the pressure drop in the main supply line from the roof to the basement.

The aerosol supply for the WAA, Royco optical counter and for the GE nuclei counter was provided through a common flexible pipe directly from the main manifold. All aerosol connections of these instruments were kept short to minimize diffusion losses of small particles. The detailed dimensions and distances are indicated in the rectangular boxes in Fig. I-2.

All three instruments had separate in-line aerosol diluters. The highest required dilution was for the Royco sensor, with a total dilution of 1:100, accomplished by using two diluters in series, while for the nuclei counter a dilution of 1:12 was found to be sufficient. The main diluter, before the inlet of the WAA, was not used as a diluter because dilution was found to be not necessary and also because some difficulties arose with its operation.

The design of the passive in-line diluter used to dilute the aerosol for the optical counter and the condensation nuclei counter is shown in Fig. III-1. It is constructed from a Gelman No. 12100 membrane filter cartridge having a pore size of 3 µm. The only modifications to the standard filter cartridge are the installation of a short length of glass capillary tubing of about 0.5 mm I.D. in the center of the cap that closes the top of the filter and the insertion of a U-shaped piece of cardboard or metal in the outlet hose connector to mix the aerosol stream as it leaves. In this type of capillary leak diluter a small stream of aerosol passes through the capillary and is then remixed with the clean air that has passed through the filter. The dilution ratio can be changed by varying the capillary length and diameter. However, capillary diameters less than 0.3 mm I.D. should not be used. Also, it has been found that dilution ratios of more than 1/25 result in unacceptable variations of dilution ratio with particle size. Higher dilution ratios are obtained by using several diluters in series.

The dilution ratios of this type of diluter must be obtained by experiment. The ratios of the diluters used in this project were measured experimentally using polystyrene latex aerosols ranging in size from 0.55 to 2.8 µm using the Royco 220 optical counter as the particle sensor. Over the given size range, the dilution ratios were found to be independent of particle size. When these diluters are used in series at high dilution ratios the overall ratio of the combination must be checked to make sure that there is adequate mixing between stages. It is best to operate the diluters in a vertical position to minimize the losses of large particles.

Most of the instruments of the MAAS are equipped with their own internally located aerosol pumping system and were thus capable of independent operation when connected to the aerosol distribution piping. Only the operation of the WAA necessitated the use of externally located vacuum pump which would have been very noisy had it not been enclosed in a sound absorbing box. The box is about 22" x 23" x 33" in size, contains the oil free, rotary vane vacuum pump, Model 3, 1200 rpm, 13.9 scfm (Condé Milking Machinery Co., Inc.), WAA sonic jet charger, Unico high volume aerosol sampler with speed control, small compressor, axial cooling blower, and the system of valves and flow rate gages for the flow rate adjustment, as seen in Fig. III-2. The box can easily be transported with the aid of four swivel casters on the bottom, and all instruments within the box can be reached after removing the box lid. All control valves, switches, and gages can be operated from outside of the box.

3. Data Acquisition System

The large number of electrical signals from the many instruments used in this project were recorded with an automatic data aquisition system. This section describes the system, gives its specifications and presents its performance characteristics that are essential to interpreting the data recorded.

Data collected for the 1969 Los Angeles air quality project consisted of strip chart records, digital print-out, and punched tape. An important objective of data collection was to record data from many different experiments and correlate these data records on a common time base. In addition, it was desirable to have one complete set of data containing results from all experiments to facilitate correlation of data taken by different investigators.

Description of Data Acquisition System

The major data recording item was a Hewlett-Packard 2010-B data acquisition system. Included in this package was a 2901-A input scanner, a 2401-C digital voltmeter, a 2509-A digital clock, a 2545-A tape punch coupler, a 2545-B power supply, a 2545-C paper tape handler, and a 562-A digital printer. The major components of the data system are illustrated schematically in Figure I-3. In addition, the basic 2010-B system was purchased with a monitor option which permits stopping the scan on a given channel in order to take more than one reading.

A. Input Scanner

The major component of the data system is the input scanner. This device transfers analog voltage, current, or frequency signals to one set of measuring and recording equipment. Data points may be scanned continuously or upon local command. The remote command capability permits automatic data logging at intervals specified by the Hewlett-Packard 2509-A digital clock. Although the system is capable of measuring frequency, resistance and ac voltages, only the dc voltage measuring mode was used.

a. Monitor Mode

The input scanner is capable of recording 25 channels of data, however, a "monitor mode" option provides additional capacity. Inserting a diode pin in the "monitor mode" row of the patch board for any of the 25 channels permits more than one data signal per scan to be accepted by that channel. Upon reaching a monitor mode channel, the scanner records one reading on that channel and stops. A ground closure output (from -26v to ground lasting approximately 3 milliseconds) is presented at connector J 108. This signal is, in turn, presented to the sensing device (in this case the Whitby Aerosol Analyzer). Upon receiving this signal, the Whitby Aerosol Analyzer issues another ground signal lasting approximately 30 milliseconds to connector J 106 of the input scanner to initiate a successive reading on the selected monitor mode channel. Another ground closure at J 108 follows. This process continues as long as the Whitby Aerosol Analyzer issues ground closures to the scanner. Stepping to the next channel is accomplished when a 3 millisecond duration ground closure from the 2509-A digital clock is issued to J 107 of the scanner.

b. Measurement Delay

Each measurement requires a finite time delay to provide stabilization time for the dc amplifiers and ac measuring devices. The system provides 4 possible delay times ranging from 30 to 910 milliseconds. For all tests conducted at Pasadena, the 30 millisecond delay was used.

c. Specifications

Number of channels: 1 to 25 floating signal pairs with shields
Maximum voltage: 750 v peak or 500 v rms

Maximum frequency: Maximum recommended frequency through scanning switch is 300 Kc
Amplitude (volts, rms) times frequency should not exceed 10
Shunt capacitance: (Hi to lo) 100 pf
Crosstalk capacitance: (Between high or low of adjacent channels) 4pf
Leakage capacitance: (Signal circuit to chassis ground) 90 pf
Signal path resistance: (Input to output) less than 0.5 Ω
Leakage resistance: (Hi to lo or to chassis ground) 10 Ω minimum at 70% RH; 10 Ω minimum at 95% RH (up to 40°C)
Thermal offset: Less than 5 µv
Common mode rejection: 85 db at 60 cps, 100 db at dc (with up to 1000 Ω between source ground and voltmeter L_o)
Connectors: Cannon 3-pin, gold-plated
Source impedance: 68K ohms
Scan start: Circuit closure or -26 v pulse, 30 ms wide (from 2509-A digital clock)
Scanning speed: recording: 85 ms per channel, minimum
skipping: 30 ms per channel

d. Channel Assignments

All channels listed below recorded one data signal except number 25. Sixteen signals were recorded in monitor mode on this channel.

Channel Number	Signal	Signal Range
1	Pyroheliometer	0-10 millivolts
2	Wind direction	0-5 volts
3	Wind deviation (direction)	0-5 volts
4	Wind speed	0-5 volts
5	Roof temperature	0-10 millivolts
6	Sampling line temperature	0-10 millivolts
7	Aerosol analyzer temperature	0-10 millivolts
8	Relative humidity	0-10 millivolts
9	OPEN	
10	Date code	0-100 millivolts
11, 12, 13	OPEN	
14	Ozone-Atlas	0-100 millivolts
15	Ozone-Mast	0-100 millivolts
16	NO - Atlas	0-100 millivolts
17	NO_2 - Atlas	0-100 millivolts
18	OPEN	
19	U of W, 675 nm	0-10 volts
20	U of W, 546 nm	0-10 volts
21	U of W, 436 nm	0-10 volts
22	U of W, 360 nm	0-10 volts
23	MRI Nephelometer	0-1000 millivolts
24	Condensation nuclei counter	0-10 millivolts
25	Whitby aerosol analyzer	0-10 volts

B. Digital Voltmeter

a. General Description

After data signals are received by the input scanner, they are diverted to the digital voltmeter. This is an all solid state electronic instrument capable of measuring dc potentials up to ± 1000 volts. There are 5 voltage ranges. the lowest full scale range, ± 0.1 volts, permits high-resolution millivolt measurements. In addition, the voltmeter is capable of frequency measurements from 5 cps to 300 Kc. A nixie tube display indicates the measurement in six digits in addition to the polarity and units being measured.

Digital coding available at the DVM is 4-2'-2-1 binary coded decimal (bcd) for recording on the digital printer and for further digital data processing. For this particular system, the data coding was further altered to teletype ASKI 33 for recording on punched paper tape.

b. Specifications

i. Circuit type: floated and guarded signal pair
ii. Ranges: 5 ranges from 0.1 v to 1000 v full scale
iii. Overranging: Overranging to 300% of full scale is permissible on all but the 1000 v scale
iv. Input impedance: 10 M on 10, 100, 1000 v ranges
1 M on 1 v range
100 K on 0.1 v range
Impedance is within ± 0.02% of nominal value in all ranges
v. Internal calibration source: ± 1 volt internal standard provided for self-calibration. Voltage reference is derived from specially aged, temperature stabilized zener diode, with guaranteed drift of less than ± 0.006% in 6 months.

C. Digital Clock

a. Purpose

The 2509-A digital clock was necessary to provide a time base for correlating data and to provide remote control signals required by the data system. For example, data recording by the digital printer and paper tape punch required control through the digital clock. Also, a scan cycle through the 25 channels could be initiated at desired time intervals specified by the digital clock. Finally, the aerosol analyzer required the use of a digital clock since data recorded in "monitor mode" required a timed pulse to initiate stepping to the next channel.

b. Description

The 2509-A digital clock is an all electronic precision instrument that accumulates time in seconds and presents it in hours, minutes, and seconds in 24 hour cycles. The time output is visually displayed in 2 digits of hours, 2 digits of minutes, and 2 digits of seconds on nixie tubes and is presented digitally in bcd 4-2'-2-1 at an output terminal at the rear of the instrument.

The digital clock also generates a train of pulses for system timing (timing monitor mode duration) and control purposes. A group of block-out latching push buttons on the front panel controls the pulse repetition rate. Intervals are available every one second, ten seconds, one minute, ten minutes, and one hour. A system option provides a thumbwheel switch with 9 multiplication positions (1-9) which, when combined with the 5 latching push buttons, provides additional timing flexibility.

Since the clock must keep an accurate time record and provide time signals for recording by the data system, the clock must operate independently of the recording system, without the need for synchronization. This is possible since the 2509-A allows time recording at any instant and allows any time reading to be held for as long as 9,998 milliseconds for recording purposes without any loss of time.

c. Specifications

Circuit reference: All voltage levels are referred to chassis ground.
Time reference: (Internal) Derived from power line frequency (60 cps standard)
Accuracy: Equal to time reference, +0, -1 second (non-accumulative)

D. Output Coupler

The bcd, 4-2'-2-1, information from the dvm and digital clock must be transferred to both the paper tape punch unit and the digital printer. In its standard form the 2545-A output coupler accepts 10 characters of externally supplied parallel bcd information and translates this to IBM 8-level code. A system modification translated this bcd information to Teletype ASKI-33 code so that the paper tapes could be processed on a standard Teletype shared time terminal.

E. Data Recording

This device, made by the Teletype Corporation (model BPRE High Speed Tape Punch Set) is designed to rapidly perforate paper tape for data storage and subsequent processing. It must be used with the above mentioned 2545-A output coupler and a power supply (2545-B). In the current configuration ASKI-33 code is punched for direct processing on a Teletype shared time terminal.

The data is also printed simultaneously on paper tape.

F. Physical Electronic Connections

Figure 2 is a schematic of the laboratory in which the 1969 Los Angeles air quality measurement study was made. Electronic cable routing and instrument locations are emphasized here. Equipment locations were the result of optimizing the allowable space and component functions.

a. Gas Analysis Equipment

All gas analysis instruments were located along the south wall of the laboratory (see Fig. III-3). The gas analysis devices that were read by the data system were: two ozone monitors, one NO sampler, and one NO_2 sampler. These instruments were owned by the State of California, Air and Industrial Hygiene Laboratory. The NO_2, NO, and one ozone monitor were made by the Atlas Electric Devices Company, 4114 North Ravenswood, Chicago 60613. The other ozone sampler, Mast, model 724-11, was from the Mast Development Company, Davenport, Iowa. All four devices are standard, commercially available shelf items.

Data from the Mast-ozone analyzer were recorded on a 0-10 mv strip chart recorder. A parallel data signal was recorded on the Hewlett-Packard data system whenever particle size distributions were being recorded. This instrument was connected to channel 15 of the data system through a 2 - conductor cable.

Channel 14 accepted the Atlas-ozone data. A two conductor plus shield cable was used for this application because signals from this instrument were easily affected by noise. Connections were as follows:

shield: Atlas case to #1 terminal of data system input
low: Atlas - to #2 terminal of data system input
high: Atlas + to #3 terminal of data system input

Channel 16 accepted the Atlas - NO signal through a 2 conductor plus shield cable as discussed above. Connections were the same as above except for the addition of a 25 µ fd capacitor attached across the + and - connections of the dymec. The capacitor was necessary in order to obtain a smooth data signal.

Channel 17 carried the Atlas - NO_2 signal. Connections were the same as for channel 16, including the 25 µ fd capacitor.

b. Particle Size Distribution Measurements

All equipment for measuring particle size was located in the northwest corner of the laboratory, as illustrated in Fig. III-3.

Particle size data from the Whitby Aerosol Analyzer were recorded on channel 25 of the data system. Signals were transmitted through a RG/58 cable and one scan was recorded once each 10, 20, or 30 minutes, depending on the experiment being conducted. All cables between the aerosol analyzer and the data system were RG/58 type with the conductor mated with the "high" or #3 pin of the data system input, and the shield tied to both the "low" and "ground" pins of the data system input.

Three electrical connections are necessary between the Whitby Aerosol Analyzer and the data system. The first connection is necessary to notify the aerosol analyzer that channel 25 has been reached by the data system, and a particle size analysis cycle should begin. A second signal then notified the data system to accept data from the aerosol analyzer. This command signal is carried via a similar cable connecting the "DVM read command" terminal at the rear of the aerosol analyzer to terminal J 106 of the data system. Finally, particle size data are transmitted from the "output" terminal on front of the aerosol analyzer to channel 25 of the data system.

G. Optical Particle Counter

Particle size data determined by the Royco PC 220 optical counter were recorded on punched paper tape and printed on paper by a teletype typewriter and tape punch. Signals were carried via a special multi-conductor cable connecting the teletype to a Hewlett-Packard 5415-A analog to digital converter and related electronics (Hewlett-Packard 5431-A display, 5421-A digital processor, and Royco 170-1 pulse converter). This group of equipment received data signals from the Royco PC-220 optical sensor and command signals from J 83 of the data acquisition system.

H. Total Nuclei Counts

Total particle concentration data were determined by a General Electric Condensation Nuclei Counter. These data were recorded continuously on a Hewlett-Packard Mosely 680 strip chart recorder, and periodically on channel 24 of the data system.

I. Nephelometer Data

Light scattering data were recorded by two nephelometers located in the northeast corner of the laboratory. Channels 19 through 22 of the data system recorded light scattering information from the University of Washington nephelometer. The following table indicates the signal carried on each channel. Data from the MRI (Meteorological Research Institute) nephelometer were recorded on channel 23.

Channel	Wavelength
19	675 nanometers
20	546 nanometers
21	436 nanometers
22	360 nanometers

J. Recording Time Sequence

Data signals for the first 24 channels were all recorded within 2 minutes (approximately 90 ms per channel and 20 channels). At the end of this scan the electrical particle counter began operating for a duration of approximately 4 minutes. The optical particle counter began counting when the record command was received by channel 1 of the data system, and continued counting for 10 minutes. After this 10 minute period, the data stored by the optical system were recorded on the teletype unit. A summary of the recording sequence appears in the sketch below.

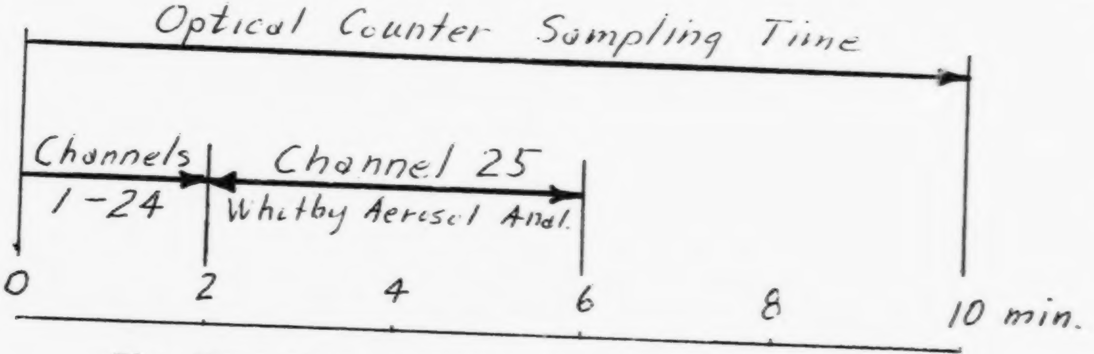

Fig. III-4 Data acquisition system recording sequence

K. Meteorological Data

Meteorological data were recorded on channels 1 to 5 of the data system via 5 pairs of 200 foot long shielded cable (provided by the Cal Tech Physical Plant). These cables carried one temperature, one pyroheliometer, and three wind signals.

L. Miscellaneous Signals

Temperature for the Whitby Aerosol Analyzer flow system was determined by a thermocouple located in the aerosol line between the three-foot cylindrical flow chamber and the collection filter. This temperature signal was carried by a 2 conductor plus shield cable and originated at a copper constantan junction, as were all thermocouples used for the project.

Sampling line temperature was recorded at the humidity sensor located at the laboratory end of the atmospheric aerosol stack. Relative humidity was also sampled here, however, after 10 September, 1969, the thermocouple was eliminated and the relative humidity measurements were made at the aerosol analyzer inlet.

4. Condensation Nuclei Counter

A standard General Electric, Cat. No. 112 L428 G 1 Condensation Nuclei Counter, Skala 1963, was used to measure the total particle concentration. Catalogue specifications for this instrument are: Theoretical lower limit of detection 0.002 μm diameter, count ranges 0-300, 0-1K, 0-3K, 0-10K, 0-30K and 0-100K linear ranges and 1M and 10M non-linear ranges, response time 2 sec., and sampling rate 6 l/min. The fluctuations of the CNC output were damped somewhat by the installation of a 1000 μF 6 volt condensor connected across the recorder output.

Four years of experience with this counter plus numerous comparisons with other particle counting instruments have shown the following characteristics and problems.

a) Factory calibrations are good only within about a factor of three. Absolute calibration of these counters is difficult and must be made by comparison with some other counter. The counter used in this study was overhauled by General Electric just before the study and was used with their calibration. The G.E. calibration is traceable to the calibration of Pollack. The only method which we have available to calibrate the CNC is to compare it with the WAA on aerosols for which the entire size range of the aerosol is within the counting range of the WAA. Such comparisons were made from data on smog aerosols during the project under conditions where coagulation had removed many of the particles below about 0.01 µm. Such conditions occurred several times during the night. These data for the CNC and the WAA are compared in Fig. III-5. It is seen that the CNC reads about 2½ times the WAA.

After the MAAS was returned to the University of Minnesota after the project, further comparisons of the CNC and the WAA on laboratory aerosols and atmospheric aerosols having no particles below 0.01 µm yielded a ratio of 1.75. From these comparisons we have concluded that the CNC reads about 1.75 times the WAA. The night time aerosols probably contain some particles below the range of the WAA, thereby giving a higher ratio than with the laboratory aerosols. This is the figure that is being used in comparing the data from the two instruments. Because as is explained in part 5 below, we have reason to believe that the number concentrations calculated from the WAA have greater absolute accuracy, the CNC concentrations reported are the measured values divided by 1.75.

b) The minimum particle diameter sensed by CNC's is usually greater than that calculated from the Thompson-Gibbs equations for the expansion ratios used because of diffusion losses of particles in the plumbing conveying the aerosols to the instrument. At the 8 inches of Hg underpressure used, the CNC should count all particles larger than about 0.002 µm diameter. However, it is estimated that with the inlet tubing and the diluter capillary will remove most particles smaller than about 0.0035 µm. Thus where a lower limit for the CNC must be assumed as for the calculation of dN/dD_p for the size interval below the lower limit of the WAA, the lower size of detection for the CNC is assumed to be 0.0035 µm.

c) Comparisons of particle counts using a diluter and the linear scales in comparisons with counts on the non-linear scale without the diluter have shown that the non-linear scales are very inaccurate. For this reason, almost all of the data was taken using the linear scales and the 1/12 diluter. On only a few occasions did the CNC concentration exceed the 1.2M limit of this combination. Most of the time the CNC was operated on the 0-100 K scale with the 1/12 diluter.

5. Whitby Aerosol Analyzer (WAA)

The aerosol size distribution in the diameter range between 0.0075 µm and 0.6 µm was measured with a modified commercial model 3000 Whitby Aerosol Analyzer (WAA)*. In the present section, the principle of its operation is reviewed and the main components of the instrument are described, including the modifications made on the standard commercial instrument. Particular emphasis is placed on the discussion of the calibration procedure and results since the present calibration was more elaborate and detailed than the earlier calibrations of the instrument. Finally, estimates of the accuracy of the WAA are given as a function of particle size.

Principle of Operation

The electrical mobility of a charged particle i.e. the ratio of the particle velocity to the applied electric field acting on it, is a function of the particle size. In a proper electrical and flow field, therefore, particles of different sizes may be classified according to their electrical mobility. For diffusion charging and for particles less than 1.0 µm in size (diameter) the electrical mibility is a monotomically decreasing function of the particle size and it varies only slightly for sizes larger than 1.0 µm. Accordingly, for particles less than 1.0 µm in diameter, the electrical mobility is uniquely related to the particle size. If diffusion charged particles are then introduced into an electrostatic precipitator through a point or line source, the precipitation distance increases with increasing particle size.

The Whitby Aerosol Analyzer (WAA) as described by Whitby and Clark (1966) was developed starting with the ideas and findings as stated above. The objective of their work was to extend these findings and to combine them in such a way that the number of particles in different size ranges could be measured by properly varying some of the parameters of the system. The five years of work on the development of the instrument resulted in the following arrangement and measuring procedure.

The aerosol first enters a jet-charger, (fig. III-6) especially developed for this purpose, where the charging results from the fast mixing of uncharged particles with high concentration of negative ions, generated on a corona needle. The physical mechanism of charging is governed by molecular diffusion and in a small part by the existing electrical field in the charger vessel.

As a result of the prevailing diffusion charging, the particles leaving the charger vessel are charged such that the number of elementary charges on a particle is approximately proportional to its diameter, D_p.

The aerosol leaving the charger is then introduced into the precipitating tube, as an annular cylinder surrounding a core of clean air. The aerosol collector, a metal rod, passes axially through the center of the tube. Depending on the voltage on the collecting rod, all particles with an electrical mobility exceeding a certain value will be collected on the precipitating rod, while those with smaller mobility (larger size) pass through the precipitation section and are then collected on an absolute filter.

---

*Manufactured by Thermo-Systems, Inc., St. Paul, Minnesota 55113

The absolute filter itself is electrically connected to a sensitive electrometer, which measures the total current due to the charges given up by the particles collected on the filter. A step increase of the rod voltage will cause particles of a larger size range to be precipitated with the resulting decrease of the filter current.

The number of particles ΔN, in a given size range ΔD_p, corresponding to the current change ΔI may be calculated from the known values for the mean number of elementary charges per particle, the flow rate and the fraction of particles lost by space charge and diffusion.

The aerosol size distribution in the size range between 0.075 μm and 0.6 μm is obtained by scanning the precipitation voltage from 225 volts (for 0.075 μm) to 14,000 V (for 0.6 μm) in 15 steps, measuring the corresponding currents on the electrometer and then, using the calibration curve, converting the voltage vs. current curve to a discrete (14 point) size distribution curve.

To allow the new particle trajectories in the precipitation tube to stabilize, the times between two consecutive voltage steps have to be kept sufficiently long. These times range from 30 seconds at the lowest voltage to 12 seconds at the highest voltage, the time required for the entire cycle being about four minutes.

The scanning cycle for a size distribution measurement is controlled by an internal timing system that also commands a digital read out for the current before each step to a higher voltage. With a digital voltmeter connected to the electrometer of the WAA, the size distribution measurement can be fully automated and the system is then suitable for monitoring time-dependent aerosol size distributions. A more detailed discussion of the electrical and timing arrangement for the Minnesota Aerosol Analyzing System (MAAS) that includes the WAA is discussed in part 2 of this section of this report.

Modifications made on the standard commercial instrument

The main components of the WAA were subjected to extensive experimental and numerical investigations as well as to changes in design and operating conditions before the instrument was shipped from Minneapolis to Los Angeles and after its return.

First, in a numerical investigation, Whitby et al. (1969) Section IV, the flow field and particle trajectories in the precipitator section of the WAA were studied with the ultimate objective of reducing the geometrical and hydrodynamical distortion effects on the quality of size classification. As a result of this numerical study, the ratio of the aerosol and clean air flow rates was reduced from 1/31 to 1/14. This reduced the standard deviation of the mobility classification from $\sigma_g = 1.4$ to $\sigma_g = 1.18$ (for $D_p = 0.5$ μm).

In Section V of the same report, Whitby et al. (1969), the results of experimental studies on the performance of the WAA are discussed, with particular emphasis on the effect of aerosol flow rate and the aerosol concentration on the resolution of the instrument. The optimal ratio of aerosol/clean air flow was found to be 1/14 at a total flow rate of 2.12 l/sec (4.5 cfm). The aerosol concentration was found to affect the level and quality of the charging only slightly, if the total current due to the deposited charged aerosol was between 2 x 10-12 and 50 x 10^{-12} Amp.

In a further series of experiments (unpublished) aerosol losses due to diffusion and space charge in the charger were investigated. The results indicated that the losses in the charger depend strongly on the particle size and on the aerosol flow rate, decreasing in magnitude with increasing particle size and increasing flow rate. For particle size of 0.08 µm for instance, the aerosol penetration through the original 22 l charger was found to be 20% at an aerosol flow rate of 0.15 l/sec (optimal flow rate for the classification) and increased to 40% at a flow rate of 0.5 l/sec.

A significant reduction of the aerosol losses in the system was achieved by replacing the charger vessel of the standard instrument which had a volume of 22 liter, with a much smaller, 1.7 liter vessel. The new cylindrical charger vessel is 7.5 cm in diameter and 34.0 cm long with its axis coinciding with the jet axis. The aerosol exit is placed radially on the cylindrical vessel, 3.0 cm from the jet entrance (Fig. III-6). The penetrations for a particle size of 0.08 µm with the small charger vessel were 58% at an aerosol flow rate of 0.15 l/sec and 70% at 0.5 l/sec. The increase in the aerosol penetration is attributed to the reduction of the aerosol residence time in the small vessel. In a highly recirculating flow field, such as the jet-driven recirculation in the larger charging vessel, the aerosol is forced several times to the vicinity of the walls before it leaves the vessel. In the small vessel, this contact time is reduced, by that reducing both the diffusion and space charge losses. The jet entrance and the primary aerosol mixing section of the charger remained unchanged.

There were also several minor changes and adjustments made on the electrical circuit of the standard model 3000 TSI instrument.

First, it was found that the stepping of the lower to a higher voltage on the collecting rod occurred simultaneously with the read command to the digital voltmeter. This caused a distorted current reading. The interaction was eliminated by inserting a time delay of about 0.2 seconds between the read command and the subsequent voltage stepping.

In the intermittent cycling mode, the instrument automatically scans through the 15 voltages, then returns to zero voltage and awaits the pulse from the digital clock to start a new cycle. In a further modification, a switch was installed which permitted the selection of either a zero or 15 Kv voltage, for the time period when the instrument was standing by awaiting the pulse for a new cycle. With the added choice of 15 Kv in the stand-by position, the instrument could be used for size distribution measurement, let's say every hour (for four minutes that is needed for the scanning) while for the rest of the time it would be classifying the aerosol on the rod. This mode permits then the correlation of size distribution data with those obtained by classification.

The scanning times between the steps 1 through 6 were found to be too short, so that the corresponding currents were not stabilized before the next voltage step occurred. Accordingly, the time between first and second step was prolonged from 23 seconds to 30 seconds, then the step between 2 and 3 from 20 to 25 and those between 3 and 6 from 15 to 22 seconds. The stepping times for the remaining steps were unchanged at 12 seconds.

The stepping voltages were adjusted according to the newly calculated calibration curve discussed in the following paragraphs.

Calibration of the Whitby Aerosol Analyzer

After the main components of the WAA had been restudied and the necessary modifications made, the instrument was calibrated before its use in L.A. However, the calibration for sizes smaller than about 0.02 μm was still inadequate primarily because of the lack of good monodisperse aerosols smaller than 0.02 μm.

After the return of the instruments to Minnesota, Mr. Husar made a more thorough calibration as part of his Ph.D. thesis work. Means were found to generate adequately monodisperse aerosols smaller than 0.02μm. The principal effect of the recalibration was to change the constants for sizes smaller than 0.03 μm. The new calibration has been used in all data reduction.

The calibration required the determination of two parameters as a function of particle size, namely the average number of charges carried by a particle and secondly the fraction of particles lost in the system.

The complexity of the instruments' geometry and of the flow field did not permit a sufficiently accurate theoretical prediction of the fraction of particles lost in instrument. The losses (or the penetration) therefore had to be determined experimentally.

The average number of charges on a particle as a result of diffusion charging was studied by several investigators both theoretically and experimentally and it can be predicted with fair accuracy if the so called $N_o t$ product is known, where N_o is the number concentration of ions and t is the time the particle spent in the ion cloud. In the presently used jet-charger, however, neither the ion concentration nor the time the particle spent in the ion cloud is known with sufficient accuracy to permit accurate calculation of the $N_o t$ product. Furthermore, for particles less than about 0.05 μm in diameter, a fraction of the aerosol escapes charging entirely, so that the average charge, based on the total number of particles, may be less than unity. For this latter charging range the available theory is only applicable for the free molecular regime and experimental data to test its validity are missing entirely. For the above stated reasons an experimental determination of the average number of charges seemed most desirable.

In order to arrive at a fair estimate on the size resolution of the WAA, not only the mean number of charges n_p, but also the charge spectrum had to be investigated at several different sizes. Such data for the ion-jet diffusion charger were not available prior to this study.*

An experimental determination of the penetration P, and of the level of charging n_p, for particles below 0.1 μm presented considerable difficulties since several of the techniques used here had to be developed for this particular study.

The experimental procedures to determine the two parameters, P and n_p, are discussed in the following section.

The Average Number of Charges n_p and the Charge Distribution on Particles

The average number of charges and the charge distribution on particles of different sizes were determined from the distribution of their electrical mobilities. The electrical mobility Z_p is defined as

$$Z_p = n_p \cdot e \cdot B \qquad \text{(III-1)}$$

where n_p is the number of elementary charges carried by the particle, e is the elementary electron charge, 4.8×10^{-10} stat coul. and B the fluid dynamical mobility. The electrical mobility of the singly charged spherical particle Z_{ps} depends only on the properties of the fluid surrounding the particle and on the particle size, D_p.

The electrical mobility of an arbitrarily charged particle is most easily determined from the deposition distance, x, in an electrostatic precipitator. For an annular type of precipitator with the inner tube (with radius r_1) charged oppositely from the charge of the aerosol, and with particles entering the precipitator at the outer tube radius r_2, the following relation holds for the mobility:

$$Z_p = \frac{Q_t \ \ln(r_2/r_1)}{2\pi x V} \qquad \text{(III-2)}$$

where Q_t is the total flow rate and V is the precipitation voltage. Combining (III-1) and (III-2), the number of charges may be obtained from the following relationship:

$$n_p = \frac{Z_p}{Z_{ps}} = \frac{3 \ \mu_g D_p Z_p}{C \ e} \qquad \text{(III-3)}$$

where μ_g is the gas viscosity and C the Cunningham slip correction.

The electrical mobility distribution as a function of particle size was determined by two methods: First, monodisperse Polystyrene Latex (PSL) was charged and deposited on the central rod and counted on optical microscope and secondly, polydisperse methylene blue particles were classified on the rod and the mobility distribution was obtained from size-selecting electromicrograph counts.

---

*The charge spectrum for diffusion charged particles is presently being investigated in considerable detail analytically and experimentally in our laboratory.

PSL Classification Runs

The mean electrical mobilities, and the mobility distribution for 0.5 μm and 0.365 μm PSL particles were obtained by collecting the PSL particles on the black painted rod and then counting the number of particles collected on a unit area of the rod.

The PSL aerosol, generated by a Collision atomizer, was first passed through a radioactive neutralizer (Kr-85, 1 mc) and then through two diffusion batteries connected in series. The first in the line was a glass bead diffusion battery (a 5 cm diameter, 50 cm long tube filled with 0.3 cm glass beads) and as a second battery, a 1000 cm^3 silica-jel air dryer was used. With the two batteries in line, small particles from the PSL suspending liquid were eliminated by diffusion and larger agglomerates were precipitated by interception and impaction.

The concentration distribution on the rod with 16 Kv precipitating voltage is shown in Fig. III-7. The experimental points, circles for 0.5 μm and squares for 0.365, are fitted with log-normally distributed mobilities (solid line) in order to obtain the mean and standard deviation of the mobility spread. Both concentration distributions could be closely fitted with a logarithmic standard deviation of, $\sigma_g = 1.18$ while the mean mobilities, $\bar{Z}_p$ were 6.15×10^{-4} cm^2/sec, V, and 6.78×10^{-4} cm^2/sec, V, for 0.5 μm and 0.365 PSL respectively. By eqn. (III-3) the number of elementary charges were calculated as $\bar{n}_p = 25.0$ for 0.5 μm PSL and $\bar{n}_p = 19.5$ for 0.365 μm PSL.

In a previous work, Whitby et al. (1969), it was pointed out that the mobility spread obtained by the above discussed method is the result of two major factors, namely the charge distribution of particles and hydrodynamic distortion effects. There is experimental evidence, Whitby et al. (1969), that the hydrodynamical distortion effects are small compared to the effect of the charge distribution.

The mean number of charges and charge distribution for 0.075 μm and 0.125 μm particle diameter was determined by selective electromicrograph counts of atomized 0.1% methylene blue particles, collected on the rod. In order to obtain statistically representative counts, the size interval for the selective counts was chosen to be between 0.075 μm and 0.1 μm. The measured distribution is shown in Fig. III-7. The indicated dispersion is partly due to the charge distribution. The mobility spread shown in Fig. III-7 corresponds to $\sigma_g = 1.28$ but it is estimated that the actual spread of n_p for 0.075 μm particles (and not for the size interval 0.075 μm to 0.1 μm) would be at most $\sigma_g = 1.25$ with a mean charge of $\bar{n}_p = 3.9$.

The four values obtained for mean number of charges is in close agreement with previously obtained data, Whitby & Clark (1967), Whitby et al. (1969). For the charge spectrum of jet-diffusion charged aerosols, however, no data are available for comparison.

The experimental points for $\bar{n}_p$ as a function of particle size are shown in Fig. III-8 along with the fraction of particles charged, discussed in the following paragraph.

Figure III-9 shows the measured electrical mobilities $\bar{Z}_p$, as a function of particle diameter.

Fraction of Particles Charged

When particles of less than 0.1 μm are charged by a conventional diffusion (or field) charger, a fraction of the particles will escape the charger vessel without acquiring a single charge, i.e. without colliding with a negative ion.

Since for size distribution measurements the concentration of particles in a given size range is calculated from the current due to the particles giving up their charge, it is of basic importance to know the mean number of charges, with respect to the total number of particles, charged plus uncharged.

The fraction of particles charged was determined by passing relatively monodisperse aerosol through the charger and analyzer sections and then measuring the concentration of particles penetrating to the collecting filter, Fig. III-6. The concentration was then measured twice, first with no voltage on the rod so that particles, charged plus uncharged, would penetrate to the collecting filter and the second time with high (15 Kv) voltage on the rod such that all the charged particles would be collected and only the uncharged would penetrate to the collecting filter. The ratio of the number of particles penetrating the analyzer section with high voltage on the rod to the total number at zero voltage is the fraction of particles that are not charged.

The most difficult part of the calibration procedure was to find proper test aerosols in the size range around 0.01 μm. Fast diluted, combustion generated aerosols were found to serve surprisingly well for this purpose. By controlling the aging process in a proper way, the size of the aerosol could be varied by a factor of ten (0.005 - 0.05) still retaining adequate monodispersity.

The test aerosols up to 0.05 μm number median diameter (NMD), were produced by aging propane torch aerosols in a 4.5 m^3 mylar bag (fig. III-11). For .007 μm NMD aerosol, the propane torch was inserted for about 2 seconds in the glove box, Fig. III-11, where it was diluted in the first stage and subsequently transported to the nearly filled mylar bag. After a short mixing period the aerosol was ready for calibration purposes.

The larger aerosols were obtained by inserting the propane torch for longer periods in the glove box to grow the particles by reinforced coagulation. For 0.05 μm NMD aerosol, the torch was inserted for 5 minutes. Polydispersity was reduced by aging the aerosol for 30 minutes to eliminate the small particles. The size distribution of the test aerosol was measured before every calibration run.

All of the concentrations were measured with the General Electric condensation nuclei counter, since for the calibration only relative concentration measurements were required. For such measurements the linearity of the instrument's reading was important rather than the absolute concentration it indicated. The linearity of the GE CNC was established in a series of experiments using different type of diluters.

The monodispersity of the aerosol was evaluated by running a current I vs. voltage V curve before every test. The steepness of the I (V) curve was taken as a measure for the monodispersity of the aerosol. If the I (V) curve for a run was not steep enough, the run was rejected and a new aerosol was generated. The particle size was determined using the median voltage to calculate the mobility according to formula (III-1) and with the known mobility from Fig. III-9, the particle size was obtained.

The geometrical mean particle size for $D_p < 0.03$ μm was also measured by the diffusion battery method described by Fuchs, Stechkina and Storoselskii (1962). The mean aerosol sizes obtained by the two methods agreed within ten percent. Further details on this comparison are given by Husar (1971).

The results of the test for the fraction of particles charged, f, are shown in Fig. III-10. At about 0.06 μm practically all the particles carry at least one elementary charge but at 0.025 μm practically all the particles carry at least one elementary charge but at 0.025 μm only 50% of the particles are charged, the fraction decreasing rapidly to 15% at 0.01 μm.

The data for the mean number of charges $\bar{n}_p$ and for the fraction of particles charged are plotted on the same figure, because it is believed that such a presentation permits a more useful interpretation of the data. If the mean number of charges is defined as the mean with respect to the total number of particles, charged or uncharged, then for f less than about 0.2, n_p and f are equal. This follows from the low probability that there will be double-charged particles if $f < 0.2$. Using this observation, the n_p and f curves may be joined as shown in Fig. III-8. This approach appears to be useful for obtaining reasonably accurate mean n_p in the size range $0.01 < D_p < 0.05$ where the discrete nature of the charge distribution makes such an estimate otherwise rather difficult.

Figure III-8 also yields some information about the charge distribution in the size range between 0.01 μm and 0.04 μm. Let us consider for instance the probable charge distribution at 0.02 μm: the fraction of particles charged is 0.4 while the mean number of charges $n_p = 0.5$. This means that 10% of the particles must carry double charge in order to have a mean charge of 0.5. Intuitively, it is suggested that the fraction of particles carrying three charges is negligible. Accordingly, the charge distribution at 0.02 μm would be: 40% uncharged, 50% singly charged, 10% double-charged. Similar estimates are made for 0.03 μm and 0.04 μm NMD.

Figure III-12 presents the estimated cumulative charge distributions for several particle sizes between 0.01 μm and 0.075 μm. Since the mobility analyzer detects only charged particles, the cumulative charge distribution in Figure III-12 are normalized with the number of charged particles instead of the total number used for n_p.

The standard deviations σ_g of charging from 0.075, 0.125, 0.365 and 0.5 μm particles were obtained from microscope and electron-micrograph counts discussed on p. 43. The measured ($D_p > 0.075$ μm) and estimated ($D_p < 0.075$ μm) geometric standard deviations of charging are shown in Fig. III-13. The σ_g (charging) vs. D_p curve in Fig. III-13 was used to construct the discrete charge distributions for $D_p > 0.075$ μm in Fig. III-12. The objective of these intuitive estimates as well as the charge distribution measurement for larger sizes is to obtain data which can be used to calculate the size resolution as a function of particle size.

The main features of the curves, plotted in Fig. III-12 is the obviously discrete nature of the charge distributions, particularly for the size range $0.01 < D_p < 0.1$ μm and secondly that the number of charges are nearly log-normally distributed on particles. This latter property of the charging was used to show the "quality" of the charging in Fig. III-13 where the logarithmic standard deviation of the charge distribution σ_g is plotted vs. D_p. The σ_g for $D_p = 0.02$ μm was estimated to have an equivalent geometric standard deviation of $\sigma_g = 1.17$ for the discrete, two point distribution (single and double-charged particles only).

For particles less than 0.01 μm the σ_g of the charged particles is unity since the particles either carry a single charge or no charge at all. Accordingly there is no charge distribution (on the charged particles) and the electrical resolution of the instrument is perfect. The σ_g of charging increases rapidly to 1.29 at 0.04 μm which corresponds to the greatest electrical dispersion of the size resolution. For $D_p > 0.04$ the σ_g slowly decreases to about 1.18 at 0.365 μm and .5 μm. In a later paragraph on the size resolution of the WAA, Fig. III-13 will be related directly to the size-classification ability of the instrument.

With the known mean number of charges on the particles, the particle mobility vs. D_p may be constructed, using the known values of the singly charged particles and eqn. (III-3). The derived Z_p vs. D_p curve is shown in Fig. III-9.

Diffusion and Space Charge Losses in the System

Simultaneously with the experiments for the evaluation of the fraction of particles charged, the aerosol losses were also determined. In a similar manner as described in the previous paragraph, the concentration of monodisperse particles was measured at the aerosol entrance to the WAA, 1, Fig. III-6, after the charger, 2, and then at the collecting filter, 3. The ratio of the concentrations 1 and 3, corrected by the dilution ratio for the clean air core, gave the fraction of particles penetrating through the system, P, which is plotted in Fig. III-10. The ratio of the concentrations 1 and 2, also corrected by the fraction of clean air introduced by the jet, gave the losses in the charger alone.

The aerosol losses to the walls of the system were caused mainly by Brownian and turbulent eddy diffusion, space charge and image force on the unipolarly charged mixture of aerosol particles and ions. For the separation of the diffusion and space charge losses the assumption is made that the two mechanisms are mutually independent. This assumption is not strictly correct, but for the determination of K itself the separate contributions are not important as long as the total loss is known and that can be measured accurately. As a matter of interest, most of the losses occurred in the charger section where there is high turbulence level and recirculation. The measured penetration curve, along with the fraction of particles charged, is shown in Fig. III-10.

Evaluation of the Calibration Constants

With a knowledge of the previously discussed parameters, namely the electrical mobility, mean number of charges, and the fraction of particles lost in the system, one can calculate the constants which are used to transform the current vs. voltage curve into a particle size distribution curve.

The differential current ΔI between two voltage steps is $\Delta I_m/P$, where ΔI_m is the measured current and P the penetration through the system. The number of particles ΔN, in a discrete size range (corresponding to a voltage range) is calculated from the relationship:

$$N = \frac{\Delta I_m}{P\, q_a\, \bar{n}_p\, e} \tag{III-4}$$

where q_a is the aerosol flow rate, $\bar{n}_p$ is the mean number of elementary charges in the size range under consideration, and e is the unit electron charge.

In order to set the 15 voltage steps, the size intervals were chosen(with approximately equal $\Delta \log D_p$) using the mobilities obtained from Fig. III-9, and the precipitating voltages were calculated from eqn. (III-2). The selected size intervals for the size range between 0.0075 μm and 0.6 μm, the n_p and P values as well as the resulting calibration constants are listed in Table I.

In the course of this work it was found that the size distributions of coagulating aerosols around 0.01 μm NMD, were very narrow. For a typical size spectrum in that range, the use of the calibration data of Table I would give only four points in the aerosol size spectrum. In order to obtain more detailed information for the smaller sizes, a second calibration table was prepared which covered the size range between 0.004 and 0.033 μm.

The same calculation procedure that was used to prepare the range 0.0075 to 0.6 μm was applied, except that for the range $D < 0.070$ μm, no experimental data being available, the data for P and n_p were extrapolated. The precipitating voltages for this range of operation were set manually.

In Table 2 the corresponding size intervals, voltages, and calibration constants are listed.

The Resolution of the WAA and Error Estimates

In this paragraph, an attempt is made to interpret the available calibration data in terms of the WAA's resolution. The particular question of interest for this study is to what degree the measured size distributions are distorted as a result of non-ideal classification characteristics of the instrument.

First, the factors limiting the WAA's resolution, namely the shape of the mobility curve, the hydrodynamic distortion effects and the charge distribution are discussed and subsequently numbers are given for the errors involved.

The inherent limit for the use of the WAA as a classifier is given by the vanishing dependence of the electrical mobility on particle size for $D_p > 1.0$ μm (see Fig. III-9). The particle size dependence of the electrical mobility decreases to essentially zero for $D_p > 1.0$ because in eqn. (III-1) the number of elementary charges is $n_p \sim D_p$ while the fluid dynamic mobility approaches $B \sim D_p^{-1}$. Accordingly in that size range and for diffusion charging ($n_p \sim D_p$) particles with different sizes cannot be classified according to their electrical mobility. From these considerations and further error estimates, the upper size limit for the WAA was set to 0.6 μm.

The second factor affecting the size classification of the instrument is hydrodynamic distortionl due to: 1) the finite width of the aerosol sheet entering the precipitation section, and 2) axial non-uniformities of the flow field in the annulus.

In an earlier work, Whitby et al. (1) it was demonstrated that by reducing the aerosol/clean air flow rate ratio the hydrodynamic distortion effects may be reduced to a small fraction of the charging effects. The effect of flow distortions was neglected.

The third and most significant factor limiting the resolution of the WAA is the charge distribution on the aerosol, discussed on page III - 18. The WAA sizing resolution will now be derived using recently acquired experimental data on the aerosol charge distribution and the aerosol losses in the instrument. The effect of the instruments imperfect sizing resolution on the smog aerosol spectra measured in Los Angeles are calculated and discussed.

If we denote the charge distribution function as $f(n_p,D_p)$, noting that $f(n_p,D_p)$ is a log-normal distribution defined by the mean charge $\bar{n}_p(D_p)$, Fig. III-8 and $\sigma_{gn_p}(D_p)$ show in Fig. III-13. The distribution function $f(Z_p,D_p)$ for the electrical mobility is related to $f(n_p,D_p)$, for simplicity written as $f(n_p)$, by the transformation

$$f(Z_p)dZ_p = f(n_p)dn_p \qquad \text{(III-5)}$$

and using eqn. (III-1)

$$f(Z_p) = f(n_p)\cdot \frac{1}{e\,B} \qquad \text{(III-6)}$$

Attention may now be directed to Fig. III-14 which shows the mobility distribution $f(Z_p)$ as it changes with particle size. We also recall that the instrument classifies particles according to their mobility and that between two voltage steps it cuts out a band (shadowed in Fig. III-14) from the Z_p-D_p plane. If we follow the shadowed area it is evident that instead of sharp size cut-out at the mean of the stochastic distribution there is a particle distribution that satisfies the criterion of constant Z_p. The smaller size particles at a constant Z_p are the ones carrying "less than average" charge and the larger ones in the collected particle population are those charged by "higher than average" number of charges.

In the presently used data evaluation a mean charge $\bar{n}_p$ is assigned to each mobility band and the aerosol number spectrum, $g(D_p)$ for unit flow rate is calculated from the relationship:

$$\Delta I = K\cdot\bar{n}_p\cdot e\cdot g(D_p)\,\Delta D_p \qquad \text{(III-7)}$$

where ΔD_p is determined from the voltage step to calculate ΔZ_p by eqn. (III-2) and the Zp vs. D_p figure (Fig. III-9) is used to obtain the corresponding ΔD_p.

The accuracy of the presently used data evaluation may be tested by constructing a mathematical model which takes into consideration the charge (and mobility) distribution as well as the size dependent losses in the system. In the following, a numerical experiment is presented which in judgment of the authors could be easily adapted to the resolution analyses of other size distribution measuring instruments such as the single particle optical counters, Coulter counter, etc.

Referring to Fig. III-14 the current carried by the particles in a given mobility interval, dI/dZ_p, is made up of the contributions from different sizes, and it can be expressed by the following integral:

$$\frac{dI}{dZ} = \int_0^{\infty} K(D_p)\cdot f(Z_p)\cdot n_p\cdot e\, f(D_p)\,dD_p \qquad \text{(III-8)}$$

The product $f(Z_p)\cdot n_p\cdot e$ denotes the amount of charge carried by a particle of size D_p and mobility Z_p. The number of charges n_p is obtained from eqn. (III-1) with known D_p and Z_p. The true aerosol distribution function is $f(D_p)$ and K accounts for the losses in the system and for the uncharged fraction as shown in Fig. III-10.

We note that eqn. (III-8) which was used to calculate the "apparent" size spectrum $g(D_p)$ may be written as

$$\frac{dI}{dZ_p} = K\,\bar{n}_p \cdot e \cdot g(D_p)\,\frac{dD_p}{dZ_p} \qquad \text{(III-9)}$$

Equating the left hand sides of eqns. (III-8) and (III-9) we obtain an integral equation which relates the apparent distribution $g(D_p)$ and the true distribution $f(D_p)$:

$$g(D_p) = \frac{dZ/dD_p}{K \cdot \bar{n}_p \cdot e} \int_0^\infty K \cdot f(n_p)\frac{n_p}{B}\, f(D_p)\, dD_p \qquad \text{(III-10)}$$

Solution of the above integral equation for $f(D_p)$ would, in principle, permit the determination of the true size distribution.

A simpler procedure for the error estimate is to insert a known, say log-normal size distribution for $f(D_p)$ and to observe the difference between $f(D_p)$ and $g(D_p)$.

This latter method was used to obtain $g(D_p)$ for log-normal $f(D_p)$ with $\sigma_g = 1.02$ and $\sigma_g = 1.35$ and for mean sizes 0.03 and 0.1 μm. The results of the numerical experiment are shown in Fig. (III-15) on a log-probability plot. Essentially monodisperse aerosols, $\sigma_g = 1.02$ are indicated by the instrument as size distributions of $\sigma_g = 1.22$ and $\sigma_g = 1.21$ for 0.03 and 0.1 μm respectively. Aerosols with $\sigma_g = 1.35$ are also distorted on the lower and the upper ends but their geometric standard deviation is essentially preserved in the main portion of the distribution. There is in addition a systematic shift to smaller D_p for the "apparent distributions", which may be attributed to the polydisperse ($\sigma_g > 1.35$) small ($D_p < .02$) aerosols used for the calibration of the instrument. This is in accordance with the observation that for $\sigma_g = 1.35$ the number median diameters are closer to the true NMD than for $\sigma_g = 1.02$. For $\sigma_g = 1.7$, which is typical for the Los Angeles smog aerosol, the difference between the indicated spectra $g(D_p)$ and the true spectra is small. The principal difference is a less than 10% shift in mean size. These data are shown as a dotted line in Fig. (III-15).

The above discussion of the size resolution of the WAA suggests that the Los Angeles size spectra evaluated by our procedure does represent a close approximation of the true size distributions.

6. Optical Particle Counter

A single-particle optical counting system was used to measure the size distribution of aerosol particles in the size range between 0.33 and 6.8 μm. the system, consisting of a Royco PC 220 optical sensor, a Royco 170-1 pulse converter, a Hewlett-Packard 5400A multi-channel analyzer and a Teletype printer, is shown schematically in Figure I-3. A special diluter was placed at the sensor inlet to reduce the particle concentration by a factor of 100 and to a level acceptable to the system.

The system was operated automatically and was programmed to measure the aerosol size distribution for a period of 10 minutes at periodic intervals. At the end of each 10 minute measurement period the data were recorded automatically on printed and punched tapes by the Teletype printer. The command signal to begin each measurement cycle was provided by the digital clock which also started the data acquisition system by which other data were recorded. Thus a precise time correlation of all recorded data could be obtained.

The lower sizing limit of the system is approximately 0.33 μm. The upper sizing limit, corresponding to the saturation level of the preamplifier in the optical sensor, is approximately 6.8 μm. Thus no sizing information was obtained for particles larger than 6.8 μm, although these particles were counted by the instrument. The size distribution data were spread over 58 channels in the multi-channel analyzer, giving an average size increment of 0.11 μm per channel.

Optical Sensor

Except for the modification described below, the sensor used, a Royco* model PC 220, is a standard commercial instrument of the 90° scattering type. The operating principle of the sensor is well known. As each particle passes through the illuminated sensing volume, it scatters a pulse of light which is detected by the photomultiplier tube. The output from the sensor is in the form of voltage pulses, each approximately 100 μs wide. The amplitude of a pulse provides a measure for the particle size.

The sensor was operated at the standard flow rate of 2.83 liters per minute (0.1 cfm). According to the manufacturer, at a particle counting rate of 5000 particles/sec, the loss of particle count due to coincidence is approximately 10%. This corresponds to a particle concentration of 106 particles/cc at the standard flow rate of 2.83 liters/min.

In order to improve the resolution of the sensor, the standard inlet tube of the sensor was replaced with the sheath-air inlet tube shown in Fig. III-9. In the sheath-air inlet tube, part of the sample drawn in is by-passed through an absolute filter. The particle-free air thus obtained is reintroduced as a clean air sheath around the unfiltered sample and the combined stream then enters the illuminated viewing volume where the particles are counted. Of the 2.83 liters/min total sample drawn in by the sensor, 2.36 liters/min is by-passed through the filter, while the remaining 470 cc/min is unfiltered. Thus the effective sampling rate of the instrument, on which measurement is made, is reduced from 2.83 lpm to 0.470 lpm using the sheath-air inlet.

---

*Royco Instruments, Inc., 141 Jefferson Drive, Menlo Park, Calif. 94025

The sheath-air inlet was used primarily because it was found that the light intensity in the sensor viewing volume was quite non-uniform and that by confining the particles to a smaller diameter stream the sensor output, when sampling a monodisperse aerosol, could be made considerably more uniform, thus greatly improving the resolution of the sensor. With this modification the sensor was found to have a resolution of approximately 10% in terms of particle diameter (see Fig. III-15).

In addition to improving the resolution of the optical sensor, the sheath-air inlet has the following effects upon the operating characteristics of the sensor: (a) As discussed previously, the effective rate of flow of the aerosol on which measurement is made is reduced from 2.83 liters/min to 470 cc/min. While a disadvantage for such applications as clean-room monitoring where the particle concentration is low and a higher counting rate can produce a given statistical counting accuracy in a shorter time, this is not a problem for such a concentrated aerosol as the smog. In fact, with the sheath-air inlet, the maximum particle concentration acceptable to the sensor is increased. Theoretically, for the same coincidence loss of 10% the acceptable particle concentration is increased to (2830/470)(106) = 638 particles/cc by means of the sheath-air inlet. Unfortunately, the Royco 170-1 pulse converter imposes an additional limit on the system and the maximum particle concentration acceptable to the system is considerably lower than what the sensor can accept. (b) The calibration of the sensor, i.e. the relationship between particle size and pulse amplitude, is affected by the sheath-air inlet. This shift in calibration is apparently due to the change in the average light intensity in the illuminated area of the viewing volume as the diameter of the stream containing the particle is reduced. (d) With the sheath-air inlet, aerosol particles can no longer spill into the cavity surrounding the viewing volume as they do with the regular inlet. This has the effect of reducing the sensor response time from the order of 1 minute to what may be described for all practical purposes as instantaneous response.

Diluter

A two-stage series diluter was used to reduce the particle concentration of the smog aerosol by a factor of 100 and to a level acceptable to the optical counter. Each diluter stage consists of an absolute filter (Gelman Model 12103) punctured with a small capillary tube. The capillary tube, approximately 0.61 mm in diameter and 2.5 cm or 5 cm long, serves as a controlled "leak". A mixing baffle at the outlet of each diluter stage insures that the particles are uniformly mixed before entering the next diluter stage or the optical sensor. The design of the diluter is shown in Fig. III-1.

The series diluter was calibrated with a monodisperse latex aerosol. The aerosol concentration was first measured without the diluter and then with the diluter in series with the optical sensor. The dilution factor, as calculated from the ratio of aerosol concentrations thus determined was found to be independent of the size of the latex aerosol within the size range of the latex aerosol, 0.5 to 1.97 μm, used in the calibration. It was found also that the dilution factor thus determined was sensibly the same as the value calculated using the flow rates through the filter and the capillary.

Pulse Converter

The Royco 170-1 pulse converter provided the necessary electronic interface between the optical sensor and the Hewlett-Packard 5400A multi-channel analyzer. Its function can best be described with reference to Fig. III-10.

The sensor output, shown as A in Fig. III-17, is in the form of a voltage pulse approximately 100 μs wide. The amplitude of the pulse is a measure of the particle size. This pulse is amplified and held at its peak by the pulse converter. Curve B shows the pulse converter output, which is applied to the input of the multi-channel analyzer. The pulse converter, after detecting an incoming pulse at its input, and after a suitable interval of delay, then issues a "gating" pulse to the multi-channel analyzer, shown as curve C, causing the latter to read the voltage present at its input at that particular instant. The delay time is variable and can be set by a front panel control to one of the following values: 50, 100, 200, 400 and 800 μs. The delay time used for a specific optical sensor must be sufficiently long to insure that the incoming pulse has already reached its peak at the time when the gating pulse is issued. However, it was discovered, and for reasons still unknown to us, that the pulse converter would occasionally issue two gating pulses after it was triggered. The problem was especially severe when the delay time used was short. At a delay time of 400 μs, however, this double pulsing phenomenon was not observed. For this reason, a constant delay time of 400 μs was used in all these experiments.

A baseline voltage can be established in the pulse converter to prevent the converter from being triggered by the noise in the incoming signal. However, the actual baseline voltage used does affect the amount of dilution required for the aerosol. In these experiments the baseline voltage used was such that particles with an "equivalent latex sphere diameter" of 0.33 and smaller did not trigger the converter. With this baseline voltage it was found that a 100 to 1 diluter was adequate for the range of particle concentrations encountered in the smog. However, had the baseline voltage been lowered to, say, a level corresponding to an equivalent latex diameter of 0.165 μ, which is still possible considering the noise level in the instrument, the concentration of particles above the minimum triggering level would have been increased by an approximate factor of $(0.33/0.165)^3 = 8$, assuming that the size distribution in the optical range is given approximately by the Junge distribution. Thus a diluter with a dilution ratio of 800 to 1 would have been required. For this reason, the baseline was not set to a lower level, even though it was possible to do so from the standpoint of the noise level that was present in the signal.

In using the pulse converter in an optical counting system such as the present one, two additional effects must be considered which further limit the maximum rate at which particles can be counted. One such effect is the increased coincidence loss due to the dead time in the converter. As the converter is triggered by an incoming pulse, there is a certain period, the dead period, t_d, during which the arrival of another pulse at the converter input would not be regarded by the converter as a separate pulse. Since the arrival of pulses at the input of the converter is a random phenomenon, the loss of particle count due to this finite dead time can be calculated by the Poisson law

$$P(x) = \frac{\text{Exp}\ (-f\ t_d)(f\ t_d)^x}{x\ !} \qquad \text{(III-11)}$$

where P(x) is the probability that x pulses will arrive at the converter during the time interval, t_d, and f t_d is the average number of pulses arriving during this same time interval, t_d. Here, f is the mean rate at which pulses arrive at the converter input, or the average rate at which particles are counted by the system. Since there is no coincidence loss only when x = 0, the fraction loss of particle count due to coincidence is therefore,

$$\delta = 1 - \exp\ (-f\ t_d) \qquad \text{(III-12)}$$

For the pulse converter, the dead time, t_d, is approximately equal to the delay time, which was set to 400 µs in these experiments. Therefore, at a coincidence loss level of 10%, the maximum particle counting rate would be 250 particles/sec, or an equivalent particle concentration of 32 particles/cc at the aerosol flow rate of 470 cc/min.

A second, and a more serious effect, is one that could have been avoided, perhaps with a better converter circuit design. It was discovered that as the count rate exceeded approximately 10 counts/sec, the dc level of the converter output was depressed, causing the apparent pulse amplitude to decrease, since the pulse amplitude was measured from the ground level. This had the curious effect that as the count rate exceeded approximately 10 counts/sec there would be a shift of particle count from a higher to a lower channel, in the multi-channel analyzer, corresponding to an apparent decrease in the particle size. With the system operating under the standard conditions normally no counts should appear below channel 10 since this is the first channel above the minimum trigger level of the pulse converter. This was found to be indeed the case when the count rate was below approximately 10 counts/sec. However, as the count rate exceeded this limit counts would begin to appear, first in channel 9, and then in channels 8, 7, etc. as the count rate continued to increase. For this reason, data in channels 7, 8 and 9 were also recorded during these experiments. They serve as a useful index for determining whether the count rate limit of the converter was exceeded. Although there were a few instances when the smog was very heavy and this count rate limit was exceeded, the effect on the overall accuracy of the data was not considered to be serious. The particle concentration corresponding to a count rate of 10 counts/sec is 1.28 particles/cc for an aerosol flow rate of 470 cc/min.

The input-output (transfer) characteristics of the pulse converter were determined by calibration with simulated pulses of a trapesoidal shape produced with a Tektronix Model 115 pulse generator. The repetition rate of the pulses were kept low to insure that the output dc level of the pulse converter was not depressed. Input and output pulse amplitudes were measured with the multi-channel analyzer. The results are shown in Figures III-18 and III-19 which also include a detailed specification of the shape of the calibrating pulses used.

D. Multi-Channel Analyzer

A Hewlett-Packard Model 5400A multi-channel analyzer was used to measure and record the amplitude distribution of the pulses from the converter. Its operation will not be described here as this information is available in the technical literature published by the company.*

For the present application, the instrument was operated on the "sampled voltage analysis" mode. In this particular mode of operation the instrument measures the instantaneous voltage at its input and registers one count in the appropriate channel upon receiving a gating pulse at the input gate. It was not possible to measure the pulse amplitude directly in the "pulse height analysis" mode because the maximum rise time permitted for this particular mode of operation is 12.6 μs, which is considerably shorter than the rise time of the pulses produced by the optical sensor.

E. System Calibration and Performance

A prime system calibration is needed in order to determine accurately the relationship between the size of the particles and the corresponding channels in which the counts are registered. The calibrating procedure consists of feeding a monodisperse latex aerosol of a specific size to the optical sensor and recording the corresponding pulses with the multi-channel analyzer for a specific interval of time. Results of such a calibration performed in Minneapolis are shown in Figure III-20 . A complete system calibration was performed again after the system was installed in the Keck Laboratory in Cal. Tech. The results are shown in Figure III-21. If these results are compared it will be seen that they do not completely agree, indicating that there is a shift in the system calibration. This shift in system calibration was found to result from the slight damage the optical sensor suffered during its shipment from Minneapolis to Pasadena. The optical system in the sensor was realigned upon its arrival in Pasadena.

In operating the system, it was decided to chose a specific set of conditions as standard and to operate the system under these standard conditions over the entire experimental period. The standard conditions chosen are as follows.

---

*Hewlett-Packard Co., 1101 Embarcadero Road, Palo Alto, Calif. 91604.

Optical Sensor: 2.83 liters/ min total flow
470 cc/ min aerosol flow

Pulse Converter: Coarse Gain = 2
Fine Gain = 0
Baseline = 0
Delay time = 400 μs

Multi-Channel Analyzer: Input sensitivity = 10 volts into 128 channels
Baseline = 0
Data output: channel 7 to 68

The system calibration was checked twice with monodisperse latex aerosols of 0.5 μm during the entire experimental period. The system was found to retain its calibration well during this period.

The prime system calibration was performed only with monodisperse latex aerosols of five different sizes, 0.36, 0.5, 0.79, 1.305 and 1.97 μm. The manufacturer provides a calibration curve relating particle size and pulse amplitude for the 200 sensor up to a diameter of 5 μm. However, this curve, shown in Figure III-14, does not agree with our calibration of the sensor after the sheath-air inlet modification. If we assume that the ratio of the pulse amplitudes for two different sized particles is given correctly by Figure III-14 for our sensor, then a calibration curve can be constructed for our system up to a particle diameter of 5 μm. Curve B in Figure III-22 is constructed on this basis using the actual system calibration point at 1.97 μm as a base, and the pulse amplitudes ratio as determined from Figure III-14. However, if we assume that the pulse amplitude is proportional to the square of the particle diameter for particles of 1.97 μm and larger, then curve C is obtained. Since the true calibration of the system is not known above 1.97 μm, it was decided that data reduction would be done on the basis of the straight line relationship, shown as curve A in Figure III-22. This straight line is given by the equation

$$D_p = 0.11\ (N - 7) \qquad \text{(III-13)}$$

where D_p is the particle diameter in μm and N is the corresponding channel number. It is hoped that this question will be resolved in the future as we make further calibration studies on the optical counting system. However, it should be noted that the difference in particle diameter as determined from these three curves is less than 28% in the range, 1.97 μm to 6.8 μm, where actual calibration data are not available.

The size distribution data in the first channel, and the last few channels of the system are not reliable for the following reasons. According to equation (3), the first channel, i.e. channel 10 has a nominal particle size of 0.33 μm, and a nominal interval width of 0.11 μm. On a relative percentage basis, both of these values could be in substantial error. Further, as the signal to noise ratio is decreased with reducing particle size, the pulse amplitudes resulting from a monodisperse aerosol would show an increased spread as the noise voltage becomes increasingly significant compared to the signal voltage. Thus some of the pulses would fall below the trigger level of the pulse converter, causing only a fraction of the particles to be counted. Therefore the counting efficiency should be less than 100% for this first channel. The data in the last few channels of the system (channel 68 is the last channel in which counts were registered) are difficult to interpret because all particles larger than the minimum size needed to saturate the preamplifier are registered there.

E. Effect of the Refractive Index of Particles

Since the current practice in calibrating optical counters is to use monodisperse latex spheres as the standards of calibration, we wish to propose that the size of a particle measured with an optical counter should strictly be referred to only as an "equivalent latex sphere diameter". Here, the equivalent latex sphere diameter of a particle is defined as the diameter of a latex sphere that produces the same response in the optical counter as the particle under consideration. The use of equivalent diameters in the science and technology of aerosols is quite common. Familiar examples include the Stokes diameter, the aerodynamic diameter, etc.

The equivalent latex sphere diameter of a particle generally depends on the optical design of the optical counter and for counters of a specific optical design, it is also a function of the size, the shape and the optical properties of the particle. Since the majority of the smog particles are probably liquid drops, they are probably all spherical in shape. Therefore, the equivalent latex sphere diameter for a spherical particle with various indices of refraction is of interest in interpreting the data obtained in the present study.

Figure III-15 shows the relationship between the geometrical size of a spherical particle and its equivalent latex sphere diameter for various refractive indices. The curves are constructed according to theoretical results presented by Hodkinson* for the Royco PC 200 sensor whose optical design is similar to that of the 220 sensor. The refractive index of the smog aerosol is not known. However, if it is within the range of 1.4 to 1.8, then the ratio of the geometrical size to the equivalent latex sphere size varies from a maximum of 1.5 to a minimum of 0.9, with the mean ratio being on the order of 1 over the size range of our measurements.

---

*Hodkinson, J.R. and J.R. Greenfield, "Response calculations for light scattering aerosol counters and photometers", Applied Optics 4:1463-1474 (1965)

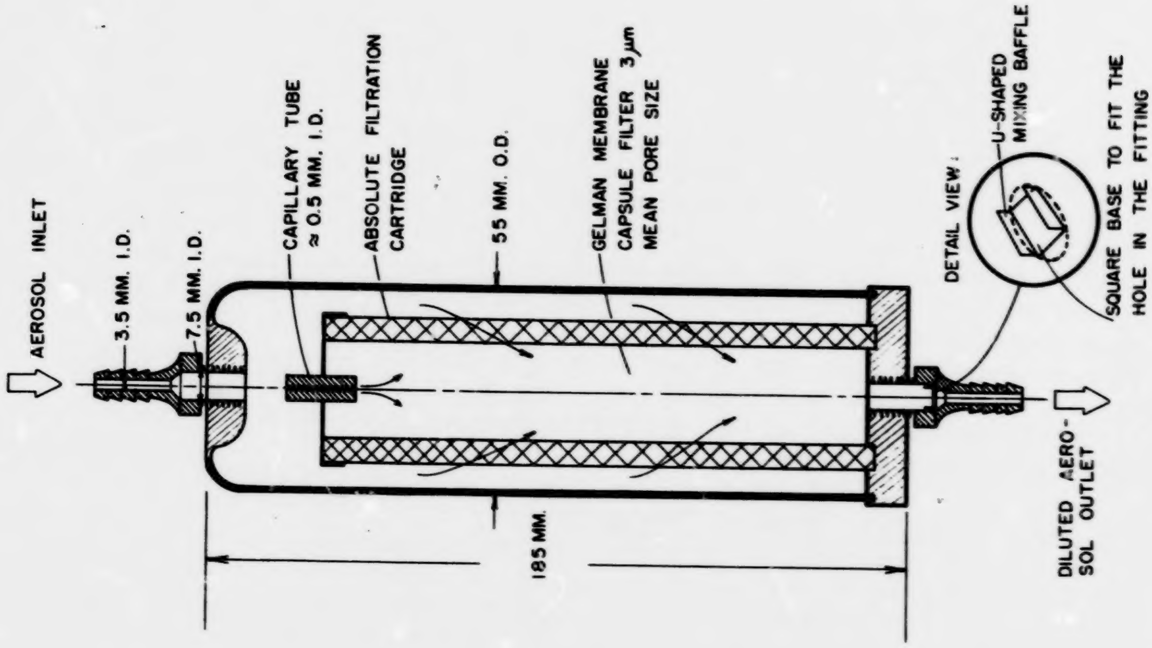
AEROSOL INLET
3.5 MM. I.D.
7.5 MM. I.D.
CAPILLARY TUBE ≈ 0.5 MM. I.D.
ABSOLUTE FILTRATION CARTRIDGE
55 MM. O.D.
GELMAN MEMBRANE CAPSULE FILTER 3 μm MEAN PORE SIZE
DETAIL VIEW:
U-SHAPED MIXING BAFFLE
SQUARE BASE TO FIT THE HOLE IN THE FITTING
185 MM.
DILUTED AERO-SOL OUTLET

Figure III-1 In-line passive diluter used on the condensation nuclei counter and optical counter.

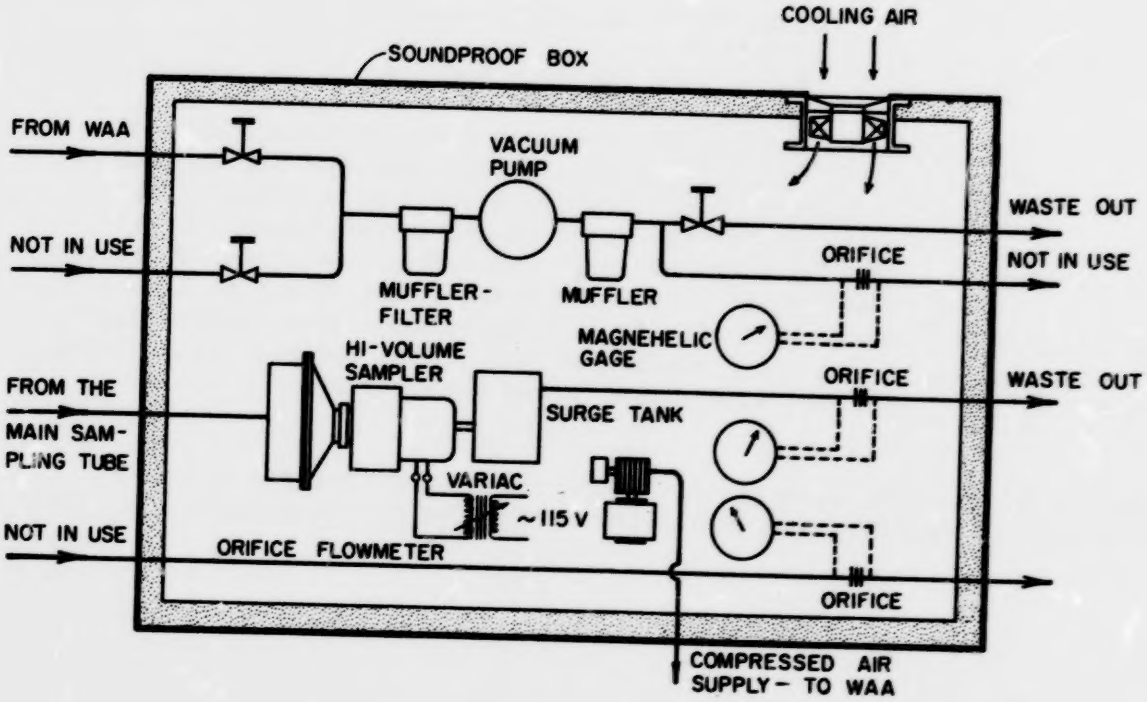
SOUNDPROOF BOX
COOLING AIR
FROM WAA
NOT IN USE
VACUUM PUMP
MUFFLER-FILTER
MUFFLER
WASTE OUT
ORIFICE
NOT IN USE
MAGNEHELIC GAGE
HI-VOLUME SAMPLER
FROM THE MAIN SAMPLING TUBE
ORIFICE
WASTE OUT
SURGE TANK
VARIAC
~115 V
NOT IN USE
ORIFICE FLOWMETER
ORIFICE
COMPRESSED AIR SUPPLY - TO WAA

Figure III-2 Schematic of the air handling box used for the MAAS instruments.

Channel Number	Equipment
1	Pyrohelicmeter
2-4	Wind Instruments
5	Temperature
6	Temperature
7	Temperature
8	Relative Humidity
9	open
10	Date Code
11-13	open
14	Atlas - O_3
15	Mast - O_3
16	Atlas - NO
17	Atlas - NO_2
18	open
19-22	Univ. of Washington Nephelometer
23	MRI Nephelometer
24	G.E. Nuclei Counter
25	Whitby Aerosol Analyzer

-----Data Signal

-·-·-·-Control Signal

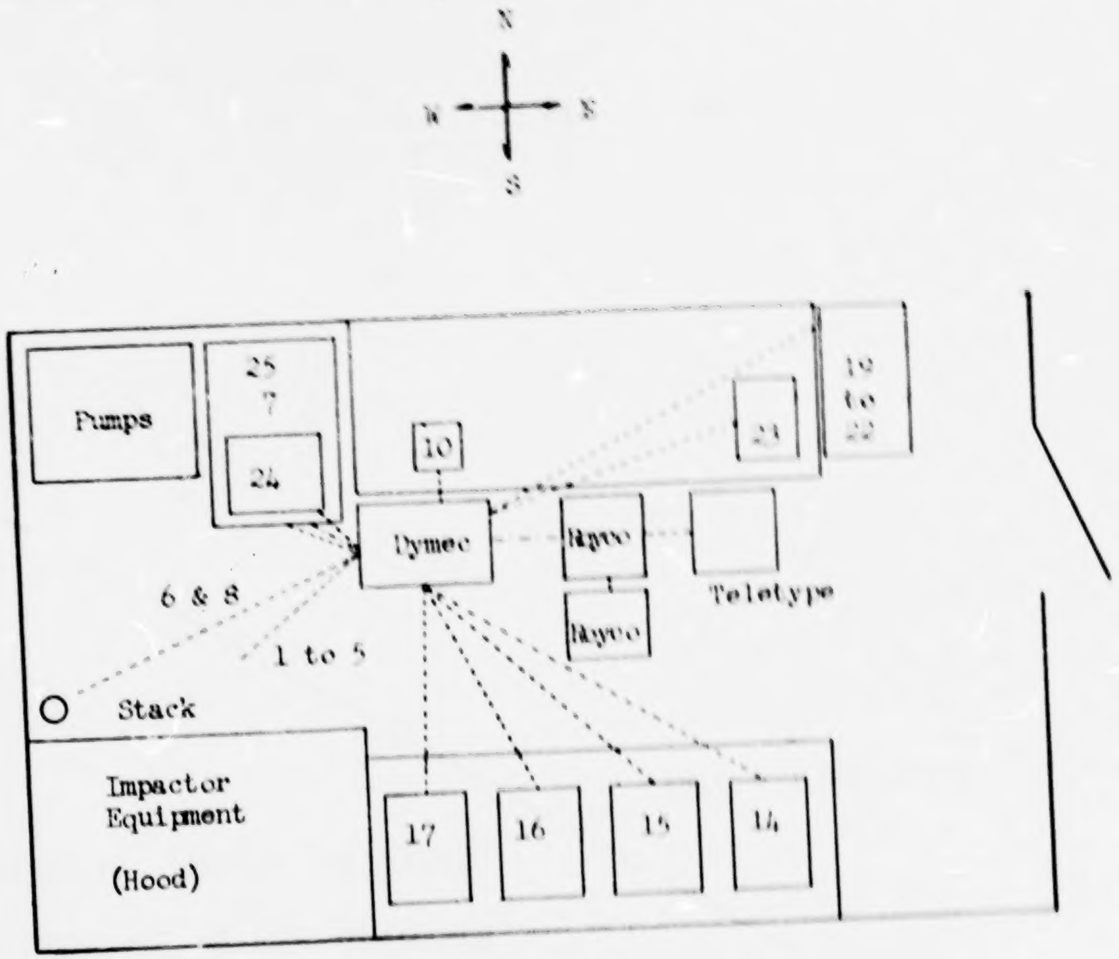
N
W
E
S
Pumps
25
7
24
10
Dymec
23
19
to
22
Teletype
6 & 8
1 to 5
Stack
Impactor
Equipment
(Hood)
17
16
15
14

Figure III-3 Sketch of Room #10, W.M. Keck Laboratory (not to scale)

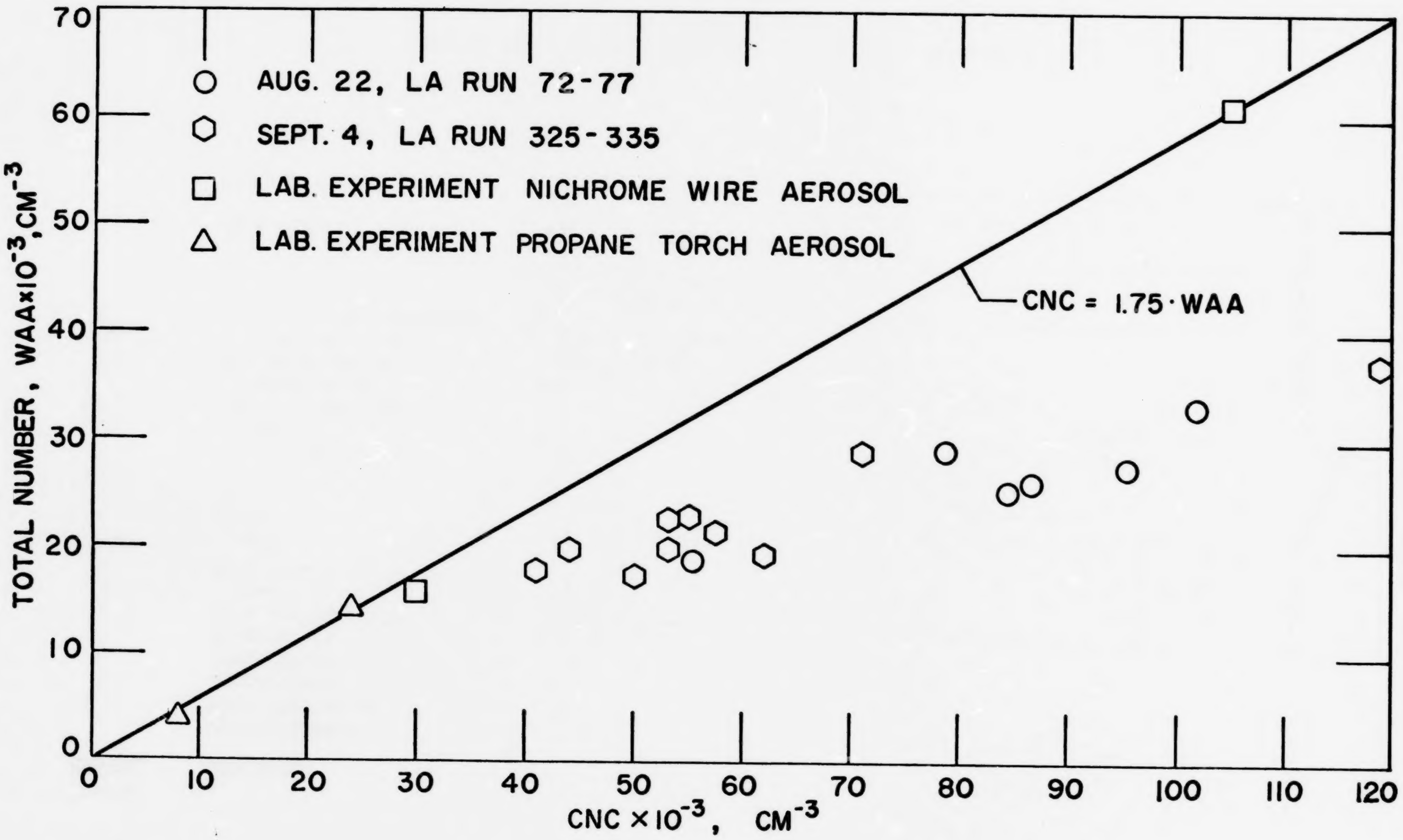

Fig. III-5 Comparison of total numbers measured by the GE Condensation Nuclei Counter and calculated from the number spectra obtained by the WAA.

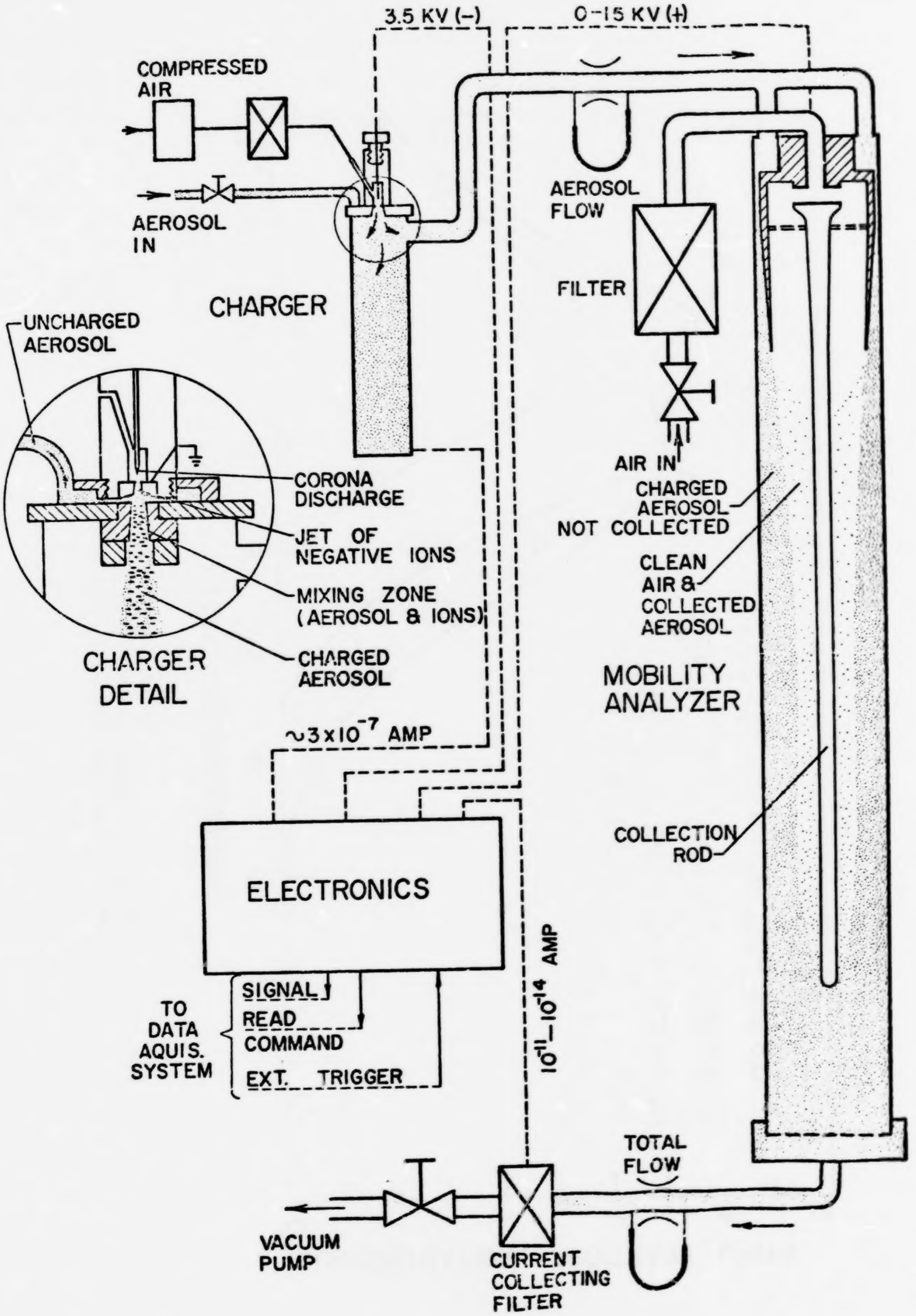
3.5 KV (−)
0−15 KV (+)
COMPRESSED AIR
AEROSOL IN
CHARGER
AEROSOL FLOW
FILTER
AIR IN
UNCHARGED AEROSOL
CORONA DISCHARGE
JET OF NEGATIVE IONS
MIXING ZONE (AEROSOL & IONS)
CHARGED AEROSOL
CHARGER DETAIL
CHARGED AEROSOL NOT COLLECTED
CLEAN AIR & COLLECTED AEROSOL
MOBILITY ANALYZER
~3x10^{-7} AMP
COLLECTION ROD
ELECTRONICS
10^{-11}–10^{-14} AMP
SIGNAL
READ COMMAND
EXT. TRIGGER
TO DATA AQUIS. SYSTEM
TOTAL FLOW
VACUUM PUMP
CURRENT COLLECTING FILTER

Fig.III-6. Schematics of the Whitby Aerosol Analyzer

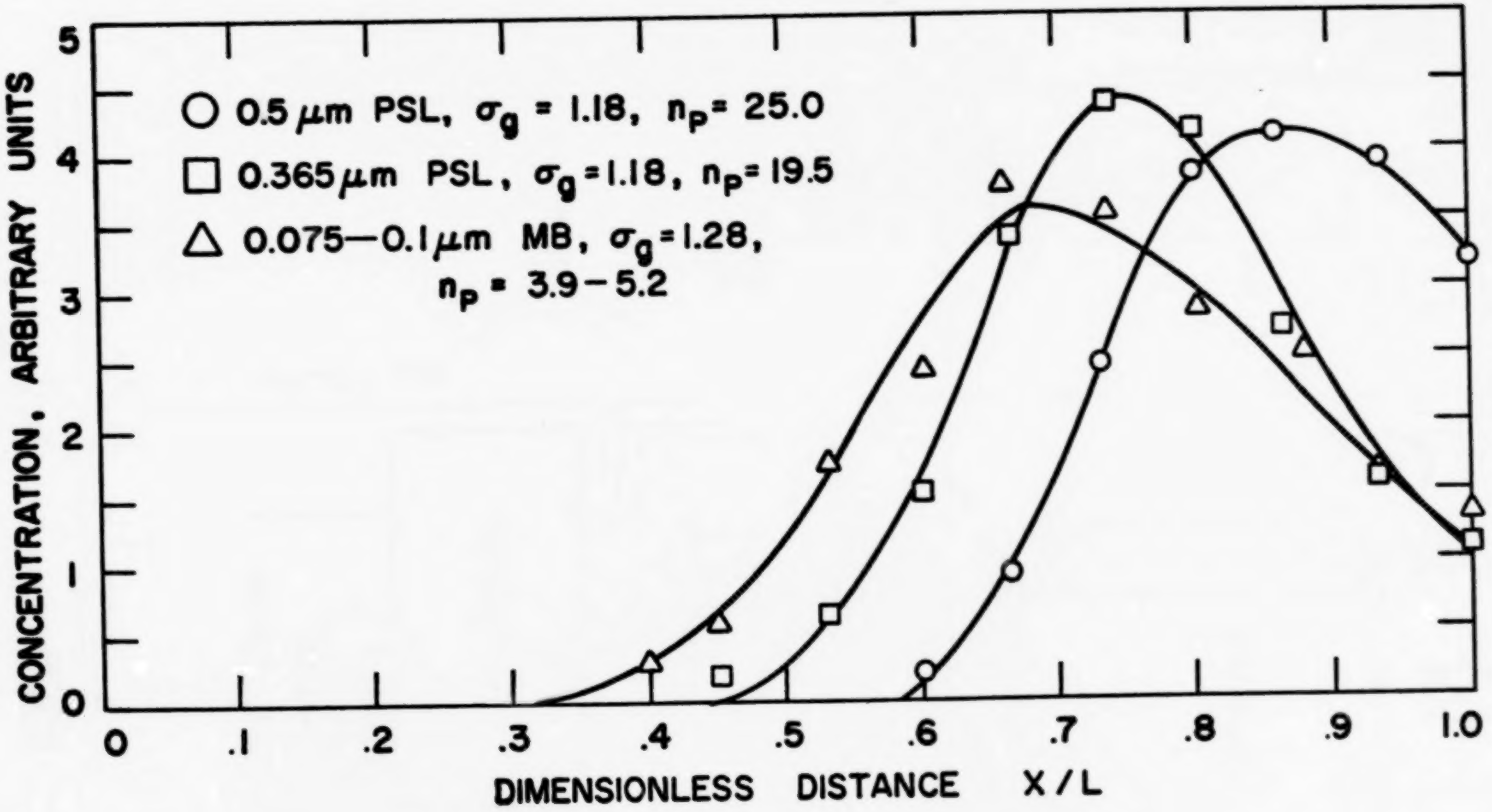

Fig. III-7. Deposition pattern of Polystyrene Latex and Methylene Blue particles on the rod of the WAA.

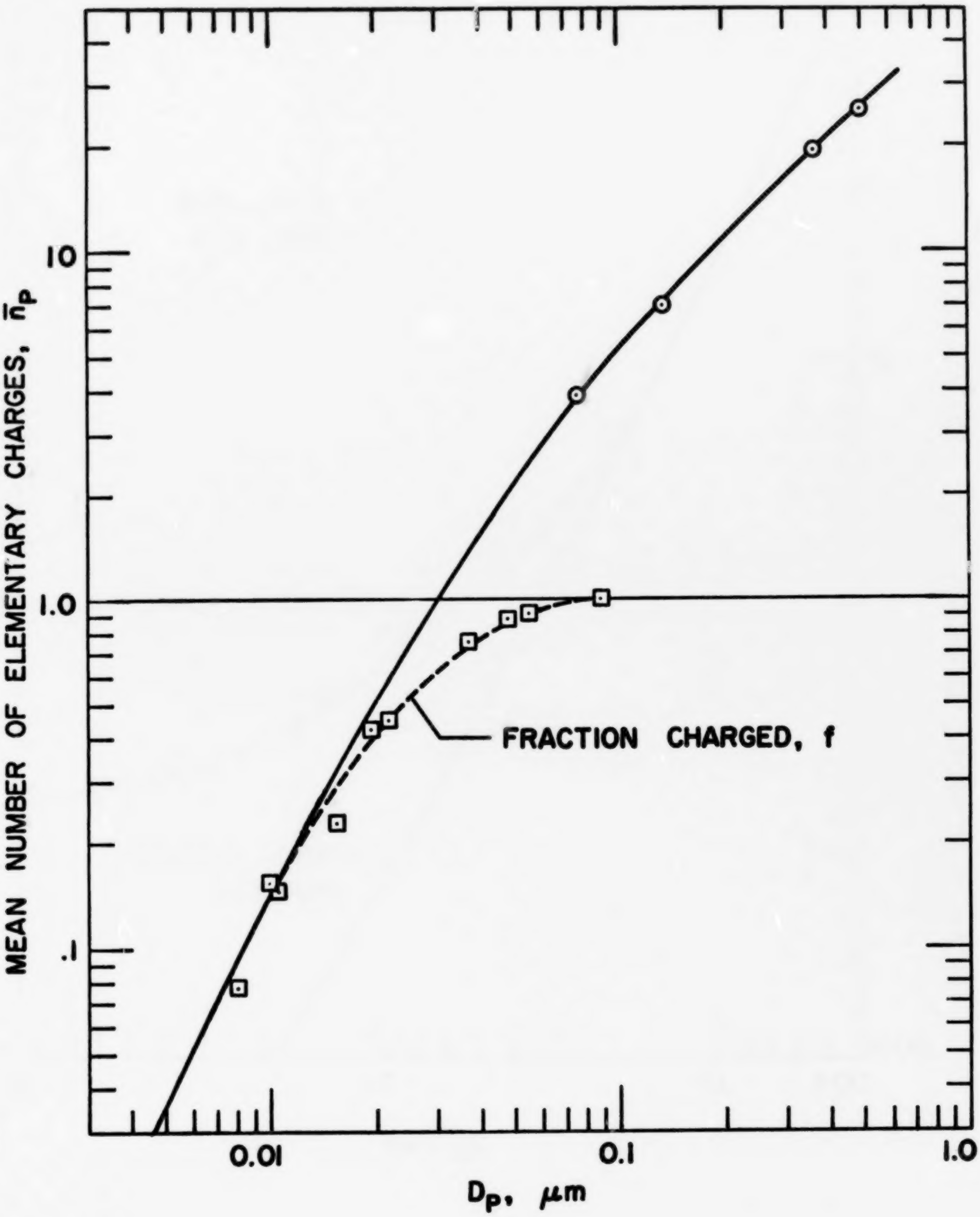

Fig. III-8. The mean number of charges $\bar{n}_p$ and the fraction of particles charged, f as a function of particle size.

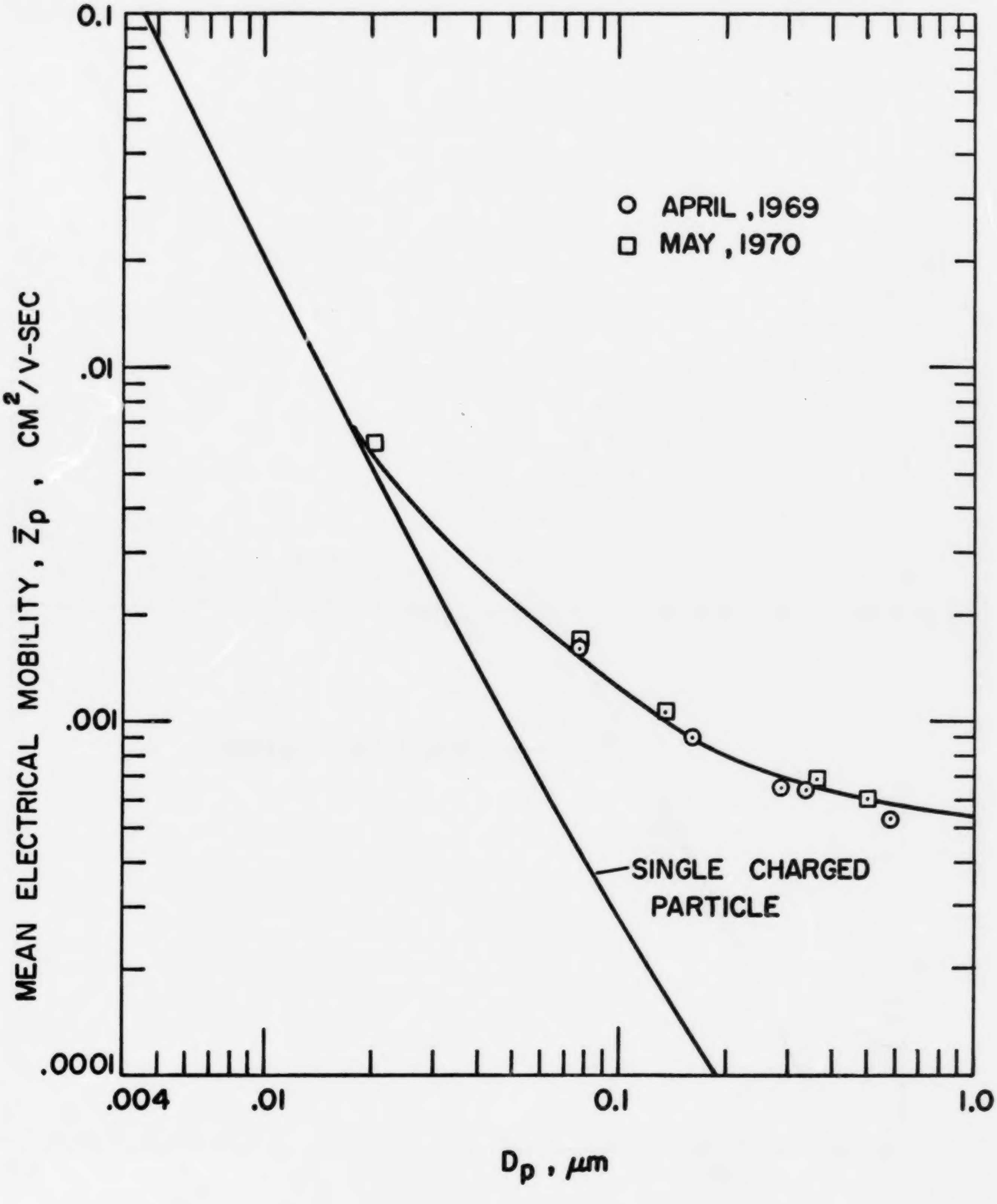

Fig. III-9. The mean electrical mobility $\bar{Z}_p$ as a function of particle size.

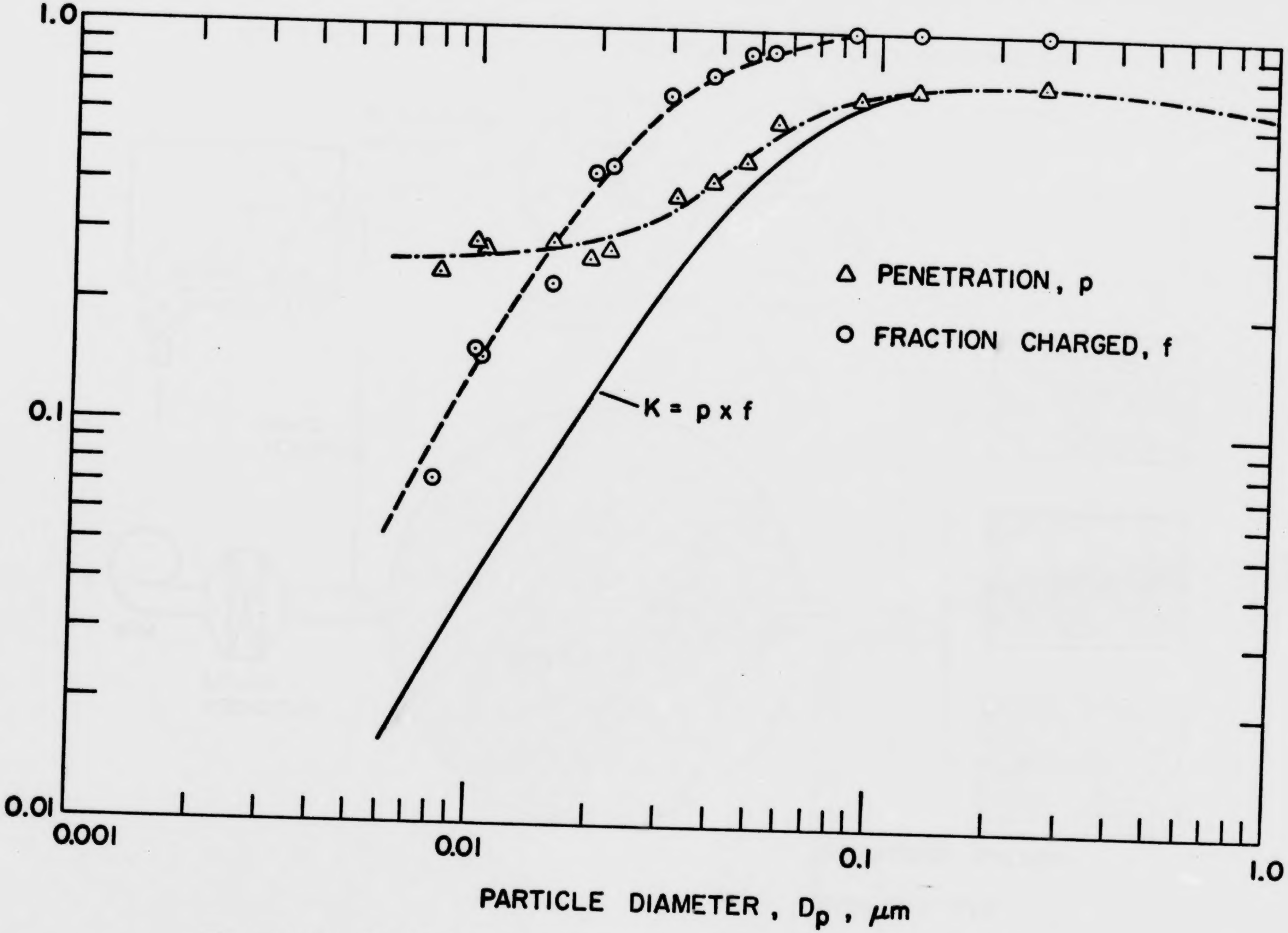

Fig. III-10. The fraction of particles charged and the aerosol penetration through the WAA.

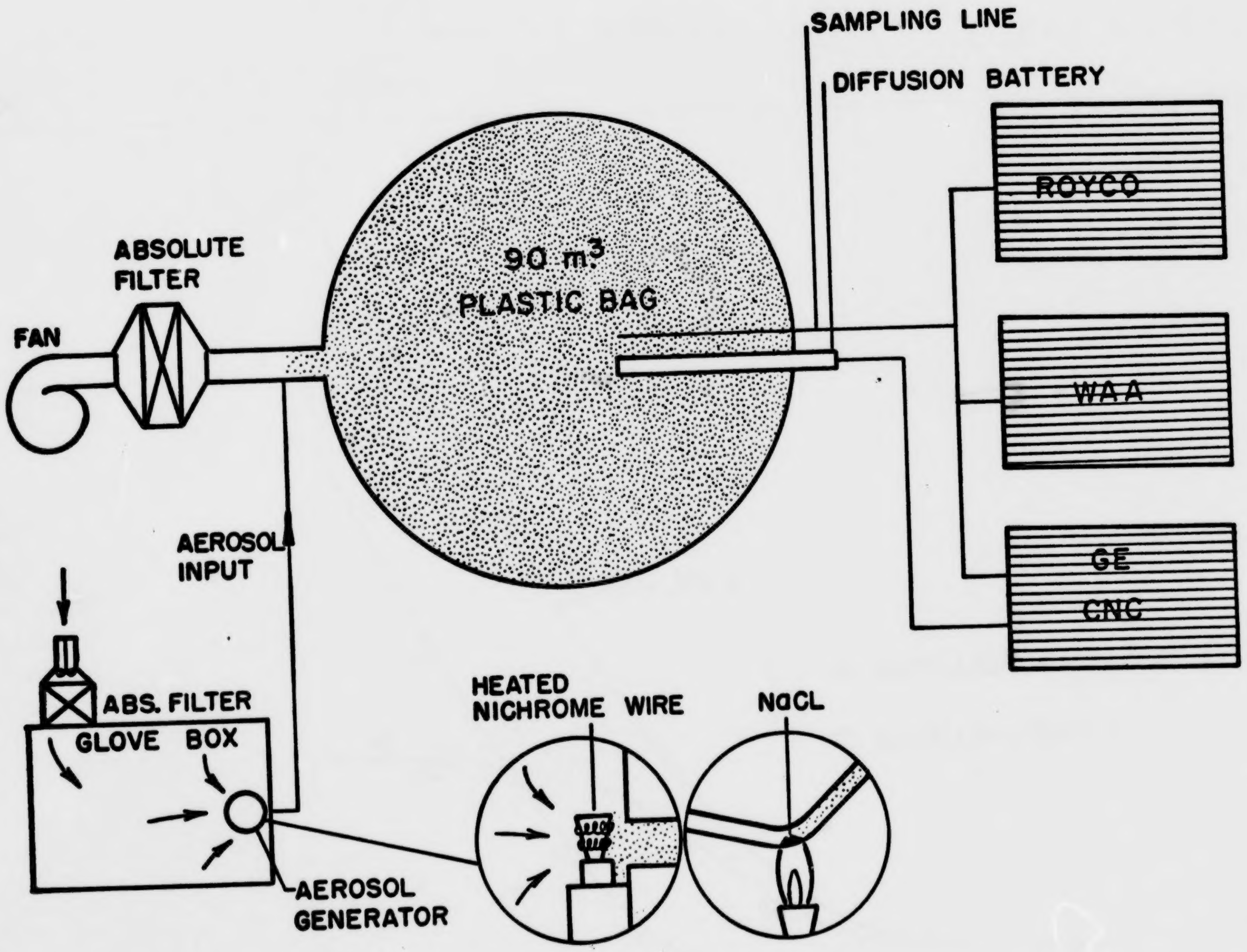
SAMPLING LINE
DIFFUSION BATTERY
ROYCO
WAA
GE
CNC
ABSOLUTE FILTER
FAN
90 m³
PLASTIC BAG
AEROSOL INPUT
ABS. FILTER
GLOVE BOX
AEROSOL GENERATOR
HEATED NICHROME WIRE
NaCL

Fig. III-11. Experimental set-up for the calibration of the WAA showing the method for generating the small aerosols.

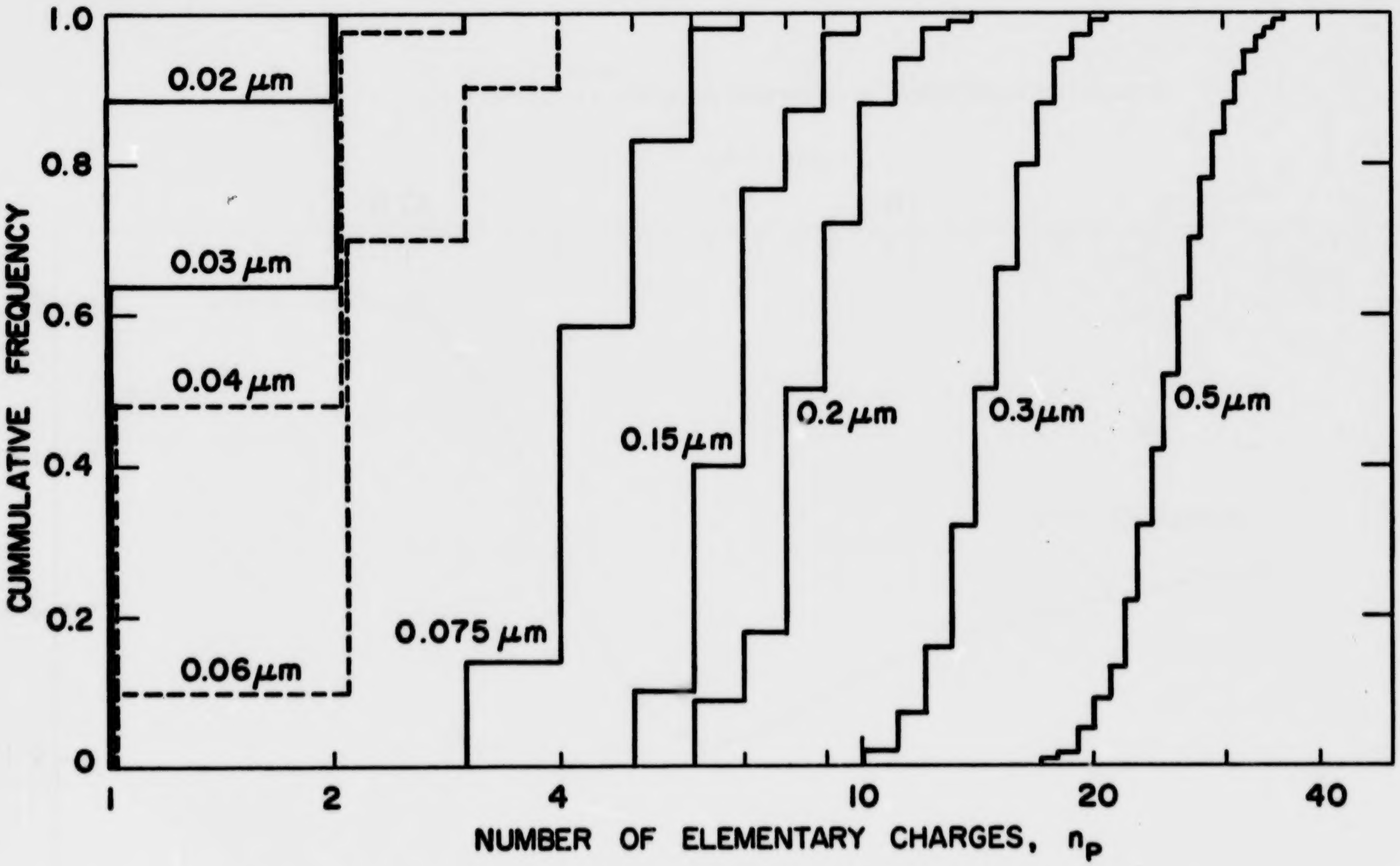

Fig. III-12. Cumulative change distributions on particles of different sizes.

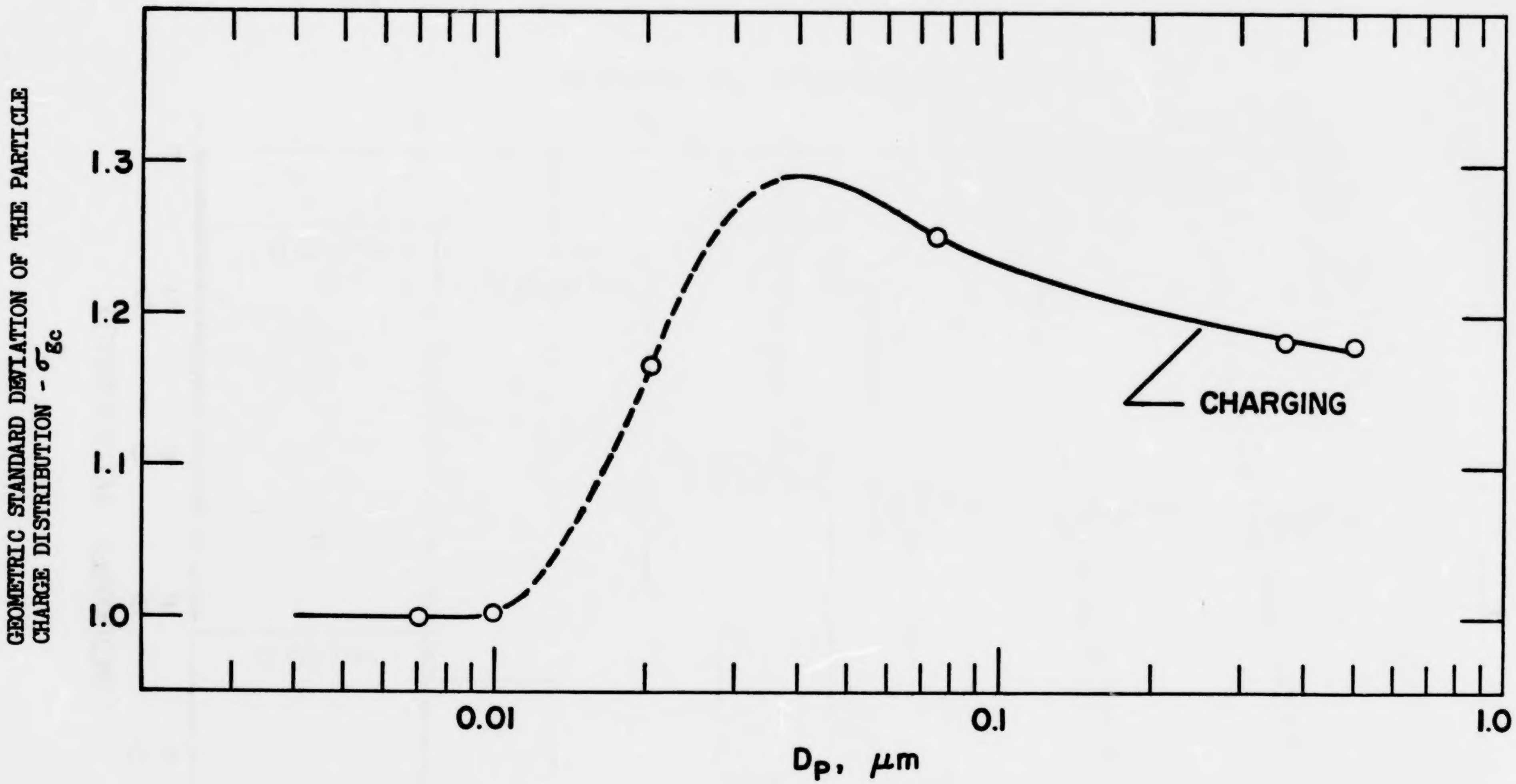

Fig. III-13. The logarithmic standard deviation of charging as a function of particle size.

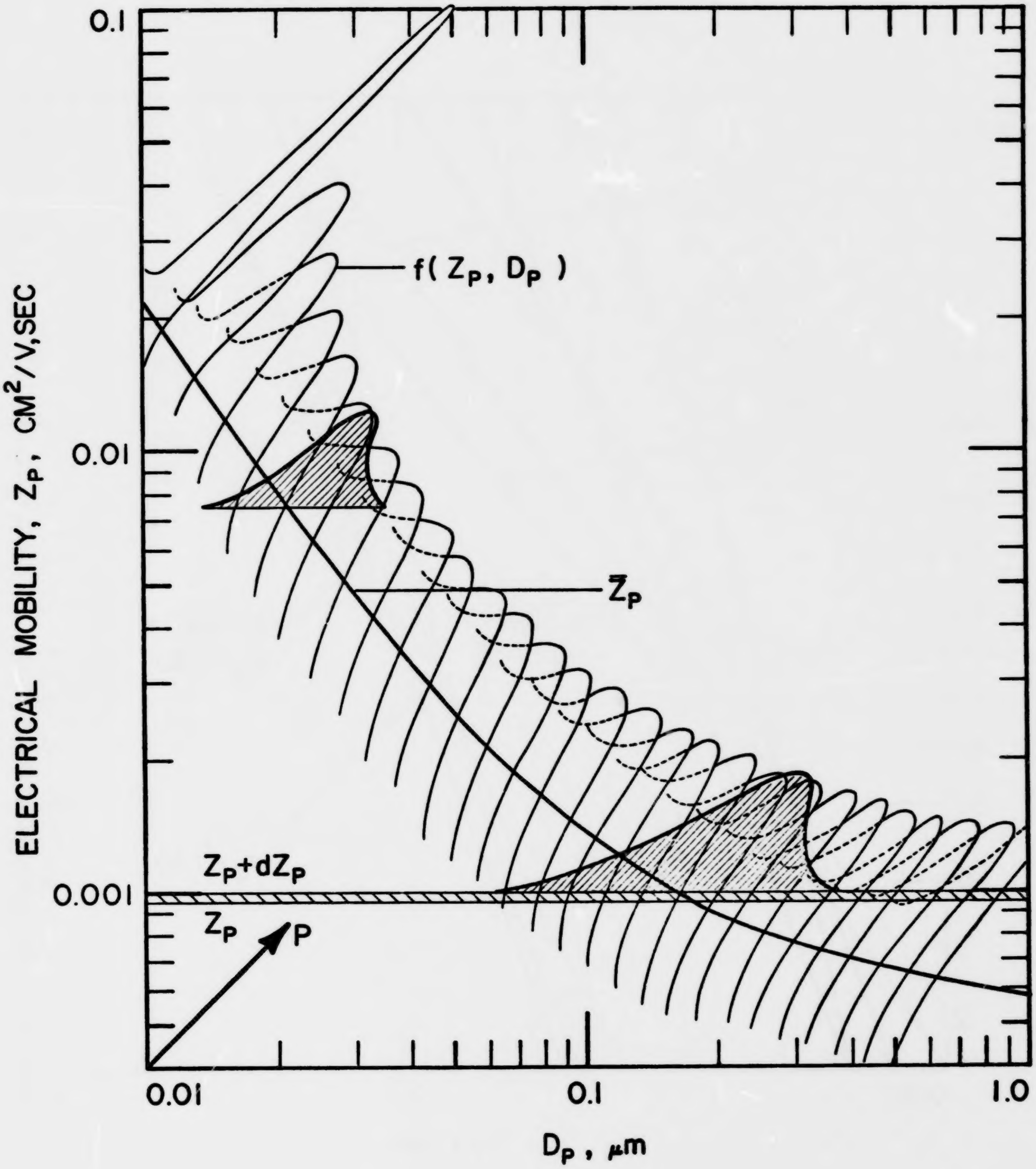

Fig. III-14. The mobility spectrum of particles charged with the jet charger.

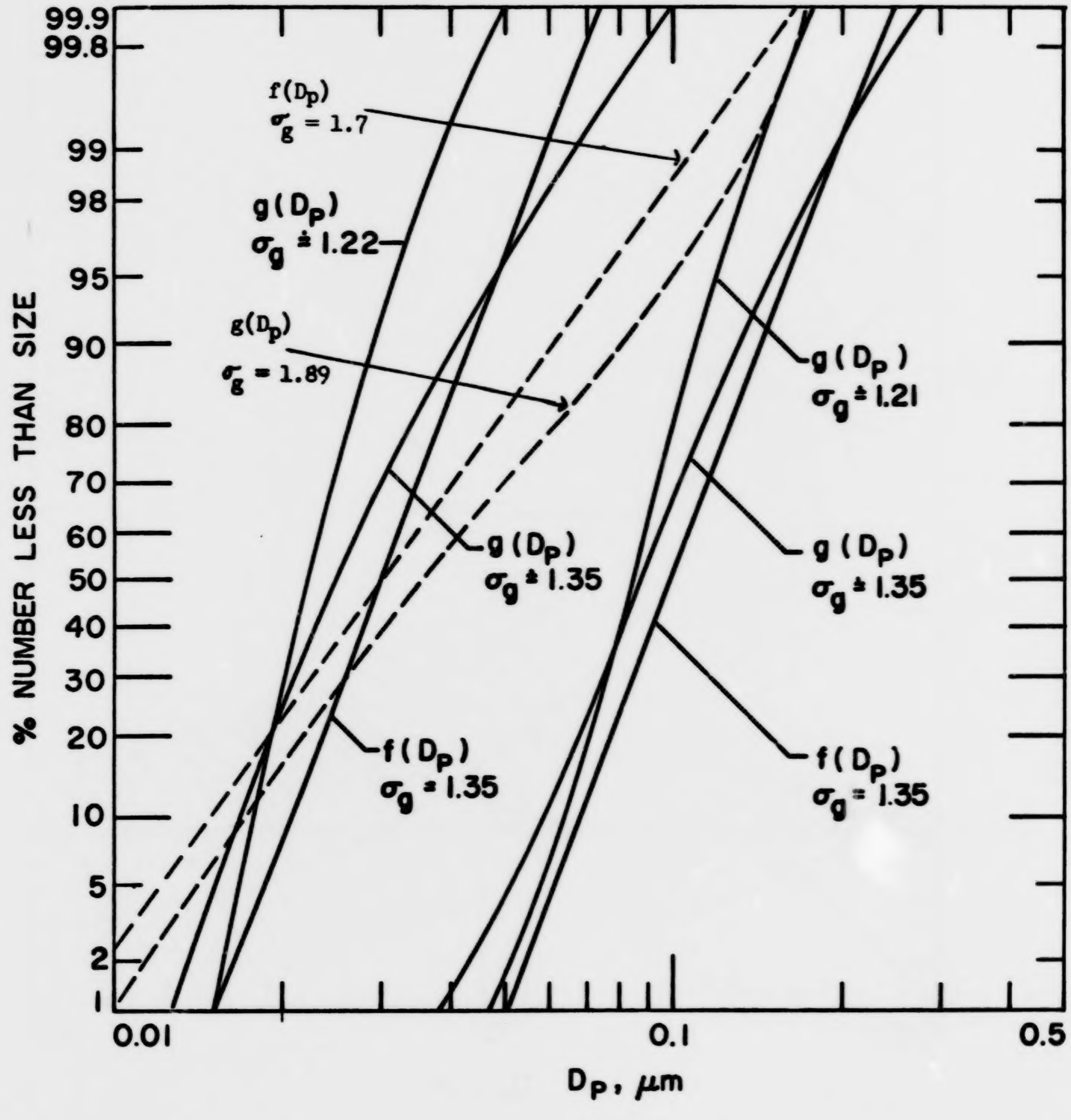

Fig. III-15. Comparison between the true size spectra, $f(D_p)$ and the indicated spectra $g(D_p)$. The dashed lines show $f(D_p)$ and $g(D_p)$ for a σ_g typical of the smog.

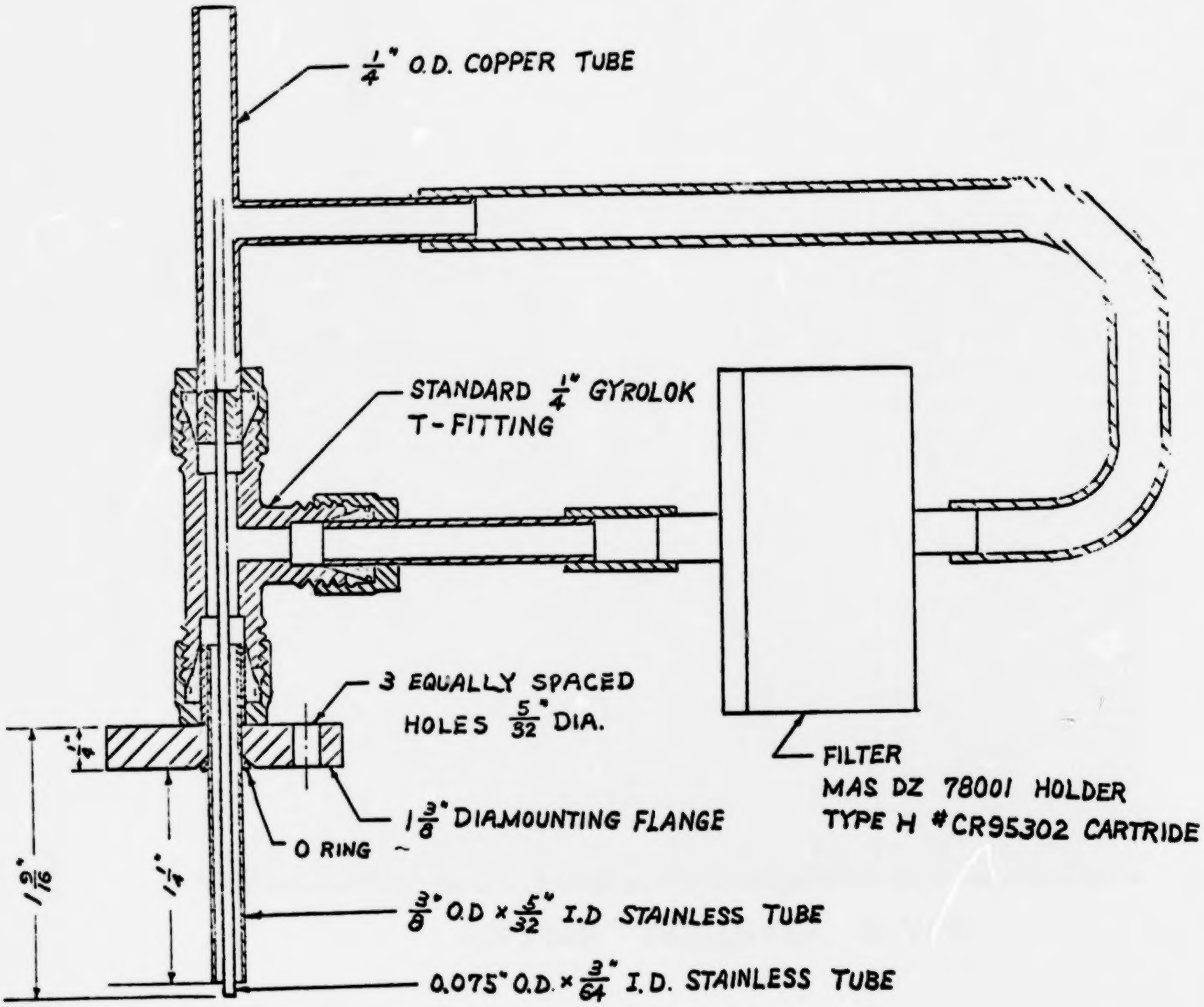

$\frac{1}{4}$" O.D. COPPER TUBE
STANDARD $\frac{1}{4}$" GYROLOK T-FITTING
3 EQUALLY SPACED HOLES $\frac{5}{32}$" DIA.
$1\frac{3}{8}$" DIAMOUNTING FLANGE
O RING
FILTER
MAS DZ 78001 HOLDER
TYPE H #CR95302 CARTRIDE
$\frac{1}{4}$"
$1\frac{9}{16}$"
$1\frac{1}{4}$"
$\frac{3}{8}$" O.D × $\frac{5}{32}$" I.D STAINLESS TUBE
0.075" O.D. × $\frac{3}{64}$" I.D. STAINLESS TUBE

Figure III-16. Sheath-air inlet for Royco 220 optical sensor

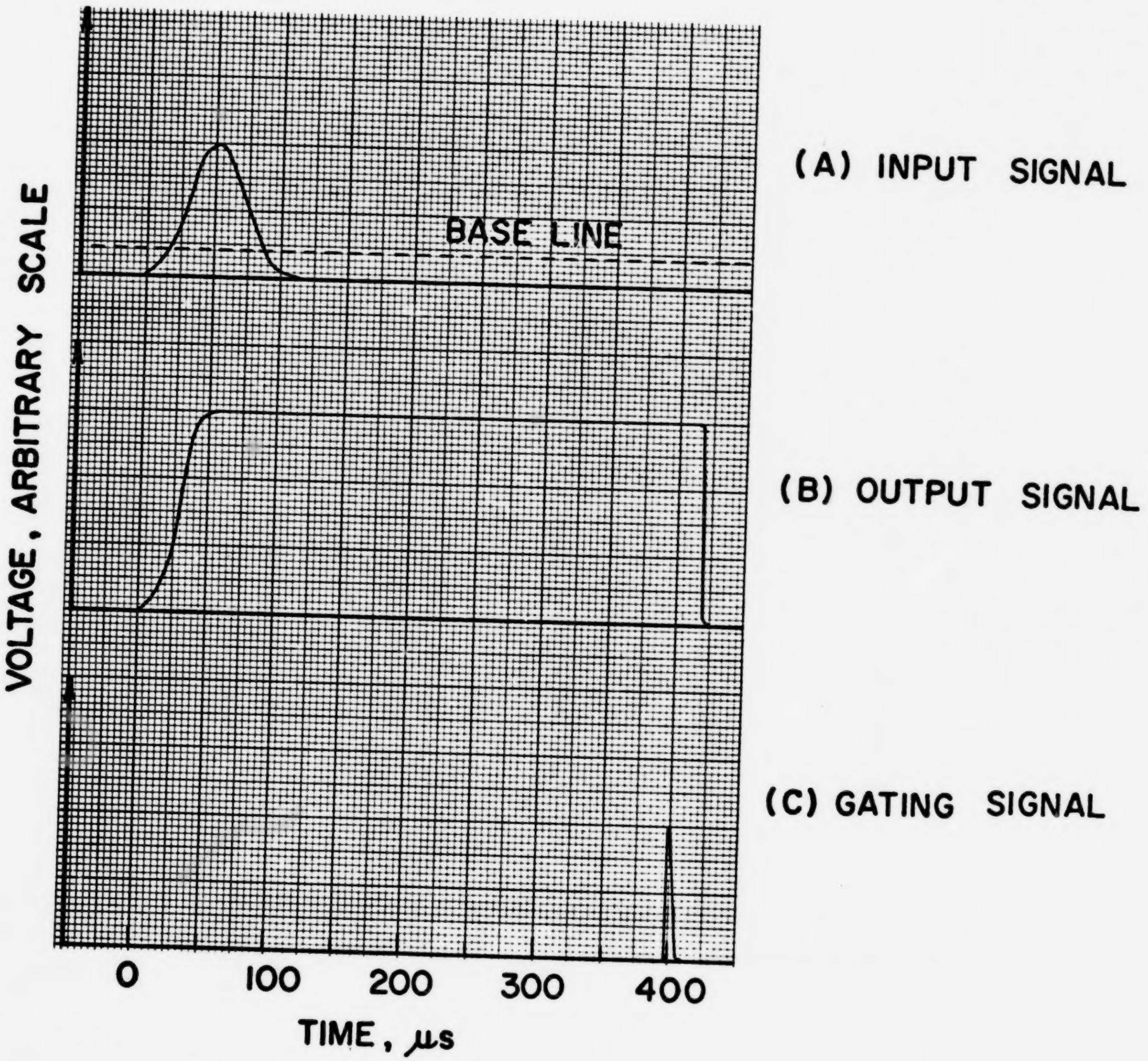

Figure III-17 Input and output signals from Royco 170-1 pulse converter

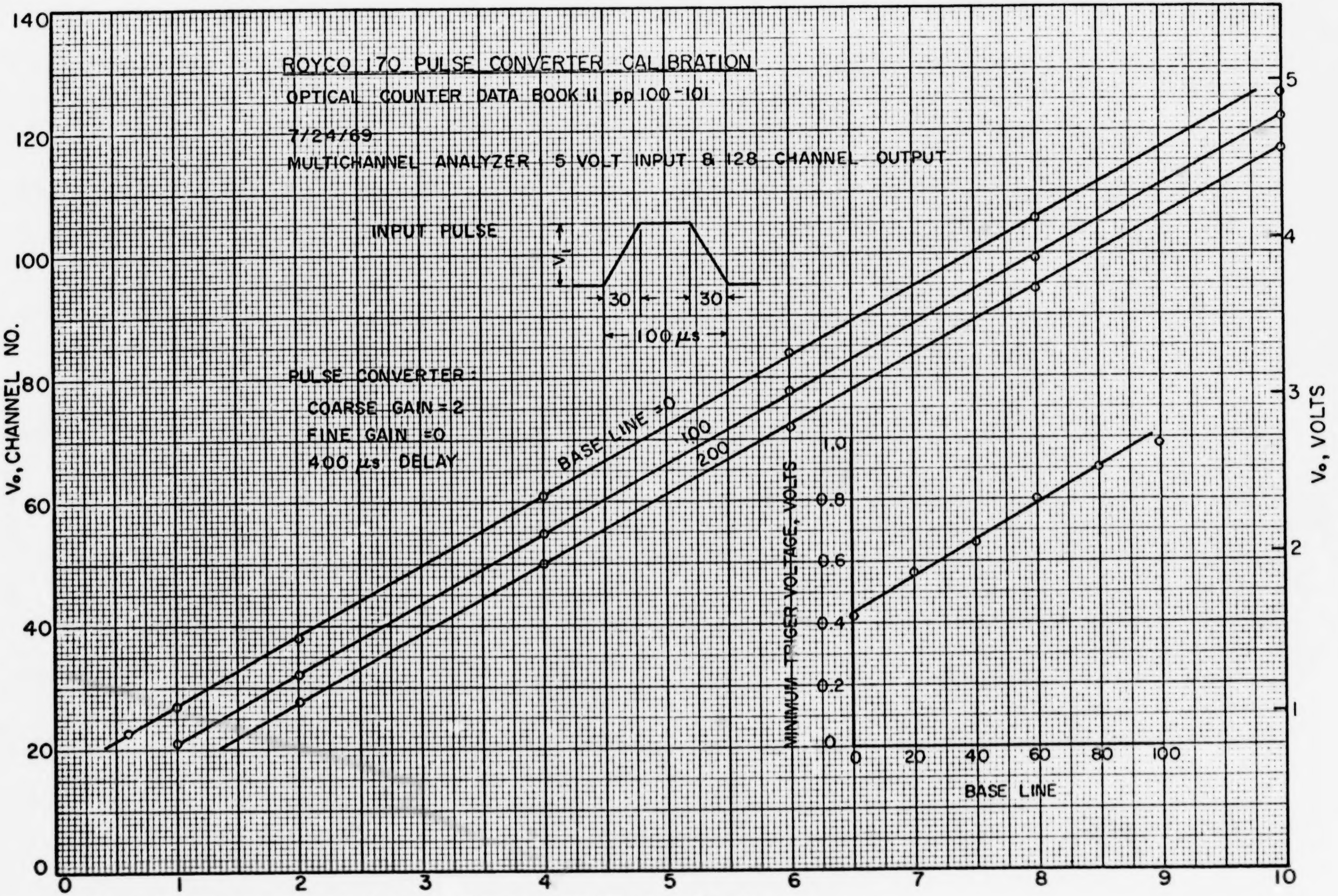

Figure III-18 Royco 170-1 pulse converter calibration

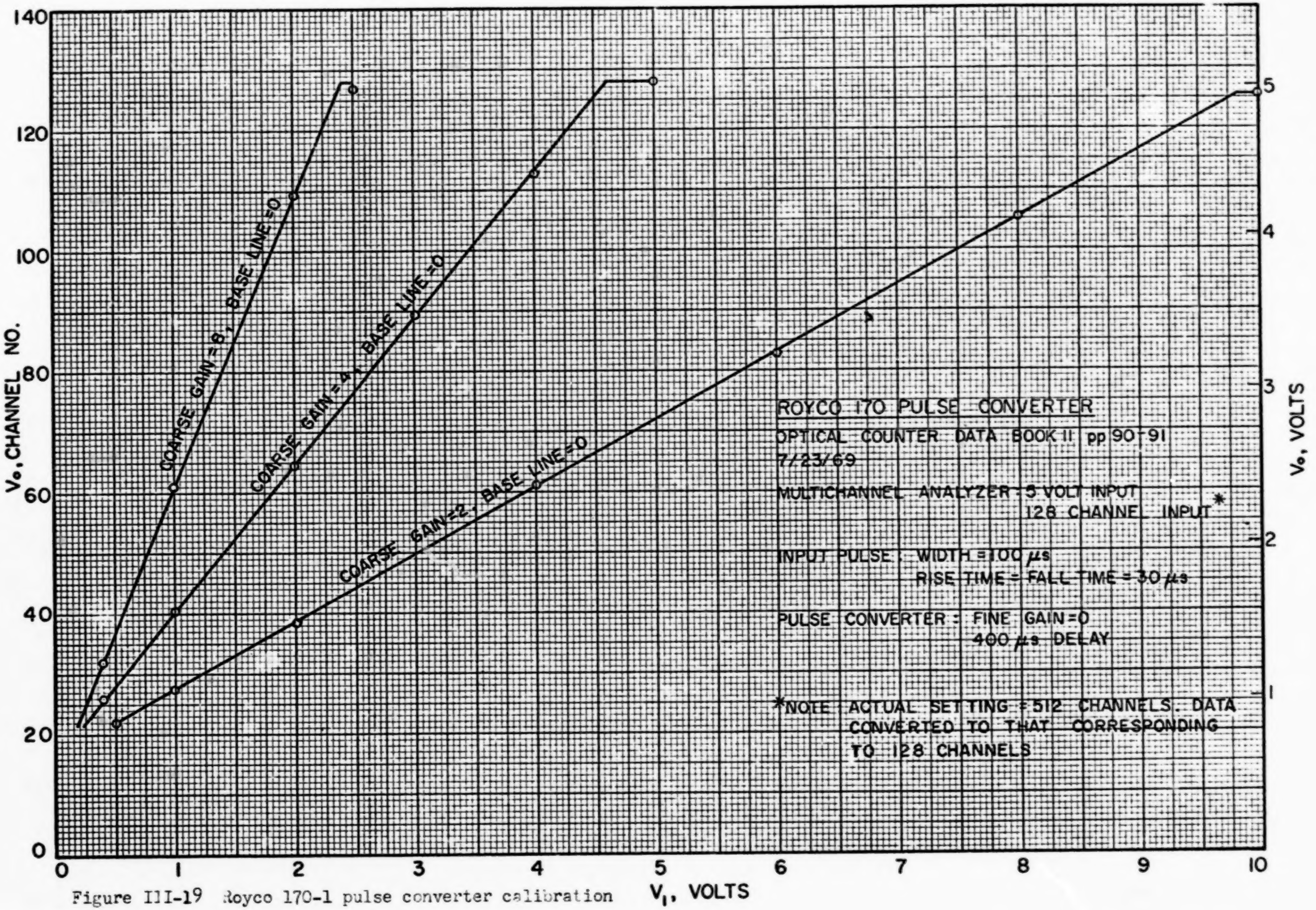

Figure III-19 Royco 170-1 pulse converter calibration

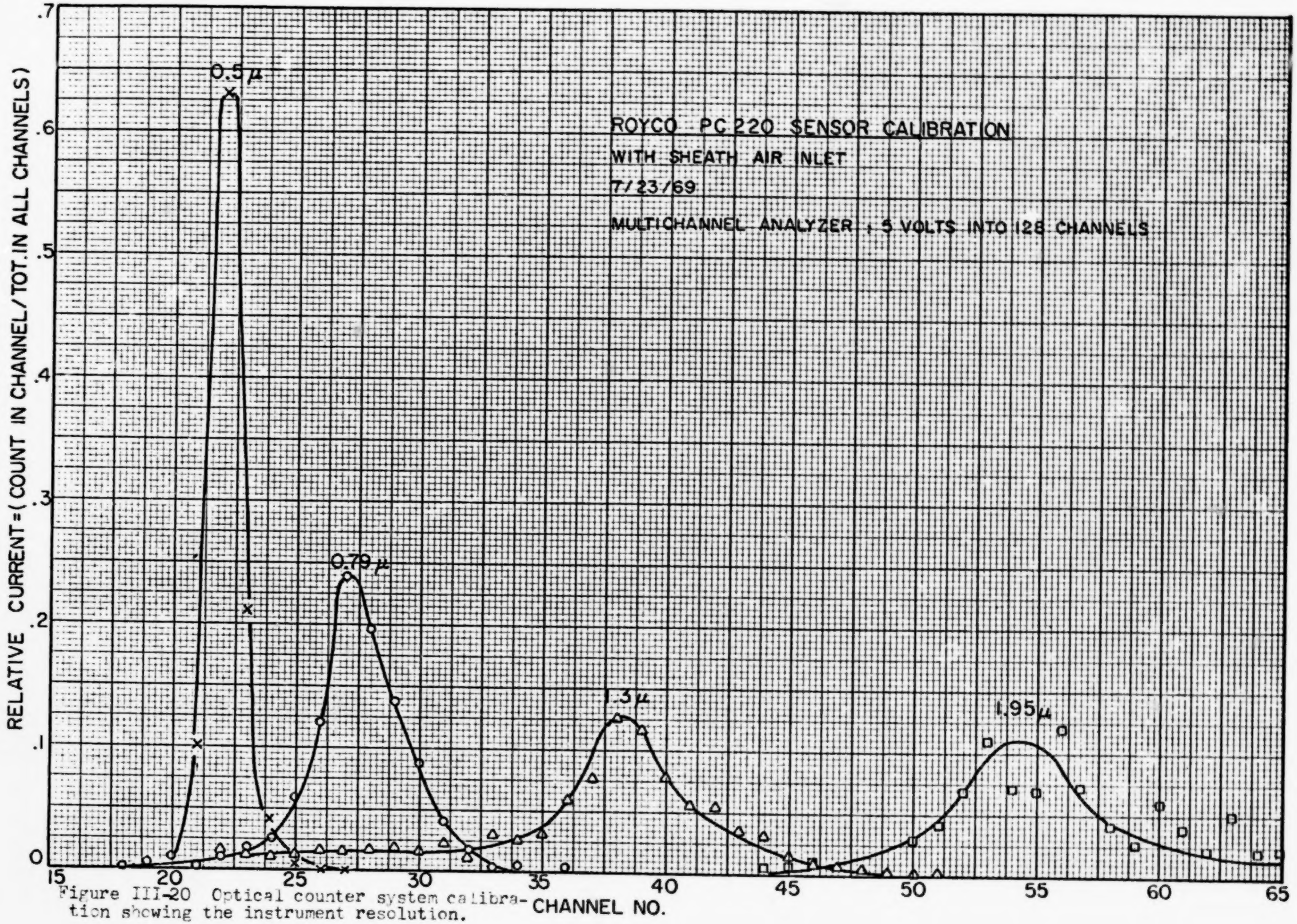

Figure III-20 Optical counter system calibration showing the instrument resolution.

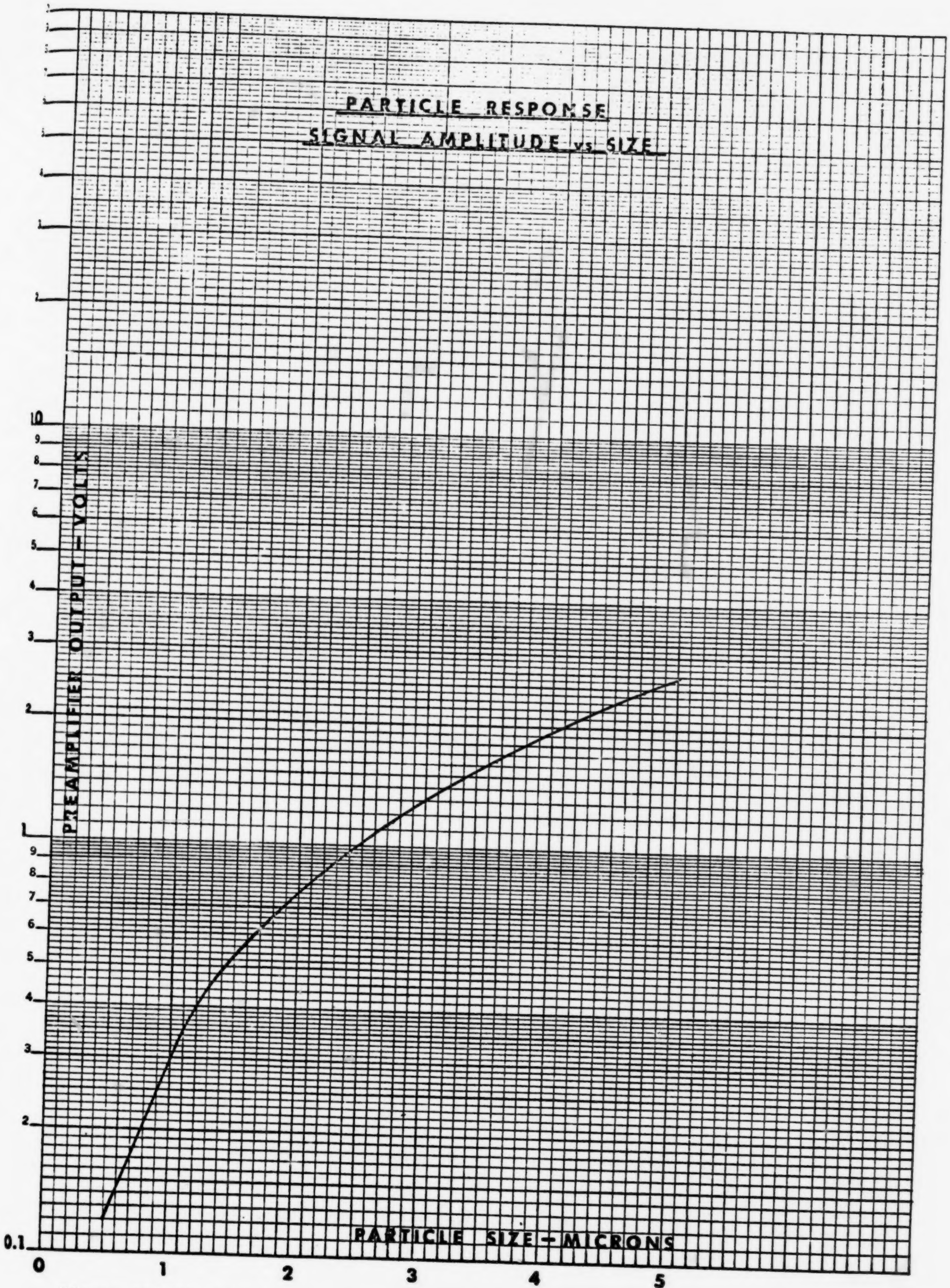

Figure III-21 Royco 220 sensor calibration according to the manufacturer.

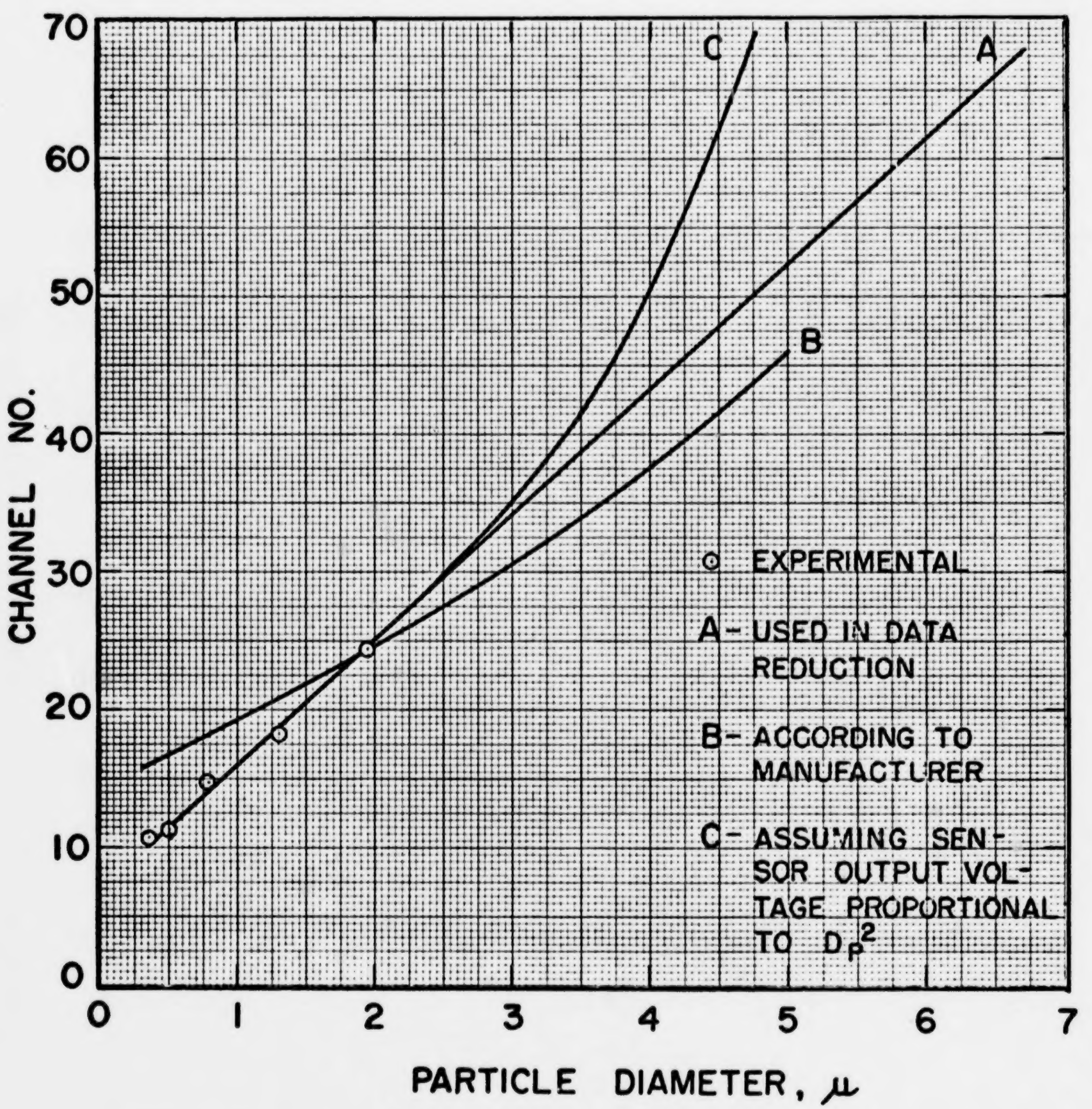

Figure III-22 System calibration for the optical counter under the standard operating conditions

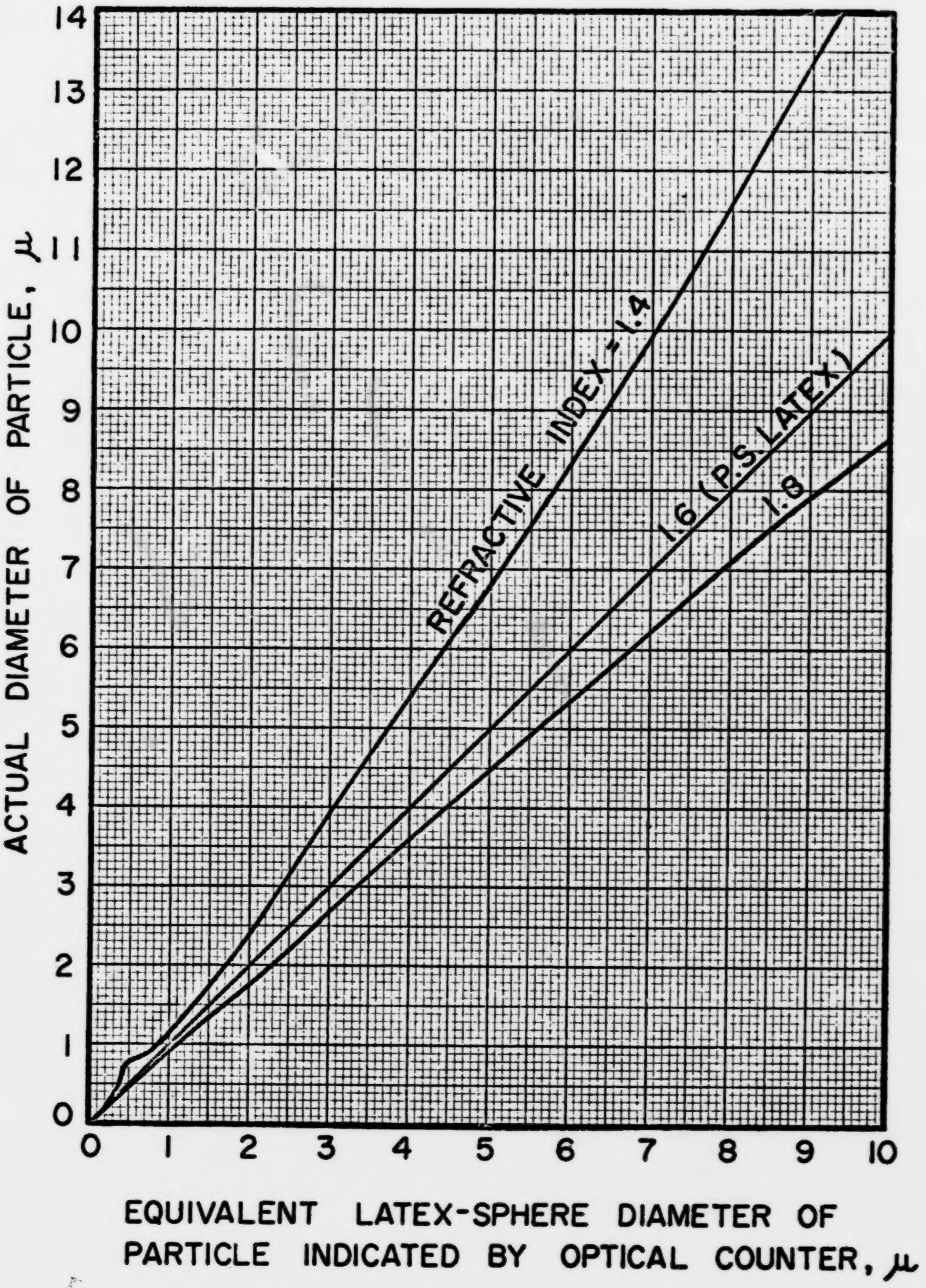

Figure III-23 Effect of refractive index on the response of the optical counter.

Table III-1. Calibration constants for WAA, particle size range 0.0075 - 0.6 μm.

Date__________

WHITBY AEROSOL ANALYZER, Calibration May 1970, RBH
Aerosol Flow Rate: 0.32 cfm

Test__________

D_p	ΔD_p	D_{pi}	$\frac{\Delta N}{\Delta I}$	$\frac{\Delta N}{\Delta I \ \Delta D_p}$	Volts	St	I	ΔI	ΔN	$\frac{\Delta N}{\Delta D_p}$
.0075					225	0				
	.0025	.00875	1,250,000	500,000,000						
.01					400	1				
	.005	.0125	637,000	124,000,000						
.015					920	2				
	.005	.0175	343,000	68,600,000						
.02					1400	3				
	.01	.025	163,000	16,300,000						
.03					2400	4				
	.01	.035	89,200	8,920,000						
.04					3200	5				
	.02	.05	47,700	2,380,000						
.06					4450	6				
	.02	.07	26,800	1,340,000						
.08					5800	7				
	.02	.09	18,300	915,000						
.1					7200	8				
	.025	.1125	13,700	548,000						
.125					8300	9				
	.025	.1375	10,700	428,000						
.15					9200	a				
	.05	.175	8,340	166,000						
.2					10,600	b				
	.1	.25	5,790	57,900						
.3					12,300	c				
	.1	.35	4,100	41,000						
.4					13,300	d				
	.2	.5	2,800	14,000						
.6					14,000	e				

Table III-2. Calibration constants for WAA, particle size range 0.004 - 0.035 μm.

WHITBY AEROSOL ANALYZER
Calibration May 1970, RBH
Aerosol Flow Rate: 0.32 cfm

Date____________
Test____________

D_p	ΔD_p	D_{p_i}	$\frac{\Delta N}{\Delta I}$	$\frac{\Delta N}{\Delta I\,\Delta D_p}$	Volts	St	I	ΔI	ΔN	$\frac{\Delta N}{\Delta D_p}$
.004					65	0				
	.001	.0045	7,800,000	7.8 E+09						
.005					100	1				
	.001	.0055	4,000,000	4.0 E+09						
.006					145	2				
	.001	.0065	2,500,000	2.5 E+09						
.007					200	3				
	.001	.0075	1,750,000	1.75 E+09						
.008					260	4				
	.001	.0085	1,400,000	1.4 E+09						
.009					330	5				
	.002	.010	1,100,000	5.5 E+08						
.011					500	6				
	.002	.012	700,000	3.5 E+08						
.013					680	7				
	.002	.014	510,000	2.55 E+08						
.015					880	8				
	.002	.016	400,000	2.0 E+08						
.017					1080	9				
	.002	.018	320,000	1.6 E+08						
.019					1280	a				
	.004	.021	240,000	6.0 E+07						
.023					1680	b				
	.004	.025	170,000	4.25 E+07						
.027					2080	c				
	.004	.029	130,000	3.25 E+07						
.031					2450	d				
	.004	.033	102,000	2.55 E+07						
.035					2750	e				

SECTION IV

Aerosol Sampling for Determination of Particulate Mass Concentration, Chemical Composition and Size Distribution

by

Dale A. Lundgren
Staff Scientist
Environmental Research Corporation

Introduction

This paper describes the use of a Lundgren Impactor together with a total particulate filter, to determine the size distribution, concentration and chemical composition of particulate matter in air.

Determination of the above information involves:

1) Obtaining size fractionated samples of the aerosol over desired time periods.

2) Collecting out the particulate matter in such a way that it is amenable to analysis.

3) Analyzing the particulate samples by techniques capable of providing the required information.

These criteria are interrelated; therefore, the aerosol sampling method was based on knowledge of both the sampling and analysis limitations and on knowledge of the type of aerosol property data desired.

Aerosol sampling normally involved simultaneous use of the impactor (with its after filter) and a total particulate filter. Both the impactor and total filter are of the same size, use the same filter media and sample at about the same flow rate. This provided an excellent check on the total particulate concentration and particle losses within the impactor. All samples are to be analyzed chemically; this, in turn, provides a similar quantitative check on the chemical results. On several occasions two impactors were run simultaneously, each using different collection substrates and filter media. Many additional total filter samples were also obtained when the impactor was not run.

Method Description

The developed sampling-analysis method is primarily based on a fairly high flow rate four-stage impactor (called the Lundgren Impactor) originally developed for the National Air Pollution Control Administration to characterize urban particulate matter by size distribution over day-long time periods. The unit is a compact field-operational sampler having well defined operating characteristics and great versatility. A cross-section schematic of the impactor is shown in Figure IV-1. Its four impaction stages were designed so as to fractionate particulate matter at diameters of 10, 3, 1 and 0.3 microns (μ), for spherical particles of density two, at a flow rate of 4 cfm. The impactor is followed by an after filter.

Impactor flow rate is not fixed, therefore, air can be sampled at any rate from less than 0.5 cfm to over 5 cfm. A useable range is from 0.5 cfm (to prevent gravitational loss of very large particles) up to 5 cfm (to prevent excessive pressure drop in the unit and high impactor wall loss of medium size particles). This flow rate range enables classification of particles from about 0.2μ to about 40μ diameter--depending on particle density, impactor stage and flow rate--as seen in Figure IV-2. Collection characteristics of the impactor were determined experimentally.* Stage 50% cut points shown in Figure IV-2 were calculated from the calibration data. The diameters are actual diameters for spherical particles and are aerodynamic or Stokes diameter for other than spherical particles.

The total filter holder and the impactor filter holder were alike and both accommodate 90 mm diameter filter media. Total particulate concentration was determined with the total filter, while the impactor filter served to determine particulate concentration of a size too small to be collected by the impactor. Filter media for both filter holders was handled identically; therefore, the total filter sampling procedure is not discussed separately as all comments made regarding the impactor filter apply equally to the total filter.

---

*Lundgren, D. A., "An Aerosol Sampler for Determination of Particle Concentration as a Function of Size and Time". APCA Journal, Vol. 17, No. 4, April 1967.

The operation of all impaction devices is based on the fact that a particle's inertia is a function of particle velocity and mass-or particle size, density and velocity. This principle explains the separation of particles into two fractions: those having sufficient inertia to leave the airstream, and those with less inertia which follow the airstream lines. Air drawn into the impactor is accelerated in the first stage converging nozzle and then forced to flow around the first stage collection drum. Large particles have sufficient inertia to leave the airstream and impact out against the first stage collection surface. Remaining particles are carried by the airstream to the second nozzle where the air is accelerated to a higher velocity, allowing somewhat similar particles to be impacted out. This process is repeated in the third and fourth stages and then all remaining particles are collected out by an efficient after filter.

All four impactor nozzles are two inches high but of different widths, giving a fixed collection deposit height of two inches and a deposit length which is proportional to collection drum rotational speed and sampling time. The one and one-half inch diameter collection drums have a circumference of about 4.7 inches, thereby providing almost 9.5 square inches of collection area per stage. Because of this great sampling area, this unit can sample normal atmospheric air over 24-hour time periods, or sample very dusty air over short time periods--without the normal problem of collection surface buildup and blowoff. The collection drum drive can be set to provide the proper rotational speed for the desired sampling time. In all cases, a chronological collection deposit is produced with very good time resolution.

In the referenced paper describing impactor design and calibration, data on particle losses within the impactor as well as the effects of collection surface coating and deposit density on collection efficiency are given. Particles such as silica or glass beads do not. readily stick to the impaction surface; therefore, a viscous oil or grease should be used to coat the collection surface when sampling particles of that type.

Sampling Procedure

Any sampling procedure should be mated to the analysis method or methods. Because several analysis methods may be chosen, the sampling procedure should be as versatile as possible without being overly involved. The following procedure resulted from over a year of trial and is considered satisfactory in most respects.

It was stated that particles to be collected are impacted onto the collection drum. Normally the drum is coated with a thin film material and the particulate matter collected onto this removable drum coating material. Materials such as aluminum foil, stainless steel shim stock, sticky tapes, and various plastic films have been used with some success, but none have proven more suitable or desirable than a film of Teflon, about 0.001 inch or so thick. In general, the sticky tapes (such as two-sided sticky tape) were the least desirable method and are not recommended.

Teflon film has the advantages of being inert, having a low chemical background, and having a low affinity for water vapor. It is also very weight stable, is not affected by most acids or bases, and is quite transparent under the microscope. It can easily be cut into time based segments for chemical analysis.

Because of the inert nature and very low hygroscopicity of Teflon, its weight reproducibility is excellent and quite independent of humidity. This weight stability is essential if atmospheric aerosol weight distributions are to be determined accurately. Collection stage weight changes (particulate collection) of less than 0.05 mg have been determined by this method (using a Sartorius semi-micro analytical balance with an obtainable weight accuracy and reproducibility of 0.01 mg). Static charge on Teflon is often a problem in weight determination; therefore a static charge eliminator* (a radioactive ion source) is routinely used. If small weight determinations are to be made, it is essential that the film be held onto the collection drum with a mechanical type clamp; adhesives or tapes should not be used if weight changes much less than 1 mg are to be accurately determined. If only a microscopic or chemical analysis is to be performed, the Teflon film can be held to the drum with cellophane type tape; the taped end can then be cut off before chemical analysis to prevent contamination from the tape itself or from dirt it may have picked up.

---

*Nuclear Products Co., El Monte, Ca. Model 2U500 (uses 500μc of PO 210).

As mentioned, an after filter must be used to collect particulate matter passing the impactor fourth stage. Desirable characteristics of an after filter include high collection efficiency, low pressure drop, good weight stability, low chemical background, and good particulate loading characteristics (filter does not plug up). A variety of filter materials have been tested to determine their overall usefulness. Based on weight stability and low chemical background, Teflon filters (sold by Millipore Corp.) ranked highest and were normally used. These filters can be pre-cleaned by washing in acid and water to reduce their chemical background to near zero.

Teflon filters are expensive; if a low-cost filter media is desired, the standard glass fiber filter media should be considered. It has reasonably good weight stability and a fairly low chemical background, with a few notable exceptions (such as iron). Standard type membrane filters have low chemical backgrounds but are not sufficiently weight stable for small weight change determinations.

The standard impactor after filter holds 90mm diameter filters. This large area is necessary to minimize pressure drop through Teflon and other membrane filters. Even with a large size filter, problems will be encountered because of filter plugging unless large pore size filters are used. Ten micron pore size Teflon filters were tested and found to perform adequately but five micron pore size filters were found to be borderline because of pressure drop increases with time (filter plugging). Both pore size filters were found to be about 99 percent efficient by weight on atmospheric particulate matter at a test flow rate of 3 cfm. This is considered quite satisfactory and the ten micron pore Teflon is recommended for general use whenever low chemical background is important. In analysis, the particulate matter is actually dissolved out from the Teflon filter, leaving the filter intact. If the Teflon filter is pre-cleaned it will contribute almost no chemical background to the analysis.

Assuming a complete analysis of an aerosol is to be made, a stepwise procedure is outlined below. Explanations are given for several of the step procedures.

1. Drum Rotational Speed Selection

Based on a desired sampling time, sample time resolution, dust concentration and deposit density limitations, a suitable rotational speed is selected and set for the collection drums (all drums rotate at the same rate). One revolution in 24 hours is adequate for normal atmospheric sampling, one revolution per hour for factory air sampling, and one revolution per minute or less for sampling a dirty source.

2. Air Flow Rate Selection

Based on the desired particle size fractionation (which in turn is based on particle density), volume of air to be sampled, dust concentration, and amount of sample needed for analysis, a suitable flow rate is selected and set. Normally, the flow rate is set reasonably high (2 to 5 cfm) to enable collection of as much particulate material as possible and to allow particle size fractionation at the smallest size possible. The high flow rate obtainable with the impactor is often a great advantage.

3.A. Collection Surface Preparation - For Weight Determination

a) Cut pieces of film to proper size.

b) Wash film and drum in clean acetone to remove any grease or dirt.

c) Weigh film and after filter.

d) Stretch film over drum surface and fasten in place.

e) Install drums in impactor and filter in filter holder.

f) Sample for desired time.

g) Remove drums from impactor.

h) Remove films and filter (containing collected particle matter) and weigh. Weights should be made at a reference humidity because the particle matter does pick up and lose water.

i) Examine film under microscope and photograph if desired. Film (or film strip) is then ready for chemical analysis.

j) Analyze.

If weight determinations are not required, the collection surface preparation is as follows:

3.B. Collection Surface Preparation - No Weight Determinations

a) Cut pieces of film to size.

b) Wash film and drum in clean acetone.

c) Stretch film over drum surface and tape down film ends.

d) Sample as desired.

e) Remove film, cut off taped ends, examine or analyze as desired.

Analysis Procedure

Once a sample has been obtained, it is ready for analysis. If weights are to be determined, this is done first. The film is removed from the collection drums and the filter from the filter holder; both are allowed to equilibrate to some reference temperature and humidity before weighing. Microscopic viewing of a sample is done after weighing (or done first if weights are not to be made). Changes in particulate deposit density with time can often be seen directly on the film; these changes can be determined by particle count as a function of deposit position (or time) or by cutting the collection surface film into time based strips and analyzing. The large collection surface area greatly facilitates division of the collected samples. All impactor nozzles are two inches high and produce a uniform collection deposit over this height. If two different analyses or sample extraction procedures are to be run on the same sample, or if analysis replication is desired, a simple method for obtaining duplicate samples is to divide the two-inch deposit into halves--or even into fourths. Weight determinations cannot be made on the cut film sections because the initial weight cannot be determined accurately.

Heavy film deposits can be examined by techniques such as infrared absorption spectroscopy, X-ray diffraction, etc. In this way, deposit density changes or composition changes can be read directly off from the film, thereby giving the composition or concentration changes as a function of time within each of the various particle size ranges.

Normally the particulate is removed (or dissolved) from the film for analysis; using water, for example, to determine sulfate or nitrate, or acid to determine elements such as iron or lead (the Teflon film is not dissolved). Background levels for analyses such as these were found to be very low; therefore, very small quantities of material can be detected. Many methods of chemical analysis can be used to analyze the particulate coated Teflon films.

Electron microscope grids can also be attached directly to the drum for subsequent viewing or for analysis of individual particulates by electron microprobe or particulate crystals by electron diffraction. Two-sided sticky tape has worked well for fastening grids onto the drums.

All collection-analysis methods have limits. These limits are determined by: 1) the sensitivity of the analysis procedure; 2) the background level of the component to be detected; 3) the concentration of that component in the aerosol; and 4) the amount of aerosol sampled.

Example: If ambient air containing 100 $\mu g/M^3$ suspended dust is sampled for a 4-hour period at a 3 cfm flow rate, then about 2 mg of particulate will have been collected out on the four impactor stages plus the after filter, giving an average of 0.4 mg (20% of 2 mg) per collection surface. The actual amount per section will normally vary widely. Atmospheric air sampling results have shown that the cleanest film may have less than 1% of the total dirt and the dirtiest film have over 50% of the total dirt collected.

Results

Although results are not part of this method writeup, the type of information obtainable with the described sampling instrument is best illustrated by example. During November 1968, the Lundgren Impactor was used to obtain 10 samples of atmospheric particulate matter. These samples, all obtained on the Riverside campus of the University of California, were analyzed as follows:

1) Particulate weight distribution determined (based on the dry particle weight obtained by desiccating the samples for 6 hours at room temperature and pressure in a desiccator containing drierite, or $CaSO_4$).

2) Water soluble fraction extracted and analyzed for sulfate and nitrate by standard wet chemical methods.

3) Nitric acid fraction extracted and analyzed (in addition to part of the water soluble fraction) by atomic absorption spectrophotometry for lead and iron.

Results for these ten tests are plotted in Figure IV-3 as µg of the particulate, nitrate, etc., per M^3 of air sampled for each of the four impactor stages plus the impactor after filter. In all cases, samples were run from 4 p.m. of one day until 8 a.m. of the next. Air sampling rate was held constant at 2.9 cfm for all runs except number one which had a flow of 4.0 cfm. Based on a density one spherical particle and a 2.9 cfm flow rate, the impactor 50% cut point diameters are: greater than 17µ on stage one, 5.2 to 17 on stage two, 1.7 to 5.2 on stage three, 0.5 to 1.7 on stage four and less than 0.5 on the after filter. None of these tests run were divided into time fractions; therefore, the numbers given represent averages over the 16-hour sampling periods.

The data for these ten runs were used to obtain an average distribution for a total particulate weight, sulfate, nitrate, lead and iron. Figure IV-4 is a log probability plot of these weight averages vs. particle diameter. Again, the diameter is based on an assumed density one spherical particle. Microscopic examination of the collected particulates indicates this assumption was reasonably good for photochemical aerosols around one micron diameter. In noting the differences in the mass median diameters and distributions shown in Figure IV-4, it is important to remember that they are all based on the same samples--not different samples taken at different times.

Summary

The Lundgren Impactor was described as well as the procedure for using it to obtain samples of time-separated, size-classified particulate matter. This procedure was outlined in a detailed step-by-step manner. Various methods by which the obtained samples can be analyzed were mentioned. Results from the analysis of ten samples were presented to illustrate the type of data that can be obtained using the described sampling instrument.

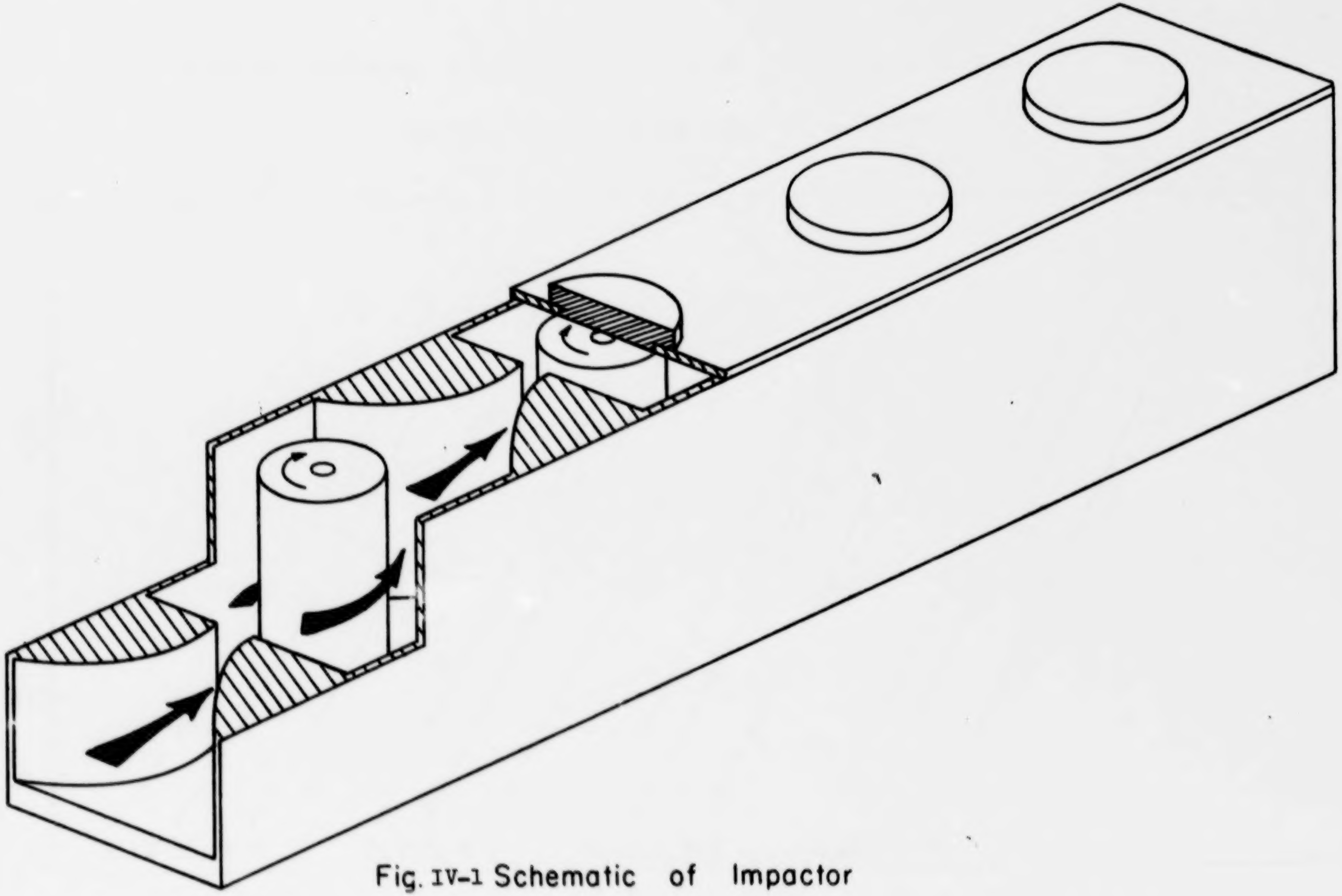

Fig. IV-1 Schematic of Impactor

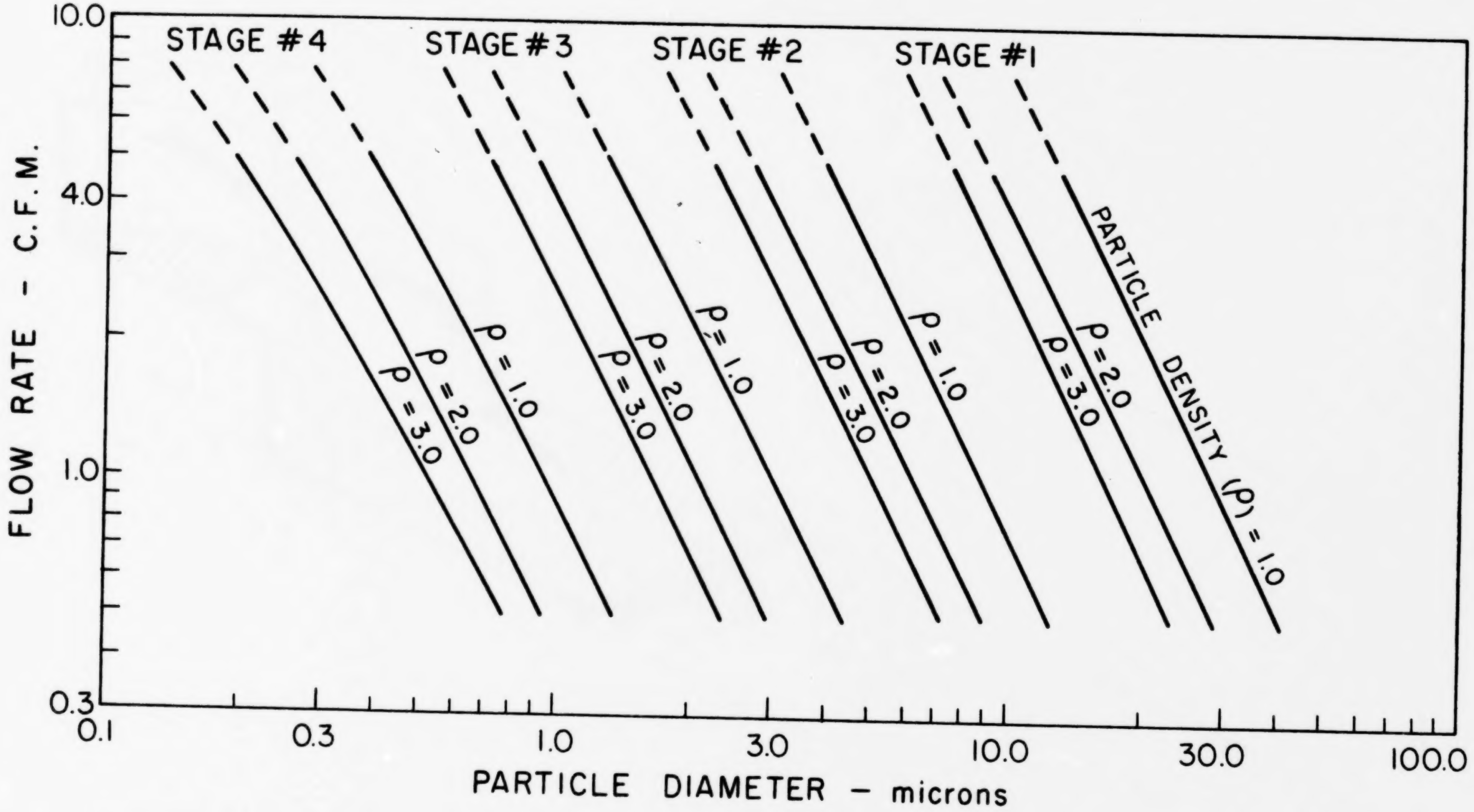

Fig IV-2 Lundgren Impactor Calibration Giving The 50% Cut Size

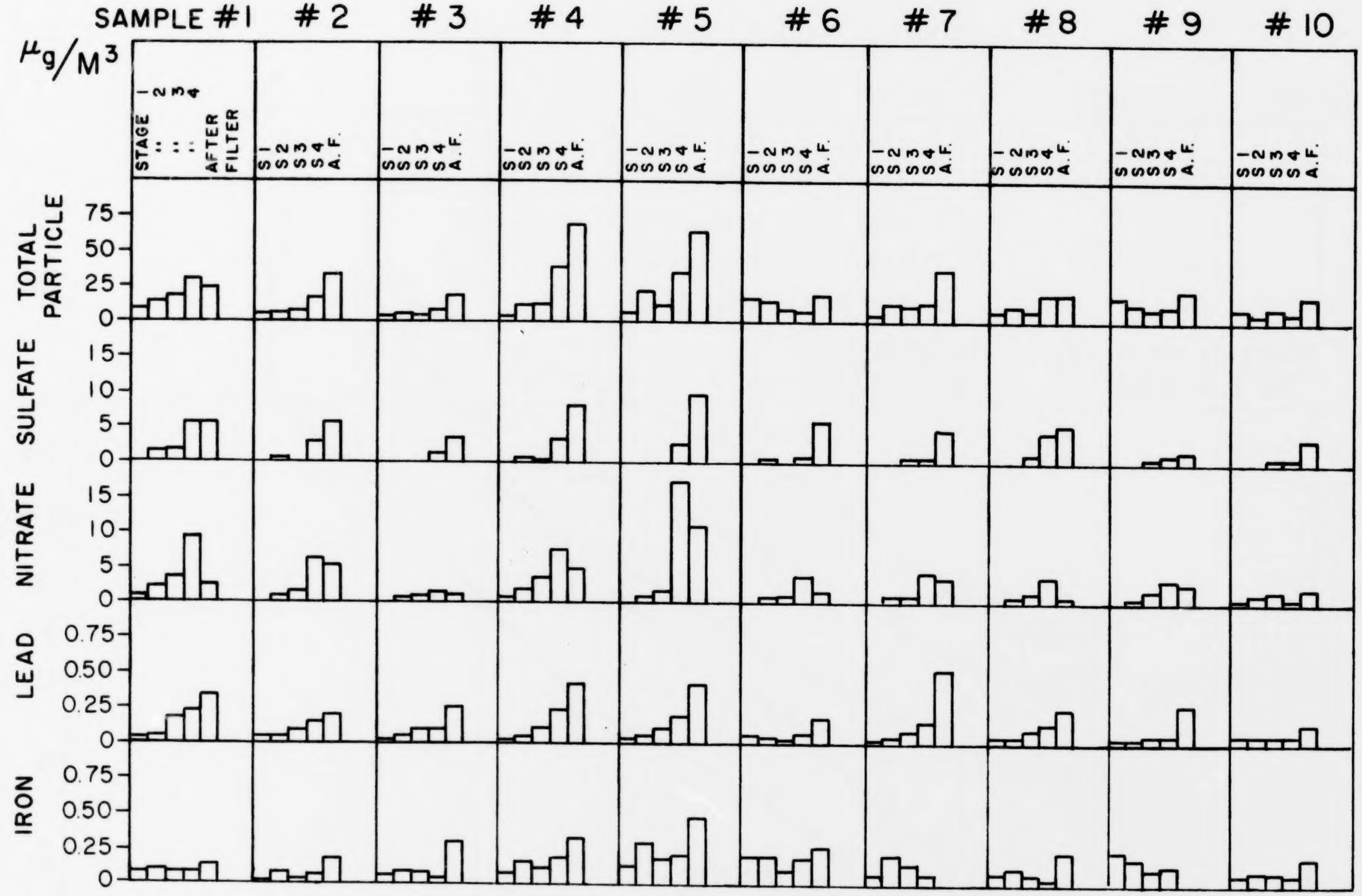

Fig. IV-3 Plot of Impactor Analysis Results. **From 1968 Riverside Study**

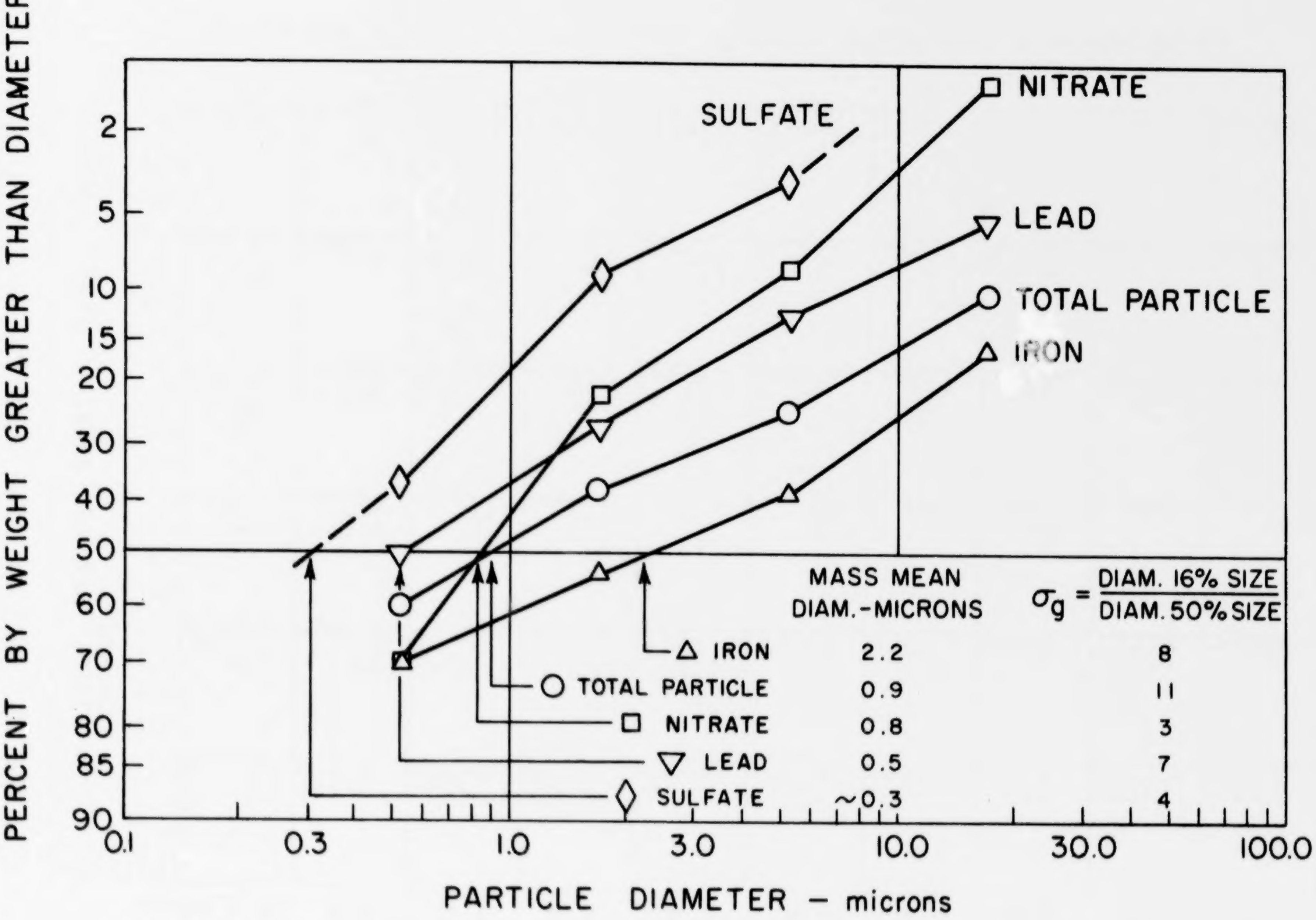

Fig. IV-4 Average size distributions for 10 impactor samples. **From 1968 Riverside Study**

References

Whitby, K.T., R.B. Husar, A.R. McFarland and M. Tomaides (1969), "Generation and Decay of Small Ions", U. Minnesota Particle Technology Lab, Publ. No. 137.

Whitby, K.T. and W.E. Clark, "Electric Aerosol Particle Counting and Size Distribution Measuring System for 0.015 to 1 μm size range", Tellus XVIII, (1966) pp. 573-586.

Fuchs, N.A., I.B. Stechkina and V.I. Staroselskii (1962), "On the Determination of Particle Size Distribution in Polydisperse Aerosols by the Diffusion Method", Brit. Journn. Appl. Phys. **13**, pp. 280-281.

Husar, R.B., "The Size Distribution of Coagulating Submicron Aerosols", Thesis, (1971), University of Minnesota

SECTION V

Short Summary
University of Washington

1969 SMOG EXPERIMENT

R. J. Charlson and N. C. Ahlquist
Water and Air Resources Division
Department of Civil Engineering

1. Description

The University of Washington experiment, conducted by Professor Robert J. Charlson and Mr. Norman C. Ahlquist, consisted mainly of light scattering measurements made with three integrating nephelometers (Ahlquist and Charlson, 1968, 1969). Dew point and instrument temperature were also recorded. The instruments were:

1) a four channel instrument operating in four very narrow wavelength bands located at 360, 436, 546 and 675 nm.
2) a broad-band device covering the wavelength range from 420 to 550 nm.
3) a device with a medium wavelength band located at 550 nm approximating the response of the human eye.

2. Purpose

The initial purpose of this portion of the experiment was to gather data on real L.A. smog. These data necessarily must be compared and correlated with the measurements by the other groups in order to put the results into proper perspective. The goals fall into three classes:

1) Experiments with 3 nephelometers and one hygrometer alone:
    a) Correlation of broad-band and narrow band light scattering coefficient with wavelength dependence as a parameter.

L. A. provides a sufficiently variable aerosol for such a study.

- b) Relation of light scattering to humidity.
- c) Relation of light scattering to visibility utilizing Weather Bureau data for visibility.

2) Experiments relating nephelometers and hygrometer data to that from other experimentors.
   - a) Relationship of wavelength dependence of light scattering (Ångström exponent, α) to size distribution (Junge exponent, β). (University of Minnesota)
   - b) Mass concentration - light scattering correlation with α as parameter (Dale Lungren).
   - c) Extinction due to light scattering compared to that by NO_2 (State of California).
   - d) Correlation of light scattering with gaseous pollutants (State of California).

3) Experiments or interpretations which will arise as a result of observations.

3. Initial Data Summary

The instruments were operated continuously for the period from 13 August to 3 September. No failures occurred except for the dew point hygrometer which began to behave erratically about halfway through the period. The light scattering levels covered a range (at 546 nm) from below $1 \times 10^{-4} m^{-1}$ to over $10 \times 10^{-4} m^{-1}$. A study of the first weeks' data show an extremely high correlation of broadband and monochromatic light scattering coefficient. Perhaps the most dramatic and interesting effect is the occasional high correlation of light scattering and dew point. At other times the correlation is nil. Data reduction is currently in progress, and more results can be anticipated.

Summary - 1969

Los Angeles Smog Measurements

University of Washington Experiments

R. J. Charlson and N. C. Ahlquist
Water and Air Resources Division
Department of Civil Engineering
University of Washington
Seattle, Washington 98105

I. INTRODUCTION

Four separate instruments, all located at the end of about 5 meters of approximately 3.5 cm diameter plastic tube, were operated for the period of 13 August to 3 September 1969, inclusive. These instruments were:

1) A multi-wavelength integrating nephelometer.
2) A broad-band integrating nephelometer.
3) A narrow band, photopic-characteristic integrating nephelometer (MRI).
4) A dew point hygrometer.

The following discussion will consider these in sequence, including calibration and accuracy information, data format and the recorder interface arrangement. Finally, the basic purpose of the University of Washington participation will be outlined.

II. MULTI-WAVELENGTH INTEGRATING NEPHELOMETER

A. Description

A detailed description of the instrument was published by Ahlquist and Charlson (1969). Briefly, it measures the extinction coefficient due to light scattering, b_{scat}, at four separate wavelengths; 360 ± 15 nm, 436 ± 5nm, 546 ± 5nm, and 675 ± 15nm. Figure V-1 is a curve of the relative response of the four channels as set up for the 1969 SMOG Experiment. The instrument includes electronic analog devices which transform the signal to a logarithmic form, i.e. so that the logarithm of b_{scat} is recorded rather than b_{scat} itself. There are two reasons for this.

1) The logarithmic format increases the usable range of the instrument.

2) The logarithms facilitate further analog computation.

Specifically, the Ångström exponent, α, defined by

$$b_{scat} = C\lambda^{-\alpha}$$

for wavelength λ and a constant C, can be given as

$$\alpha = -\frac{d\log b}{d\log\lambda}$$

This in turn can be approximated by the finite difference form

$$\alpha \cong -\frac{\Delta\log b}{\Delta\log\lambda}$$

which is rigorously correct if the original power-law holds, and is only approximate and dependent on the appropriately small magnitude of $\Delta\log b$ and $\Delta\log\lambda$ if the power law is not valid.

The instrument produces voltage signals proportional to $\log b_{scat}$ for each of the four wavelengths, and the differences between them thus provide three independent values for α. Each of the three values of α applies to a given spectral range between bands in the instrument.

Air for this (and the other devices) was pumped through the instruments with a Rotron blower (Model 250 AS) throttled at its exhaust to reduce the flow rate and pressure drop. The pressure in the instruments ran approximately 7 cm H_2O below atmospheric. The temperature of the air was typically 5° to

10°C above that outside, due to heat dissipation by the large amount of electronic equipment in the room. Temperature and dew point were therefore recorded.

B. Calibration

The multiwavelength instrument (and the other nephelometers as well) were calibrated with particle free gases (filtered through Gelman type E filters) primarily air and Freon-12 (CCl_2F_2). Figure V-2 is a graph of the light scattering coefficient of these gases as a function of wavelength, with the points for the specific wavelengths noted. In addition to the gas calibration, a wire of approximately 0.5 mm diameter coated with MgO from freshly burned magnesium was used to provide a large scattering coefficient with $\alpha = 0$, i.e. with the same scattering at all wavelength. Thus, a separate calibration for the recorded Ångström exponent was possible, with $\alpha = 4$ for Freon 12 (a Rayleigh scatterer) and $\alpha = 0$ for MgO. The only other factor effecting the independent measurement of α (that is, independent of the absolute accuracy of the log b_{scat} calibration) is the quality of the logarithmic function generator. These devices were checked and were consistently good to within 1% over three or more decades of input signal. Thus, the value of α is best obtained from the separate recording of the quantity based on this calibration rather than from calculations made on measured light scattering coefficients.

C. Accuracy

There are several necessary accuracy statements for the multiwavelength integrating nephelometer. First is the absolute accuracy of the instrument independent of strip chart reading errors or the adjustment of the position of the trace on the strip chart. This quantity is pertinent as the controlling factor for data going to the University of Minnesota data system. The absolute accuracy depends on

1) The Rayleigh scattering of the gases.
2) The angular truncation error.
3) The other "instrument constants" such as the non-ideality of the cosine source.

These have been evaluated in a preliminary study and amount to +5%, -10% of b_{scat} for most cases. This error is constant for a wide range of atmospheric aerosols.

The next accuracy figure relates to the reproduceability of the reading for a given scatterer with fixed properties such as a gas, i.e. the relative accuracy. This figure is controlled by drift and signal/noise ratio, and is less than ± 5% of b_{scat} in magnitude.

Next is the reading accuracy for b_{scat} on the logarithmic scale. This figure is pertinent for data read from the University of Washington strip chart recorder but not for data on the data system. This accuracy is determined to be about ± 15%, including the error in adjustment of signal position during Freon calibration. Last is the accuracy of the recorded and tabulated values for the Ångström exponents, of which two were recorded in the experiment. The first value of α was obtained over the spectral range from 436 to 546 nm, and the second α up between 436 and 675 nm. (The latter difference was chosen to improve the signal to noise ratio.) Both were separately calibrated with Freon-12 ($\alpha = 4$) and MgO ($\alpha = 0$). Using the reproduceability of both MgO and Freon-12 signals as a measure of system accuracy (i.e. assuming the log generators remained stable) an error of less than ± 0.1 (dimensionless) unit of α is obtained. The reading accuracy for tabulating this quantity is very good because the scale of 0 to 4 units spans eight inches of chart, so the accuracy of ± 0.1 unit is appropriate.

The Ångström exponent can also be determined from the digitally recorded values of log b_{scat} on the data system, and depends on the existence of good calibration information on the magnitude of signals for Freon-12 and MgO in the data system, or on a post-computed value from the strip chart.

Since α is obtained by the subtraction of voltages which represent log b_{scat}, the value is independent of the absolute accuracy of the measurement of b_{scat} for either the strip chart or the data-system case. In the latter case, the accuracy depends on the calibration of the data system in α units. A good calibration was obtained and the data is shown in figure V-4.

Calibration checks of the multiwavelength nephelometer were performed frequently during the experiment. The times and operations accomplished are listed in Table I for comparison with the data system.

III. BROAD BAND INTEGRATING NEPHELOMETER

A. Description

The broad band device has identical optical geometry to that of the multiwavelength version, the only difference arising in the wavelength characteristic. This instrument has been used for a large number of published experiments, for instance relating aerosol mass concentration to light scattering (Charlson, Ahlquist and Horvath, 1969). As such, it is a more or less "standard" instrument against which others can be compared. The relationship between the outputs of these instruments is a present subject of study. Particle free air and Freon-12 were again used for calibrations, and the same sort of accuracy figures result as for the multiwavelength device. The only question on calibration is the effective wavelength of the instrument. Wavelength definition is controlled by a Wratten 2A filter (minus UV) the spectral characteristic of the light source and the S-11 characteristic of the photocathode. Since the effective center of this broad band is determined by the wavelength dependence of the intensity of scattered light, and since α varies from perhaps 1 to 2 for aerosol and is 4 for calibration gas, some variation exists in the effective wavelength of the instrument. Preliminary empirical studies have shown that the shift in the effective wavelength for these different values of α is small; however, one purpose of the experiment is to more fully study this problem. The value of $3.6 \times 10^{-4} m^{-1}$ used (in the broad-band device) for Freon-12 is based on empirical studies which resulted in an effective wavelength of approximately 500 nm. This value includes a correction for angular truncation error. The strip chart recorder sensitivity used for this instrument was 0 to $20 \times 10^{-4} m^{-1}$ full scale.

B. Accuracy

As a result of these considerations, it is possible to conclude that the overall absolute accuracy of the broad band device is about ± 10% for scattering centered at approximately 500 nm. The relative accuracy or reproduceability is better than ± 5% for most scattering levels encountered. The reading accuracy on the strip chart is somewhat better than that of the logarithmic scale of the multiwavelength instrument, and amounts to 1% of full scale, or approximately $0.2 \times 10^{-4} m^{-1}$.

IV. NARROW BAND, PHOTOPIC FILTER, INTEGRATING NEPHELOMETER (MRI MODEL 1550)

A. Description

The Meteorology Research Incorporated Model 1550 prototype nephelometer, provided by MRI, was fitted with a Kodak Wratten #106 filter on 19 August 1969 in order to more closely match the instrument to the response of the human eye. The calibration was performed in a fashion identical to that of the other two nephelometers. Due to a design flaw in the prototype (corrected in production) the angular range over which integration occurs was somewhat decreased, with a resultant higher negative truncation error. As a result, the calibration necessarily had to take account of the extra truncation. The simplest calibration is to utilize the monochromatic scattering at 546 nm as determined by the multiwavelength device. Figure V-3 is a graph of percent full scale deflection for the MRI instrument on both the University of Washington and the MRI strip chart recorders versus the 546 nm scattering for several periods early in the experiment (following 19 August). Since the University of Minnesota data system was operating during the morning of 20 August the value of 13 x $10^{-4} m^{-1}$ at 13:15 hours can be used as a reference point.

The recorder sensitivity is equivalent to 0-30 full scale with zero light scatter at 2% of full scale. The accuracy of the instrument appears to be about ± 7%.

V. DEW POINT HYGROMETER

A Cambridge Instrument Model 880 thermoelectric dew point hygrometer was installed with its air sample coming from the air ducts immediately in front of the nephelometers. The calibration and accuracy figures provided by the manufacturer suggest a ± 1°C absolute accuracy and a precision of ± 0.3°C. However, this instrument began to malfunction on 31 August and data from 0000 31 August to 1200 2 September are suspect. The instrument was usable from 1200 PDT 2 September until 2000 PDT 3 September when experiment was terminated.

VI. DATA SYSTEM INTERFACE

Some, but not all, of the University of Washington data were stored by the University of Minnesota data system. All the University of Washington data were, however, recorded on a Leads & Northern Model W multichannel strip chart recorder. These data are being read and will eventually be available on punch cards for the other participants use. The data entered on the University of Minnesota system were:

Channel of U.M. Data System	Input	
19	Light scattering	675 nm
20	Light scattering	546 nm
21	Light scattering	436 nm
22	Light scattering	360 nm
23	MRI nephelometer	550 nm after 19 August

Figure V-4 is a graph of the voltage fed to the U.M. data system as a function of light scattering coefficient for the four monochromatic channels only, (i.e. channels 19, 20, 21, and 22). The Ångström exponent, which was recorded directly on the U.W. strip chart recorder, can be computed from the difference signals of the log b_{scat} signals. The difference voltages for $\alpha = 0$ are zero, and the difference voltages for Rayleigh scatter (i.e. $\alpha = 4$) are given in the figure. Figure V-5 gives the voltage for the MRI Nephelometer as a function of light scattering at 546 nm.

Punch cards with hourly readings (5 minute averages) of all variables for the whole period will be prepared. In addition, periods of special interest will be tabulated on a shorter time base. Xerox or ozolid prints of the strip charts can be prepared if necessary for selected periods. The variables recorded on the strip chart recorder at a speed of two inches per hour were:

Channel of Strip Chart Recorder	Variable
1	b_{scat}, 546 nm, log scale
2	------- blank

3	b_{scat}, 436 nm, log
4	b_{scat}, 360 nm, log
5	α ($\Delta \log b_{scat}$, 436 to 546 nm), linear scale
6	α ($\Delta \log b_{scat}$, 436 to 675 nm), linear
7	b_{scat}, 675 nm, log
8	b_{scat}, broad bond, linear scale
9	b_{scat}, MRI, 550 nm photopic, linear
10	Dew point
11	Instrument temperature
12	------- blank

Instruments response times of ∿1 minute were maintained throughout the experiment.

VII. PURPOSE OF UNIVERSITY OF WASHINGTON EXPERIMENTS

The discussions of the purpose of this effort is, of course, of primary importance since it governs the conduct of the work. In most cases, the discussion of purposes and goals precedes the technical description. However, the measurements and instrumental capabilities outlined above dictated the type of experiments which could be done in a cooperative program. As a result, the technical capability is presented first and the purpose later. It should be noted, of course, that these measurement techniques were developed expressly for the purpose of making measurements of important atmospheric properties; it is in the cooperative context that technique precedes purpose.

The boundary condition for this whole effort is that several groups of atmospheric aerosol and atmospheric chemistry researchers should study the same air in a true Los Angeles smog situation. Nonetheless, each group still had the capability for making its own independent observations exclusive of the cooperative aspect. As a result, a variety of experiments were performed. Those participated in by the University of Washington group fall into three distinct classes:

a) Experiments done by the U. W. workers alone.

b) Experiments done and pre-planned with other workers.

c) Experiments or data evaluation arising as a result of observations made during the data-taking period.

These can be further described:

a. Experiments with three nephelometers and one hygrometer alone.

 1. Correlation of broad-band and narrow band light scattering coefficient, with wavelength dependence (α) as a parameter. Los Angeles smog provides a sufficiently variable aerosol for such a study. Preliminary data indicate a high correlation without stratification with respect to α. Further data reduction should show how important α is to the measurement problem.
 2. Relation of monochromatic and broad-band light scattering coefficient to humidity. Previous experiments with maritime (sea-salt) aerosol have shown effects only above 60 or 70% Relative humidity. Preliminary L.A. data indicate an occasional strong dependence at lower values of R.H.
 3. Relation of light scattering to visibility, utilizing Weather Bureau data for visual range. No preliminary data analysis was made in this regard.

b. Experiments relating nephelometer and dew-point hygrometer data to that from other experimentors.

1. Relationship of wavelength dependence of light scattering (Ångström exponent, α) to the size distribution (Junge exponent, β). A simple relationship between these has been suggested by Van de Hulst and others (Ahlquist and Charlson, 1969) namely that:

$$\alpha = \beta - 2$$

when a power law size distribution holds. For the more complex case of a non-power-law distribution, a relationship can be obtained via Mie scattering calculations (Quenzel, 1969). The combined experiments of University of Washington and the University of Minnesota groups should provide an excellent test of the theories. Preliminary observations suggest that the simple theory may be correct if a power-law size distribution exists.

2. Correlation of light scattering coefficients and mass concentration. It has been suggested by Charlson, Ahlquist, and Horvath (1968) and by Horvath and Charlson (1969) that there exists a sufficiently high correlation between these two variables to permit the use of light scattering as an index of the atmospheric aerosol concentration. Heretofore, experiments were limited to gross measurements of broad-band scattering and total mass. This experiment has a more refined mass determination as a function of particle size, thereby testing directly the importance of size distribution. The main collaborators in this connection would be the University of Washington group, Dale Lundgren and the University of Minnesota group.

3. Extinction coefficient due to scattering compared to that by NO_2.

Charlson and Ahlquist (1969) suggested that the brown color of some smogs might be largely due to the wavelength dependent extinction due to scattering rather than that of NO_2. The University of Washington data in comparison to the State of California data (Dr. Mueller et.al.) should help to clarify this point.

4. Correlation of light scattering with other gaseous pollutants. These data (University of Washington and State of California) should shed some light on the causes of visibility reduction.
5. Experiments or data evaluation (interpretations) which developed as a result of observations made during and following the experimental period. One possible study is that of the apparent increase in particle count in the Royco counter correlated to the nephelometer indication. The full development of this portion of the experiment can only be discussed after the data on processed and thoroughly discussed by all participants.

REFERENCES

1. Ahlquist, N. C. and Charlson, R. J. (1969), Atmospheric Environment, 3, Number 5, September.
2. Charlson, R. J., Ahlquist, N. C., and Horvath, H., (1968), Atmospheric Environment, 2, 455-64.
3. Quenzel, H., (1969), presented orally at the CACR meeting, Heidelberg. To be published in JGR.
4. Horvath, H. and Charlson, R. J., (1969), J. American Industrial Hygiene Assoc., in press.
5. Charlson, R. J., and Ahlquist, N. C., (1969), Atmospheric Environment, in press.

TABLE V-1

Periods when Multiwavelength Nephelometer was being calibrated.

	CCl_2F_2	MgO
14 Aug.	1215-1315	1415-1515
15 Aug.	1745-1815	1630-1730
17 Aug.	1325-1345	1245-1305
18 Aug.	---	1145-1330
18 Aug.	2115-2245	2100-2115
19 Aug.	---	---
20 Aug.	---	1500-1630
21 Aug.	---	0900-0915 1725-1745
22 Aug.	---	2145-2200
27 Aug.	---	0800-0815
27 Aug.	---	1915-1935
31 Aug.	---	1445-1450
2 Sept.	1900-1935	1700-1730
3 Sept.	---	1825-1850

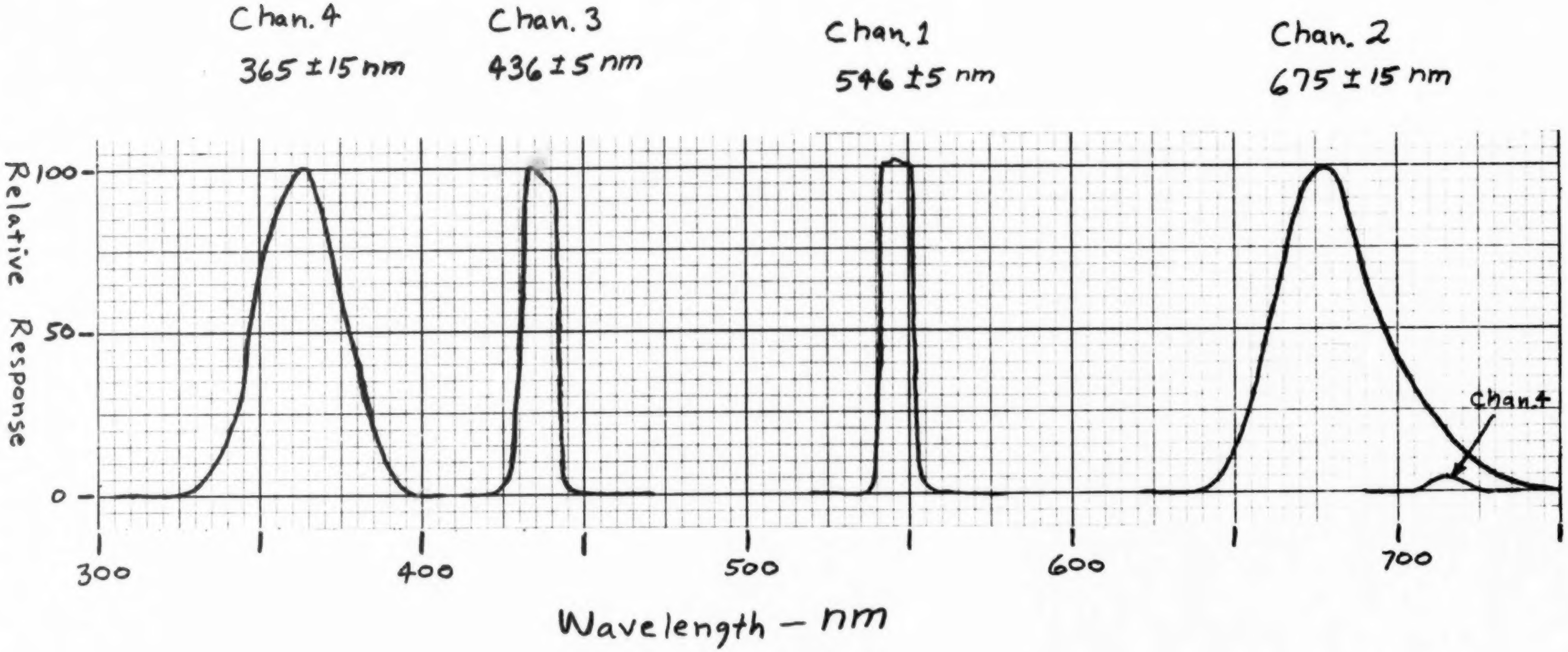

Figure V-1 Relative response of multiwavelength integrating nephelometer as a function of wavelength.

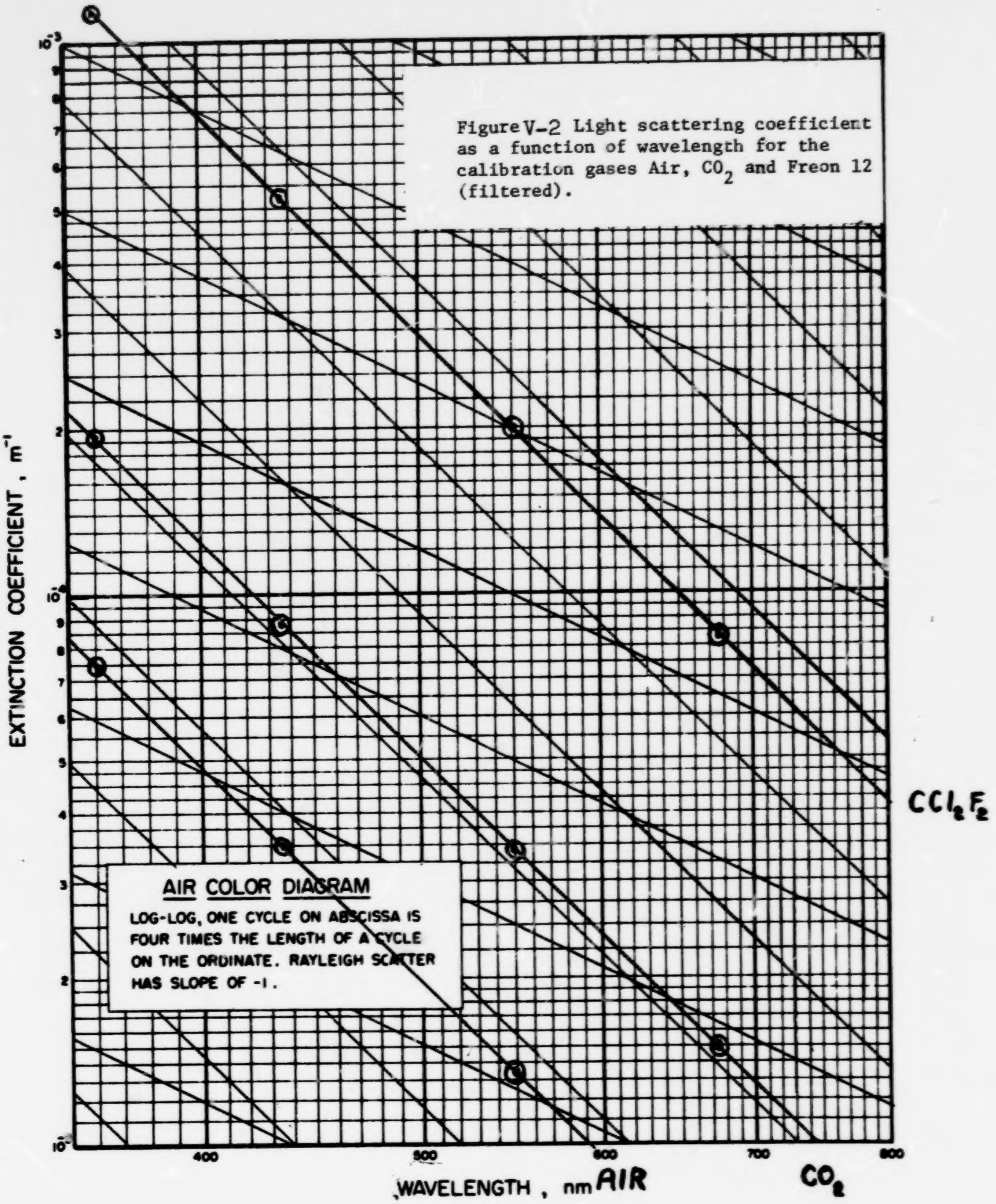

Figure V-2 Light scattering coefficient as a function of wavelength for the calibration gases Air, CO_2 and Freon 12 (filtered).

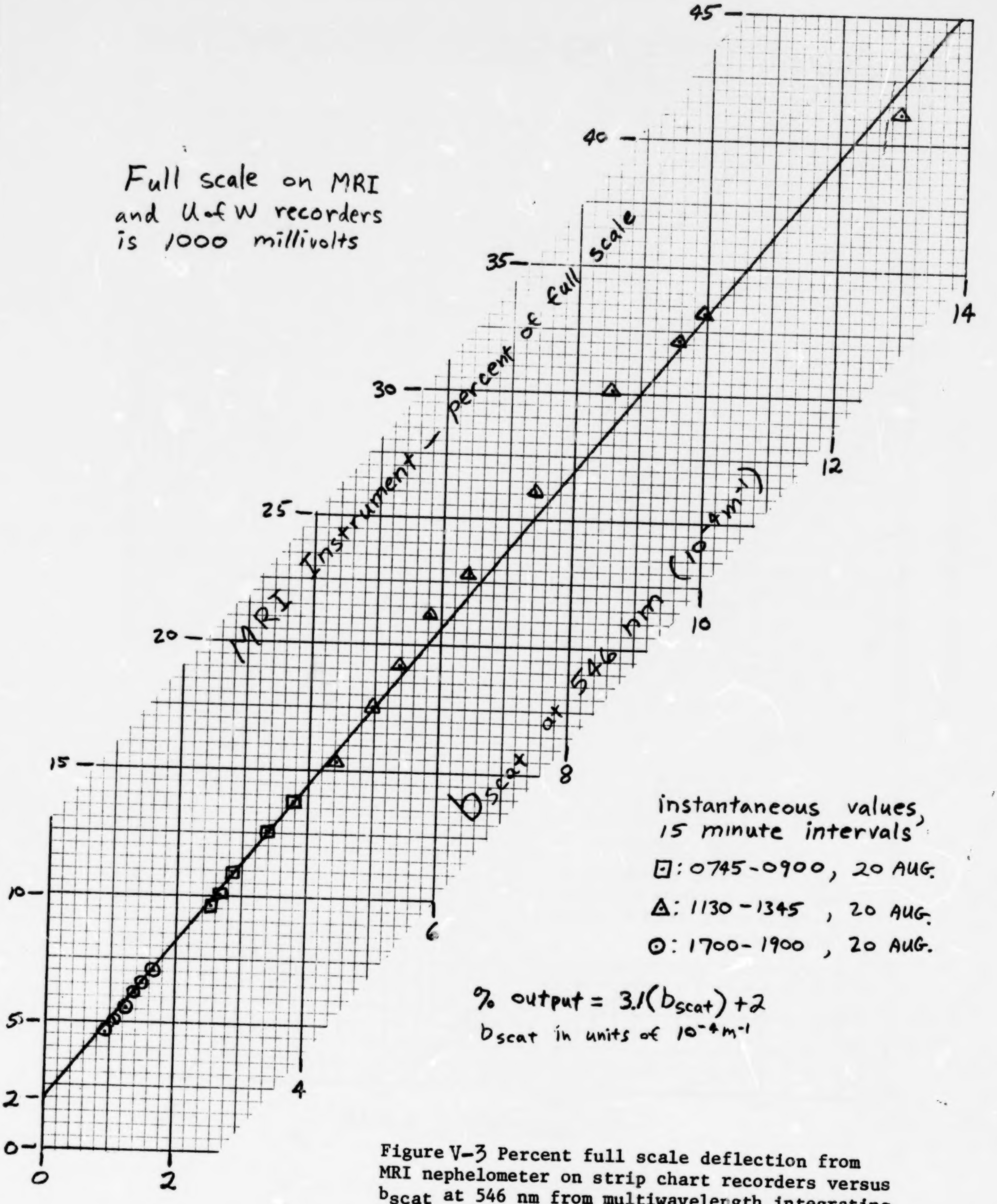

Figure V-3 Percent full scale deflection from MRI nephelometer on strip chart recorders versus b_{scat} at 546 nm from multiwavelength integrating nephelometer, demonstrating high correlation between broad band and monochromatic scattering.

Data System Channel	Wavelength	$b_{scat} \times 10^{-4} m^{-1}$ CCl_2F_2
19	675 nm	.85
20	546	2.0
21	436	5.2
22	365	11.2

Difference Signal for Rayleigh Scatter ($\alpha = 4$)

Chan:	Volts
365-436	0.938
436-546	1.175
546-675	1.07

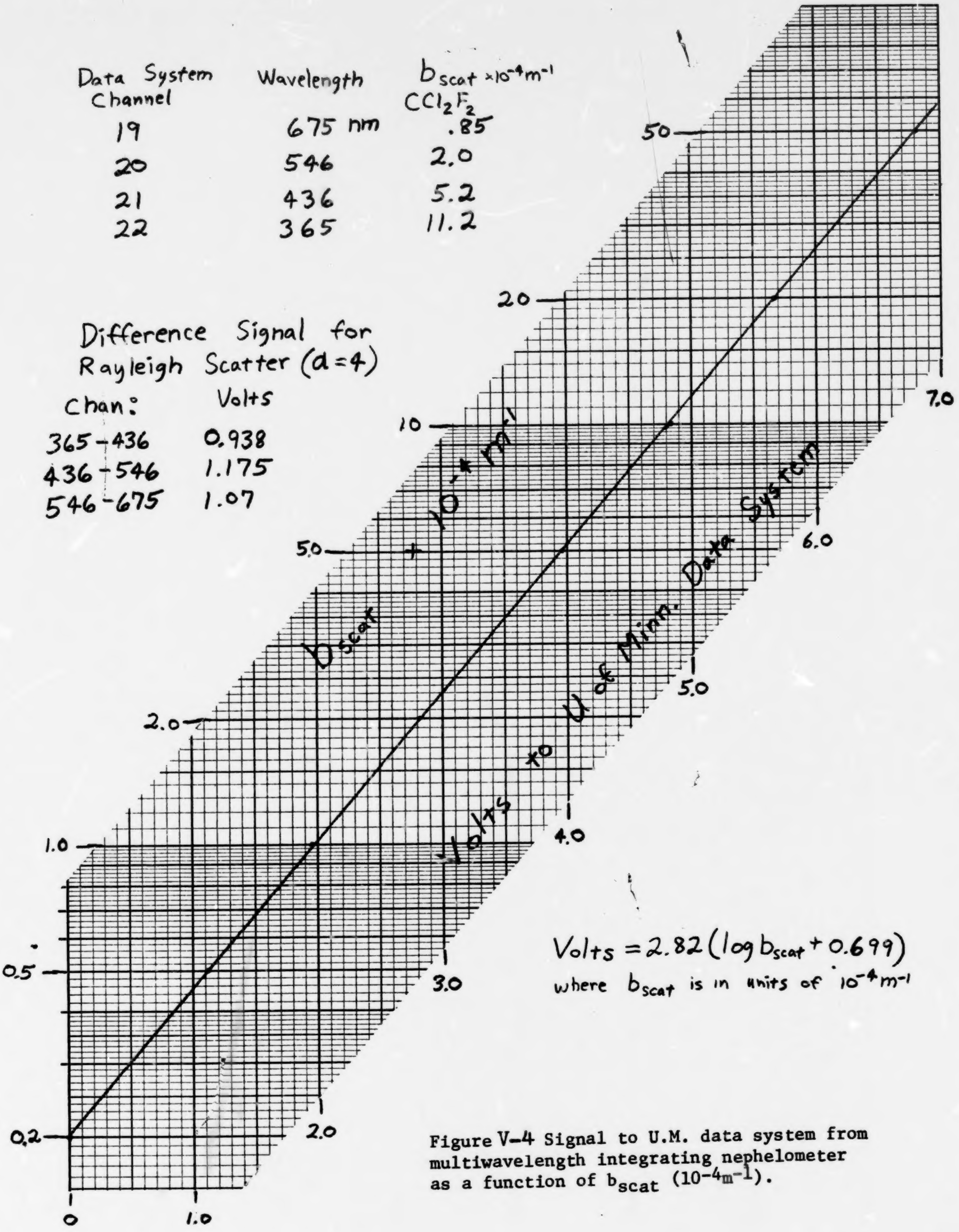

$$\text{Volts} = 2.82(\log b_{scat} + 0.699)$$

where b_{scat} is in units of $10^{-4} m^{-1}$

Figure V-4 Signal to U.M. data system from multiwavelength integrating nephelometer as a function of b_{scat} ($10^{-4} m^{-1}$).

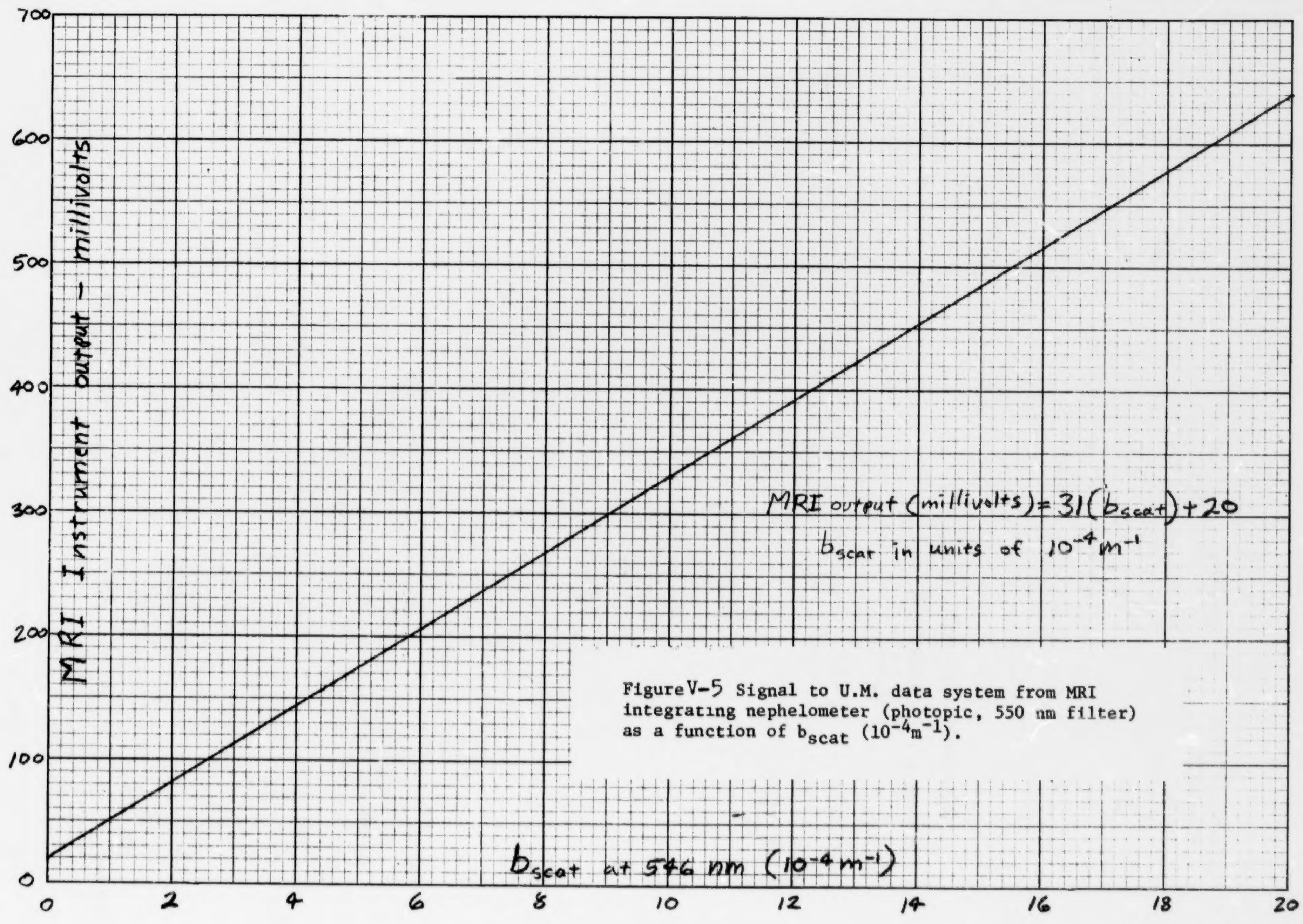

Figure V-5 Signal to U.M. data system from MRI integrating nephelometer (photopic, 550 nm filter) as a function of b_{scat} ($10^{-4}m^{-1}$).

DESCRIPTION OF CHEMICAL DETERMINATIONS IN THE LOS ANGELES SMOG AEROSOL STUDY
(Reporting Phase I)

AIHL REPORT NO. 78

Parts prepared by:

P.K. Mueller and Y. Tokiwa
Chief and Associate Public Health Chemist

February 1970

DESCRIPTION OF CHEMICAL DETERMINATIONS IN THE LOS ANGELES SMOG AEROSOL STUDY

I. Purpose

This paper is a portion of a collaborative study conducted to determine the physical and chemical properties of Los Angeles smog aerosol. As a part of this study, the levels of oxidant, ozone, NO_2 and PAN were continuously monitored with various gas analyzers. Particles were collected for chemical analysis and for electron microscopy. Visibility was measured by a nephelometer. Wind speed and direction were also monitored continuously.

The purpose of this part in the study is to provide information on gas concentrations in the aerosol sample under study and to provide auxillary information on particles in the form of mass and visibility.

The second purpose of this part in the study is to determine and compare the response of four (4) different oxidant analyzers when sampling smoggy atmospheres. Because of unresolved uncertainties in performance of these analyzers, the results of this comparison will enable making the best possible estimate of the actual ozone concentration.

The reports of this study are to be prepared in phases. The results and interpretation of the data will be subjects of other reports. There are several applications of this data. One already well under way in collaboration with Dr. Charlson's group concerns the interaction of particles and NO_2 as factors causing visibility reduction.

II. General Description

A. Location and Period of Study

The Los Angeles smog aerosol was sampled at the California Institute of Technology in Pasadena, California. All gas analyzers and equipment were located in a large air conditioned laboratory in the basement of the Keck Environmental Sciences building. The continuous gas analyzers were operated in conjunction with the study from August 19 to September 19.

In order to gain additional data concerning the comparability in performance between the various oxidant analyzers, this portion of the study was extended until the end of October. In addition to the analyzers listed on Table VI-I, a two-stage particle sampler for collecting size segregated samples on glass fiber filters was added to the study. The pollutants monitored, analyzer reagent and detector as well as the major interferences for each analyzer are summarized in Table VI-I.

In addition to the oxidant analyzers, the known interferences NO_2, PAN and SO_2 were also continuously monitored. In addition, integrated samples for carbon monoxide and C_1 through C_5 hydrocarbons were collected intermittantly during the study period. Using cascade impactors, cyclones and filters, size segregated and total particulate samples were collected on filters for chemical analysis. Continuous visibility readings by nephelometry were also taken. Single particles collected with the U of M electrostatic precipitator were studied by electron microscopy. Information on wind speed and direction were obtained continuously during the entire period.

B. Sampling System

All analyzers were located in a large air conditioned laboratory in the basement of the Keck Environmental Sciences Building. The air sample was transported from an inlet 6.7 m above the roof down through a vertical 20.5 m by 7 m internal diameter PVC pipe to the sample distribution system as shown in Figure VI-VI. The analyzers were conncected to a manifold constructed from sections of glass tubing butt-joined with Tygon sleeves. The analyzers were connected to the line with 1/4 inch O.D. Teflon tubing. Standard 12/5 ground glass ball joint connections were used at each part to facilitate making and breaking connections. Flow velocities and tubing sizes for each instrument were chosen so losses of the gas being measured were minimal.

Actual losses were determined by simultaneous manual samples of the atmosphere on the roof for oxidant and NO_2 in the vicinity of the sample inlet line and from the NO_2 analyzer port in the sampling manifold in the laboratory. The results are shown in Table VI-III. The data indicate the average less than 3% which is within the expected analytical error.

C. Analyzer Operation and Calibration

All analyzers were prepared and placed in operation as designated by the manufacturer.

All analyzers except the chemiluminescent unit were calibrated prior to shipment to Pasadena. The calibrations of all analyzers were verified upon installation and periodically thereafter. Dynamic calibrations were performed with mixtures of the pollutant gas in filtered air. The gas was measured simultaneously by the analyzer and by a standard referee procedure. (AIHL Recommended Methods #1A, 2, and 3.) A tabulation of dates and changes in response is to be made available later.

D. Performance Factors

Analyzer performance and data validity is a function of several factors defined as follows:

1. Calibration: The process of determining the output of a measuring instrument by comparing it to several values of a primary, secondary or working standard input.
2. a. Minimum detectable change: the smallest change of input concentration which can be detected for outputs at mid- and full scale. The magnitude of change may be different for positive and negative displacements.

   b. Minimum detectable sensitivity: the smallest amount of input concentration which can be detected as the concentration approaches zero.
3. Response times: The output of most continuous air analyzers is not instantaneous. Between the input sample and output data is a definite time delay. The delay is defined by two terms as:
   a. Lag time: The time interval from a change in the input concentration to a readable change in recorded output.
   b. Readibility: Half of the smallest graduated interval on the chart readout.

5. Reproducibility: The variation in response with repeated inputs of the same concentration.
6. Accuracy: is the degree of agreement between a measured and the true value which is known or assumed; usually expressed as ±% of full scale.

7. Precision: is the degree of agreement of repeated measurements of the same concentration and is expressed as the average deviation of the single results from the mean.

Data on items 2, 3, and 4 are given in Table VI-II.

III. Measurement of Oxidant

A. General Principles

Continuous analysis of oxidant is usually performed by scrubbing sample air with an iodide absorbing solution (KI or NaI). Oxidant reacts with the iodide salt to produce iodine (I_2) and triiodide (I_3^-). Their concentration is measured by a colorimeter, amperometric cell or an electrochemical cell and recorded on a strip chart recorder as ppm ozone.

The iodide reagent responds to NO_2, peroxyacetylnitrate (PAN) and sulfur dioxide (SO_2) as well as to ozone. The degree of response may also depend upon contactor efficiency and detection principle. In colorimetric instruments 2,10 and 20% KI solutions buffered at pH 6.8 to 7.0 are or have been used by various California monitoring agencies. Laboratory data with NO_2 and ozone indicate the approximate response levels are as follows: for 2% KI, 6% of the NO_2; for 10% KI, about 20% fo the NO_2 and for 20% KI, 30 to 40% of the NO_2. Amperometric analyzers which use 2% KI register about 6% of the NO_2 as ozone whereas one using 2.5% NaI registers about 20%. SO_2, on the other hand, reduces the oxidant readings by 100% of the SO_2 present.

More recently a chemiluminescent detector specific for ozone has been developed. Sample air is aspirated in the dark across the surface of a chemiluminescent substance (rhodamine B adsorbed on silica gel) which is scanned by a photomultiplier tube. NO_2, SO_2 and PAN do not interfere.

The foregoing facts in addition to the performance factors common to most instruments imply that data gathered by analyzers with different reagent formulations and principles of detection may not be comparable. In order to assess the magnitude of these differences in response, four oxidant analyzers were used. Data from the NO_2, SO_2 and PAN analyzers are to be used to correct for interferences. Descriptions of a colorimetric, two types of amperometric and one chemiluminscent analyzer follows.

B. Beckman 77 Oxidant Analyzer (colorimetric)

As shown in Figure VI-I, sample air is drawn by an air pump through the air flowmeter and enters the contactor where oxidants react with the absorbing reagent. The airflow is counter-current to the flow of reagent. The effluent air exits from the upper end of the contactor through an air control valve to the pump.

The absorbing solution metered by the solution pump enters the top of the contact column and flows in a thin film down the internal helix. The reagent reacts with the sample air and flows into the sample optical cell of the photometer. The iodine is measured at 365 nm wavelength and indicated on a strip chart recorder. The signal is logarithmic with respect to concentration. The reagent then passes into the reservoir. The reacted reagent is pumped from the reservoir through the carbon column by the solution metering pump. The carbon column contains activated charcoal which removes the free iodine to regenerate the reagent. The regenerated solution again enters the top of the contactor to react with the sample air.

Beckman oxidant analyzers are available in two models -- a portable unit for field use and a larger, stationary unit for long term monitoring. The absorber column design is different for each type. The absorber on the portable unit is a 2 turn 4 inch diameter coil of 7 mm glass tubing mounted with the axis vertical. On the stationary models a vertical 14 inch long section of 7 mm I.D. glass tube with a glass helix insert is used. The use of the portable type analyzer is limited; most oxidant data in California has been collected by analyzers using the vertical tube scrubber. For this reason, the Beckman 77 portable was modified to accept a vertical tube scrubber (9 inches long) in place of the two-turn helical absorber.

C. Mast Ozone Meter (amperometric)

The Mast amperometric oxidant meter shown in Figure VI-II consists of a solution pump, a contactor-sensor composed of a plastic electrode support (about 75% of its length is wound with many turns of a fine wire serving as the cathode and a single turn wire is the anode), a solution reservoir and a sample air pump. The absorbing reagent is metered by the solution pumped from the reagent reservoir in a fine film down over the electrode and deposited in the waste reservoir. The sample air enters at the upper end of the sensor and flows through the annulus past the cathode which is covered with the thin layer of the scrubbing solution. The air and liquid are separated at the lower end.

About 0.25 volts applied to the electrodes generates a layer of hydrogen gas which polarizes the cathode. Iodine produced by the reaction between oxidant or ozone and KI immediately reacts with the H_2 to depolarize the cathode. Removal of the hydrogen allows the current to flow until polarization is reestablished. The current is proportional to concentration of ozone. The reaction at the electrodes gives an electron yield which is less than 100% of theoretical and must, therefore, be calibrated with a known ozone source.

D. Atlas Ozone/Sulfur Dioxide Analyzer (amperometric)

The Atlas unit essentially uses the same amperometric principle as the Mast to measure oxidant as well as SO_2. The reagent formulation, however, is different as shown in Table VI-I. In the oxidant or ozone mode, a set of polarized platinum wire electrodes measure the amount of iodine produced. In the SO_2 mode, a second set of electrodes generate a constant level of triiodide from the reagent by electrolysis. Reaction with SO_2 decreases the level of triiodide which is detected by the sensing electrodes. In both systems, the generator is used for an internal standardization of the signal transducing part of the analyzer.

As shown in Figure VI-III, the absorbing solution in the reagent reservoir is metered by a peristaltic solution pump through a nylon wool filter which absorbs any residual iodine in the reagent to a shallow well at the base of the absorber or contactor (made from a one liter balloon flask). Sample air is admitted through a 0.5 to 1.0 mm orifice submerged under the solution. The solution is picked up and sprayed against the absorber walls by the jet to condense on the walls and flow down to the entrance of the sensor electrode in the arm of a glass U-tube. The reagent flow, controlled by a capillary section, circulates past the sensor electrode across the bottom of the "U" and up past the generator electrode back to the solution inlet and sample spray jet. The excess spent reagent and air are removed through a standpipe adjusted to maintain a constant head above the sensor electrode and insures constant solution flow past the electrodes. The spent reagent is returned to the reagent reservoir.

Approximately 25 mV is used to polarize the sensor electrode and currents between 20 and 300 μa is used to generate the constant iodine level for standardization and in the SO_2 mode.

Depending on the monitoring mode (O_3 or SO_2) both ozone and SO_2 interfere in this method. The sample air is passed through scrubbers to remove the interference. In the ozone mode, SO_2 is removed with boiling chips coated with a mixture of chromium trioxide (CrO_3) and phosphoric acid. This, however, is equally effective in converting nitric oxide (NO) in the sample to NO_2. In the SO_2 mode, ozone and other oxidants are removed with column filled with ferrous sulfate ($FeSO_4$) crystals. The 2.5% NaI absorbing reagent used by the Atlas is not buffered. According to the manufacturer, the sodium hydroxide produced from the electrolysis and oxidation by ozone, reacts with the carbon dioxide in the air to form sodium bicarbonate and adequately buffers the solution. However, for use in high NO_2 atmospheres, buffering at pH 5.5 to 6 with disodium citrate is recommended.

Moreover, the need for buffering was borne out in our investigations to determine the Atlas analyzer response to NO_2. Drifting response indicated continual changes in pH. Further, when iodine generated with ozone from 2% KI solution containing phosphate buffers were titrated with an electrometric endpoint detector (Mast titrator) the apparent endpoint varied with buffer concentration. Discussions with Dr. Ferdinand Schulze indicated the effect of acidity and buffer concentration on the response of the citrate buffered system due to NO_2 was largely unknown. At our suggestion and with his concurrence, the absorbing solution was buffered at pH 6.8 with 0.1 M sodium and potassium buffer.

E. Research Triangle Institute Ozone Monitor(chemiluminescent)

The sample air is aspirated in the dark across the surface of a chemiluminescent or fluorescent substance (rhodamine B adsorbed on silica gel) which is scanned by a photomultiplier tube. The chemiluminescent reaction between ozone and rhodamine B is said to be specific, the response to NO_2, SO_2 and PAN being smaller than the response to ozone by a factor of at least 5000. The unit is equipped with a built-in stable ozone source for dynamic calibration since the reaction between ozone and the chemiluminescent material is not stoichiometric. The ozone source is calibrated occasionally by a referee procedure. The chemiluminescent substance is also subject to temporary loss in sensitivity unless exposed periodically to ozone. To maintain sensitivity the unit may be programmed to check its calibration with ozone at four minutes, six hour and 12 hour intervals with the calibrated ozone source.

IV. Measurement of Other Gases

A. Nitrogen Dioxide

Analysis of NO_2 is most commonly performed by scrubbing sample air with an azo dye forming reagent. Sulfanilic acid reacts with NO_2 to form a diazotized sulfanilic acid. This is then further reacted with a napthylamine derivative to produce a pink dye which is measured photometrically at 550 nm and displayed on a strip chart recorder.

Atlas NO_2 Analyzer (colorimetric): The Atlas analyzer reagent contains 1.5% 2-aminobenzenedisulfonic acid (ABDS) as the diazotizing component and 0.1% N(2-napthyl) ethylenediamine dihydrochloride (NEDA) as the coupling agent. For longer reagent life the ABDS and NEDA solutions are stored in separate reservoirs. The ABDS solution contains, in addition, 15% ethylene glycol and 0.05% sodium benzoate or sodium carbonate as a preservative. Figure VI-IV shows the ABDS solution is first drawn by the main solution pump through a bed of activated charcoal to remove any existing color and coupling agent (NEDA) to a tee. The flow of ABDS is joined with a much smaller flow (about 1/100) of NEDA by means of a second solution pump. The main pump then passes the combined solution through the photometer reference cell to a tee at the top of the spiral contactor to join and mix with the sample air as they descend together down the absorber. Reaction of the solution with NO_2 forms dye which then passes through the photometer reference cell and then returns to the ABDS reservoir for reuse. Only the coupling agent must be replenished; the 300 ml supply is sufficient for at least a weeks opeation.

B. PAN

Panalyzer*, Wilkins Instrument (gas chromatographic): Sample air, periodically collected in a two ml sample loop, is flushed through a 1/8 inch diameter by nine inch long Teflon chromatographic column, with nitrogen at 20 to 40 ml/min. The column is packed with 5% carbowax on 60 to 70 mesh chromosorb G treated with DMCS and operated at 25°C. The emerging constituents are detected by electron capture and the signal displayed on a strip chart recorder. The unit was programmed to sample every fifteen minutes.

A stainless steel hexaport valve with an external two ml stainless steel sample loop was used instead of the glass sample valve described by Darley et al.** The rate of flow of dry nitrogen carrier gas was increased from 25 mls per minute to 40 mls per minute. With this system there was no detectable decomposition of PAN.

---

*Automatic Chromatographic Measurement of PAN. O.C. Taylor, E.R. Stephens and E.A. Cardiff. Statewide Air Pollution Research Center U.C. Riverside, California 92502. Presented at the June 1968 meeting of the Air Pollution Control Association, St. Paul, Minn.

**Darley, E.F., K.A. Kettner, and E.R. Stephens, Analysis of peroxyacetyl nitrates by gas chromatography with electron capture detection. Anal. Chem. 35(4): 589-591 (1963)

The automatic sampling mechanism attached to the outside of the chromatograph case, Figure VI-VII, consisted of: 1) a timing mechanism; 2) sample valve; 3) solenoid activator; and 4) time delay relay. The timing mechanism consisted of a microswitch, a cam to operate the micro switch, and a standard Synchron 4 RPH motor. The cam was designed to energize the solenoid for 90 seconds during each 15 minute period. The shaft of the hexaport valve was attached rigidly to the solenoid shaft and positioned so that the air sample would flow through the two ml sample loop during the time the solenoid was energized. A coil spring of proper tension installed between the solenoid and sample valve returned the valve to injection position when the solenoid was de-energized.

Dry nitrogen carrier gas was flushed continuously through the two ml sample loop of the hexaport valve for 13.5 minutes of each period when the solenoid was de-energized. When the solenoid was energized the sample loop was open to the atmosphere to be sampled and a Neptune pump Model 4-K sucked a continuous flow of air through the loop for 90 seconds. When the solenoid was again de-energized, the carrier gas flushed the two ml sample into the column.

The time delay relay, Figure VI-VI, energized the chart drive motor on the strip chart recorder at the end of the 90 second sample period when the solenoid was de-energized. The chart drive motor is allowed to run for 90 seconds which is ample time to record the chromatogram. The column is too short to separate peroxypropionyl nitrate (PPN) and peroxybutyryl nitrate (PBN), although a shoulder on the PAN peak, assumed to be PPN, appeared occasionally.

PAN was synthesized and purified* and stored in 34 liter stainless steel cylinders for use in the dynamic calibration system for the chromatograph.** The cylinders, pressurized with nitrogen to 100 psig, contained 500 to 1,000 ppm PAN and were stored at 60°F. An infrared spectrophotometer with a 10 cm cell was used to determine concentration of PAN in the cylinders using absorptivities reported by Stephens.*** In the first dilution of the dynamic system, **** one part PAN from the storage cylinder was diluted with 100 parts activated charcoal filtered air. A similar 1 to 100 dilution with filtered air in the second step of the dilution system reduced the concentration of PAN in a constant flow of gas to the ppb range. Calibration curves were plotted from calculated concentration of PAN and peak height. Calculated concentration of PAN and peak height showed a linear relationship in the range from 1 to about 50 ppb; therefore, concentration within this range could be calculated by multiplying peak height by a constant. The constant varied from one instrument to another and varied inversely with changes in standing current of a particular instrument.

---

*Stephens, E.R., F.R. Burleson and E.A. Cardiff. The production of pure peroxyacyl nitrates. J. Air Poll. Control Assoc. 15(3):87-89 (1965).

**Plata, R.L. Calibration and comparison of Coulometric and Flame ionization for monitoring PAN in experimental atmospheres. Ninth Conference on Methods in Air Pollution and Industrial Hygiene Studies, Huntington-Sheraton Hotel, Pasadena, California (1968).

***Stephens, E.R. Absorptivities for infrared determination of peroxyacyl nitrates. Anal. Chem. 36(4): 928-929 (1964)

**** See this page for ** item

The automatic system has operated continuously 24 hours a day for 11 months with only brief interruptions to clean the electron capture detector. Contamination of the detector caused a slow decline in standing current and a concomitant reduction in sensitivity. It was desirable to calibrate the instrument about once a week to compensate for the gradual reduction in sensitivity. When the detector was thoroughly cleaned the original sensitivity was regained.

Sensitivity of the detector was increased and retention time for PAN and water was decreased by modification of the procedures described by Darley.* These modifications included: 1) reduction of column lenth from three feet to nine inches; 2) increase of nitrogen carrier gas flow from 25 to 40 ml/min^{-1};and 3) reduction of oven temperature from 35 to 25°C. Retention time for PAN was reduced from two minutes 10 seconds to 60 seconds. More frequent sample periods may be feasible with this system, but care must be taken to avoid interference from the water peak which follows that of PAN. Back flushing of the column has not been necessary since there has been no indication of accumulation of contaminants.

C. Carbon Monoxide**

Integrated air samples were collected in aluminized Scotchpak bags and analyzed with a nondispersive infrared analyzer sensitized to carbon monoxide. Drying tubes containing Anhydrone and Ascarite connected between the bag and analyzer remove water and carbon dioxide and a membrane filter placed in the line following the Ascarite tube removes particles. The amount of carbon monoxide is ascertained by comparing the instrument reading obtained on the sample to a calibration curve of instrument reading vs. carbon monoxide concentration prepared from standardized carbon monoxide samples.

D. Hydrocarbons (C_1 through C_6)***

Integrated samples were collected in aluminized Scotchpak bags. The samples delivered to our Berkely Laboratory were C_1 through C_6 hydrocarbons. They were identified and quantiated down to 0.1 ppb by concentrating 100 ml of the air sample in a liquid oxygen freeze trap. The samples were then separated on β, β' oxydipropionitrate on activated alumina gas chromatographic column and detected by flame ionization.

V. Particle Measurements

A. Nephelometer, Meteorology Research Inc.

The integrating nephelometer determines the atmospheric extinction coefficient due to scatter. Sample air is drawn through a chamber where it is illuminated by a pulsed flash lamp. The light scattered by particles and aerosols is detected by a photomultiplier tube looking at an illuminated volume. The phototube output is averaged and compared with a reference from another phototube looking at the flash lamp. Further details are to be given by P.J. Charlson.

---

*See p. 6 for ** item

**Recommended Method No. 19, AIHL; Method of Analysis for Carbon Monoxide in Air

***ASTM Method D2820-69T. Tentative Method of Test for C_1 through C_5 Hydrocarbons in the Atmosphere by Gas Chromatography.

B. Size Selective Particle Sampler (two-stage)*

Size selective samples of particles in the atmosphere were collected with a single-stage and a two-stage sampler side by side. The single-stage sampler which collects total suspended particles consists of an open-face filter holder equipped with a 2.54 cm diameter tared glass fiber filter. In the two-stage sampler the 2.54 cm filter is preceded by a 1.3 cm diameter stainless steel cyclone collector. At a sampling rate of 18 liters/minute the cyclone permits only particles smaller than two microns in diameter and about one-half of the 3.5 micron particles to enter the second stage. The mass collected on the single stage filter is used to determine the total particle loading.

C. Total Suspended Particles

Samples for total suspended particles in the atmosphere were collected throughout the study on 10 micron pore diameter Teflon filters. The particles were collected by passing 35 to 101 cubic meters of sample air through tared 3.5 inch diameter Teflon filters at approximately 0.062 m^3 per minute. Details of this phase of the study will be described by D. Lundgren.

D. Electron Microscopy

This part of the report will include some preliminary quantitative data on grids exposed for two hours in the ESP on two days. Table VI-IV is a summary of the particle count on the two samples. The technique description follows.

1. Preparation of grids
   a. Nickel grids 300 mesh were coated with a thin layer of collodion
   b. A thin layer of solicon monoxide was evaporated onto the collodion surface using a vacuum evaporator.

   The SiO surface was used to stabilize the coatings in the electron beam and to provide a resistant surface to possible corrosive properties of some of the smog particles e.g., H_2SO_4 droplets.

2. Electrostatic precipitator sampling for electron microscopy

   Its principle, performance characteristic and operational aspects will have to be described by Dr. Ben Liu. The grids were placed in the ESP as shown below:

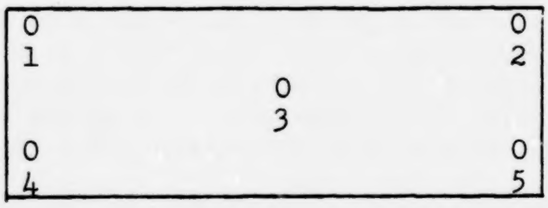

At the end of the sampling period the grid instructions were given to treat the grids as follows:

---

*Mueller, P.K. and M. Imada, AIHL Report No. 72. Two stage Particulate Matter Sampling Procedure.

a. Remove grids and place on double sticky tape mounted on microscope slide (frosted area on the left). The tape is to be put onto the center of the slide.

b. Place grids on the bottom edge of the tape.

c. Identify run on upper left ahnd corner of frosted area with pencil. Date on lower end of frosted area.

d. Grids are to be arranged from left to right, the number of the grid corresponding to the numbers in the diagram above.

e. Place slide in petri dish.

f. Identify experiment on top of petri dish with waterproof marking pen.

g. The grids in the petri dish can not go to the electron microscopist.

h. After shadowing with Pt-Pd or if not to be shadowed place slide in petri dish and tape the slide in the bottom dish with magic mending tape.

i. Tape the edge of the petri dish with masking tape.

j. If a grid is to be removed, take number 2, 3 or 4 and when the grid is replaced, put it into the equivalent place on the top edge of the sticky tape.

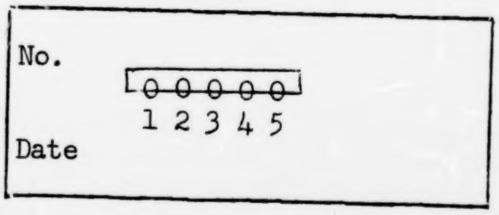

standard convention of placing grids

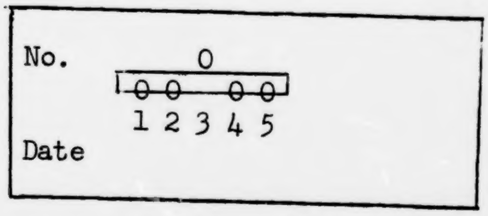

if grid is removed and replaced

3. Electron Microscopic Observations

After sampling the specimens were characterized and counted in a Siemens Elmiskop I electron microscope. Grids from two samples were examined:

LN 90790, August 20, 1300-1500 hours
LN 90786 VIII, August 22, 1300-1500 hours
LN 90786 VIII, August 22, control grid (unexposed)

Ten fields each were counted on grids 3 and 5 and nine fields were counted on grid 1 of sample 90790 (August 20). Ten fields were counted on grid 1 of sample 90786 VIII (August 22). Forty-five fields were examined on the control grid (sample 90786 VIII clean grid). Electron micrographs were taken of each field counted. No electron micrographs were taken of the control grid.

The magnification used for counting was 2000X. At this magnification, one field in the grid is approximately 50m x 50m and corresponds to a hole in the 300 mesh grid. The area of the field is therefore 2.5×10^{-5} cm^2 ± ca 10%. The image of this area is projected onto the viewing screen onto a circle of 9.0 cm diameter. The area counted is not precise because the openings in the grid are not precise.

The photographic plates of each field were taken at 2000X magnification and they cover an area of 6.5 cm x 9 cm of the viewing screen (9.0 cm diameter). These conditions were used for counting. The morphology of the particles was studied at 20,000 mag.

The count data was reduced to the form of count/cm^2 grid surface.

4. Special Samples

Dr. Barton E. Dahneke of CIT obtained particle deposits on EM grids we furnished placed at various positions in his particle beam apparatus when sampling smog aerosol. Description and results are subject of a separate memorandum from P.K. Mueller to S.K. Friedlander dated 2/26/70.

Results

The data show some differences in deposition among grids and some difference in deposition in parts of the same grid. However, the count difference in the two samples (August 20 and August 22) was significant.

Table VI-I shows that there is approximately a four-fold decrease in particle count, by electron microscopy of ESP samples from 8/20 to 8/22/69. The samples were taken over a two-hour period from 1300 to 1500, on both days. This correlates roughly with concurrent gas analyses as follows:

Date	NO_2(ppm)	O_3(ppm)
8/20	0.2	0.55 @ 1245 0.67 @ 1315 0.43 @ 1530 (triple peaks)
8/22	0.12 decreasing in time	0.40 @ 1245 0.15 @ 1500 (plateau)

A subjective report of physiological effect, namely that of severe eye irritation, correlated with the smog on 8/20/69 was received by telephone from staff on site in Pasadena on 8/20/69. Less eye irriation occurred on 8/22/69.

The electron micrographs which accompany this report show a possible difference in morphology of the particles obtained on the two days.

On 8/20/69 there were more particles than on 8/22/69. It is possible that the seeding particles were smaller in 8/20/69 samples (8/20/69 was noted for an eye burning day) than on 8/22/69 which wasn't so much an eye burner. The particles obtained on 8/22/69 seem more uniform than those of 8/20/69. More work needs to be done on the morphology of the particles hour by hour and day by day during the smoggy weather. Collection of particles by methods other than by ESP should be tried. It is possible that collection of particles on Nucleopore filters would provide valuable information. The collections are more homogeneous than one would expect.

VI. Chemical Analysis

A. Carbonate and Non-carbonate Carbon in Atmospheric Particles

The carbon content of atmospheric aerosol may be an important criterion of its origin. The carbon content of particles is in the form of the element, organic compounds and carbonates. In urban aerosol the non-carbonate carbon is probably of anthropogenic origin. Carbonates more likely result from surface erosion. To obtain information on these matters we have developed a method for measuring 10 μg or more of carbon in size-segregated collections.

The airborne particulate matter is collected on aluminum foil or other carbon free substrates covering the stages of a cascade impactor. A glass fiber filter is the final stage. The strips of the foil and filter are placed into porcelain combustion boats. A boat is inserted into a train designed to generate carbon dioxide from carbonates in a single sample by first acidifying with 1% H_3PO_4 to form carbon dioxide and water. The carbon dioxide is swept with an oxygen stream through a silica gel trap for water and then to a freeze-out trap. The concentrated carbon dioxide is moved to a 1/8 inch x 8 foot gas chromatographic column packed with 100/120 mesh Porapak Q for separating residual oxygen, water and sulfur dioxide and the carbonate-carbon is subsequently quantitated by means of a thermal conductivity detector.

The boat and water trap is then heated to 105°C to remove the water from the sample and trap. The system is purged with 50 μl/min oxygen. The organic carbon in the sample is then combusted catalytically (cupric oxide) at 900°C to CO_2 and water. The CO_2 formed is then quantitated by GLC as indicated above.

TABLE VI-I

ANALYZER DESCRIPTIONS

Pollutant	Designation	Analyzer	Model	Detection Principle	Reagent	Contactor/ Collector	Major Interferences
O_x/SO_2	Atlas	Atlas Elec. Dev. Co. Chicago, Ill.	1120	Amperometric	2.5% NaI 0.1 M Na_2HPO_4 0.1 M KH_2PO_4 pH 6.8	Spray jet	NO_2, SO_2
O_x	Mast	Mast Dev. Co. Davenport, Iowa	725-11	Amperometric	2.0% KI 5.0% KBr 0.018 M NaH_2PO_4 0.025 M Na_2HPO_4 pH 7.0	Wire helix	NO_2, SO_2
O_x	Beckman	Beckman Inst. Fullerton, Calif.	77	Colorimetric	10% KI 0.1 M Na_2HPO_4 0.1 M KH_2PO_4 pH 6.8	**Vertical tube with glass helix**	NO_2, SO_2
O_3	RTI	Research Triangle Inst. Raleigh, N.C.	-	Chemiluminescent	Rhodamine B on silica gel	Disc	none
NO_2	Atlas	Atlas Elec. Dev. Co. Chicago, Ill.	1300	Colorimetric	15% ABDS NEDA	Glass **helix**	none
PAN	PAN	Wilkens Inst. Walnut Creek, Calif.		Gas Chromatography	5% carbowax on chromosorb G	1/8 in dia x 9 in long Teflon tube	-
Particle	MRI	Meteorology Research Inc Altadena, Calif.		Nephelometry	none	-	-
Particle	2-stage	AIHL, 12 hr samples		Mass	none	Glass fiber filters	-
Particle	Total	AIHL, 12 hr samples		Mass	none	Teflon filter	-
Hydro-carbon	HC	AIHL, Integrated Sampler		Gas Chromatography	none	Mylar bag	-
Carbon Monoxide	CO	AIHL, Integrated Sampler		NDIR	none	Mylar bag	-

TABLE VI-II

ANALYZER PERFORMANCE FACTORS

Analyzer	Flow Rates Samp l/min	 Reagent ml/min	Response Times Lag min	 90% min	Recorder Size inches	Sensitivity Min Chart Div ppm	 Min Detectable Conc ppm	 Min Detectable change ppm
Atlas, O_x	3.0	4.0	0.5	12	2-1/4	0.01	0.02	± 0.01 to 0.02
Beckman, O_x	1.7	1.63	1	10	11	0.01	0.01	± 10%
Mast, O_x	0.150	0.021	0.5	2	2-1/4	0.005	0.01	± 0.01
RTI, O_3	0.100	-	0.4	0.5	5	0.005	0.02	± 0.01 0.0 ppm ± 0.01 1.0 ppm
Atlas, NO_2	3.25	2.2	3.5	5.3	2-1/4	0.01	0.02	± 0.01
Altas, SO_2	3.0	2.0	0.5	15	2-1/4	0.002	0.004	± 0.004
PAN	0.002☆☆	-			5	0.001		
MRI	280	-			11			
HC	0.078	-	-	-	-	-	0.1 ppb	
CO	0.078	-	-	-	-	-	1.0	
2-stage filter	13 M^3☆	-	-	-	-	-	10 to 20 µg/M^3	
Total filter	35 to 80 M^3☆	-	-	-	-	-	2 µg/M^3	

☆ integrated 12 hr samples

☆☆ batch system

TABLE VI-III

TEST OF SAMPLE LINE LOSSES
(10 minute bubbler samples*)

Starting Time Date/Time		Pollutant	ppm at Location Lab	 Roof
8/19	1200	Oxidant	0.27	0.26
	1215	"	0.33	0.34
	1420	"	0.33	0.37
	1450	"	0.31	0.31
Average			0.31	0.32
8/20	0830	NO_2	0.06	0.07

*Corresponding analyzer readings in the lab confirm the bubbler sample values.

TABLE VI-IV

PARTICLE COUNT ON ESP PLATE NUMBER OF PARTICLES/CM^2 SURFACE

Sample	LN	Count/Cm^2 ESP Surface
August 20 1300 - 1500 grids 1,3,5 average	90790	37.8×10^5
August 22 1300 - 1500	90786 VIII	10.24×10^5

FIG VI-1

OXIDANT ANALYZER - COLORIMETRIC

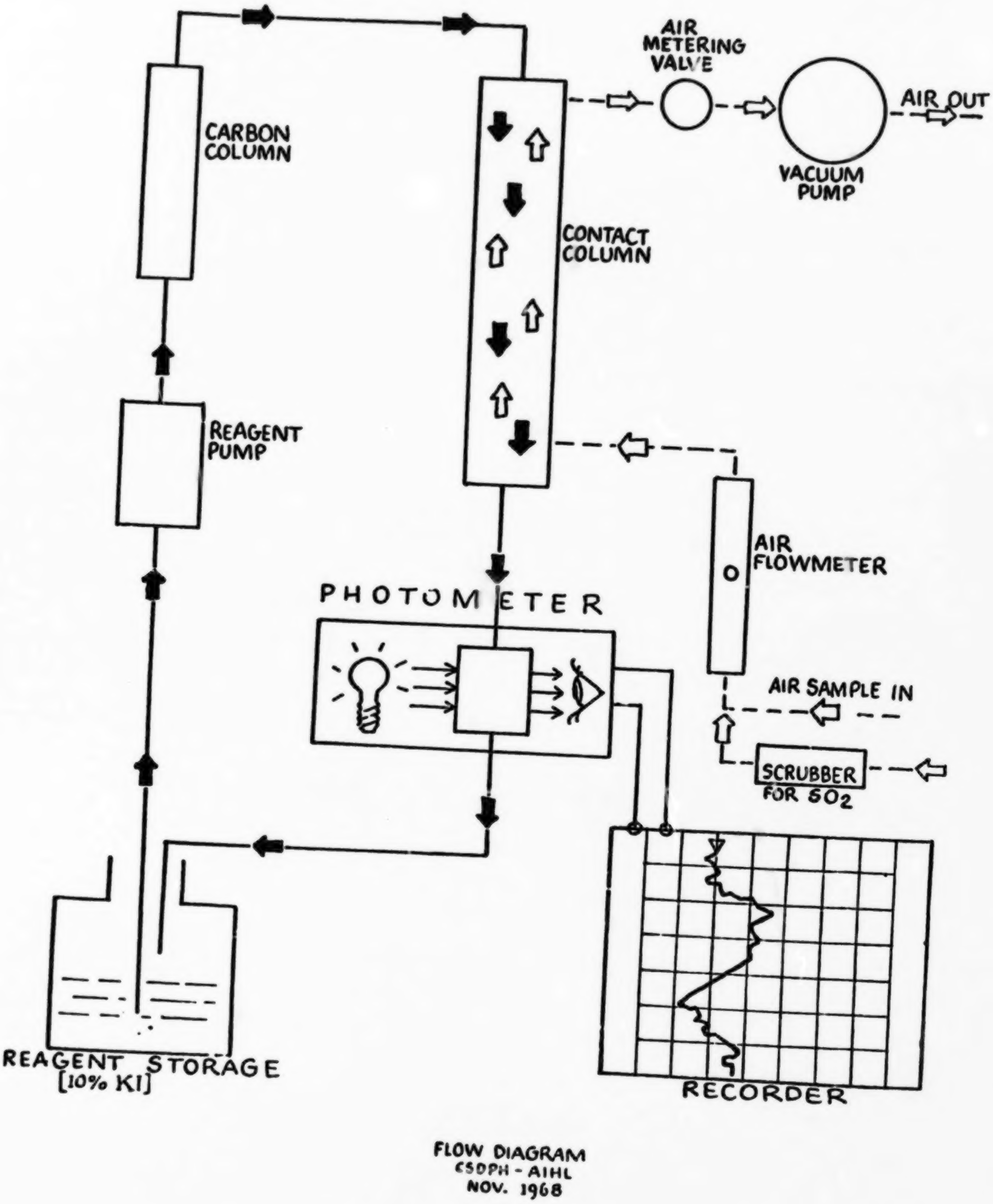

AIR METERING VALVE
AIR OUT
CARBON COLUMN
VACUUM PUMP
CONTACT COLUMN
REAGENT PUMP
AIR FLOWMETER
PHOTOMETER
AIR SAMPLE IN
SCRUBBER FOR SO_2
REAGENT STORAGE [10% KI]
RECORDER

FLOW DIAGRAM
CSDPH - AIHL
NOV. 1968

FIG VI-2

OXIDANT ANALYZER - COULOMETRIC

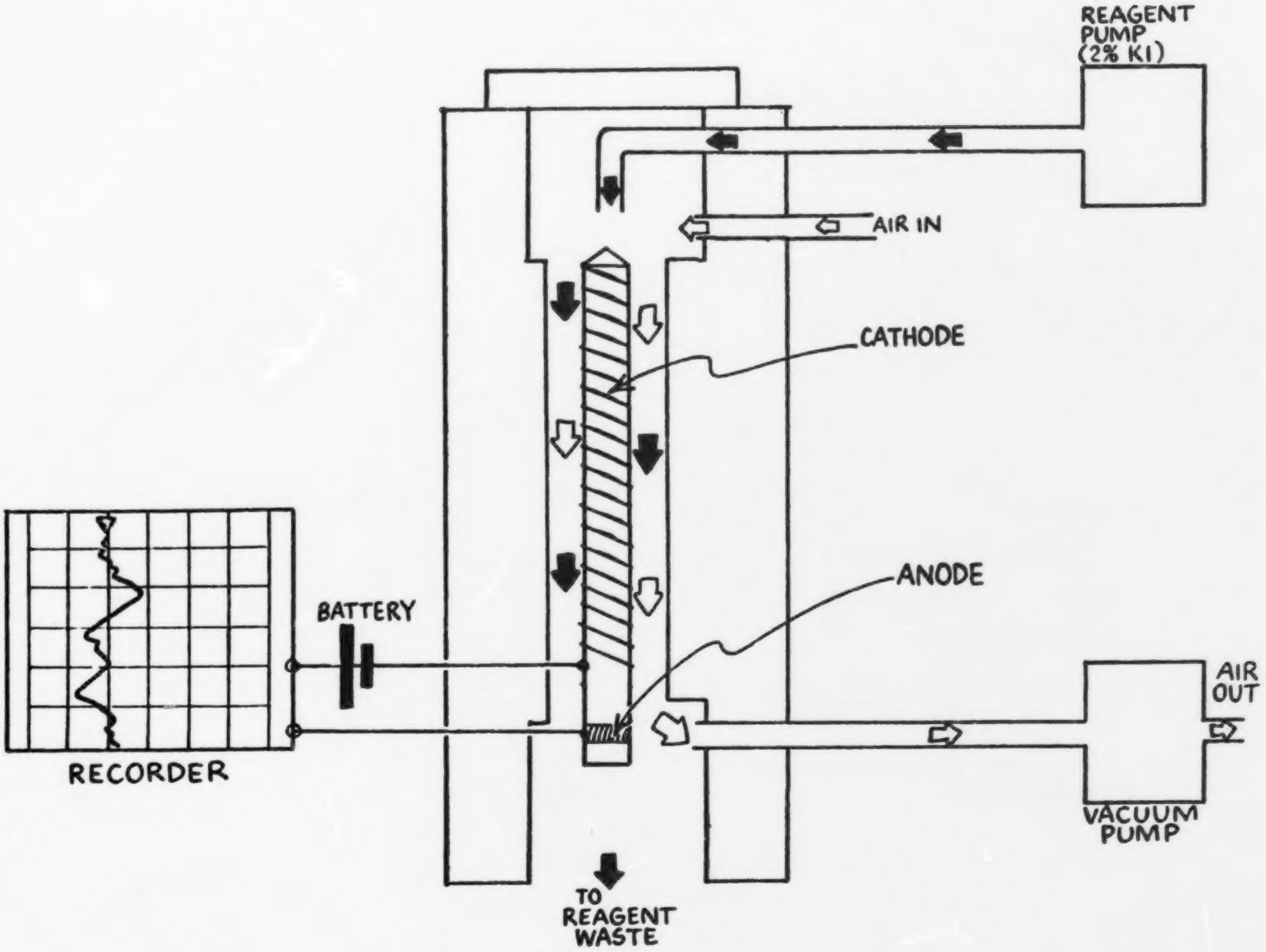
REAGENT
PUMP
(2% KI)
AIR IN
CATHODE
ANODE
BATTERY
RECORDER
AIR
OUT
VACUUM
PUMP
TO
REAGENT
WASTE

FLOW DIAGRAM
CSDPH - AIHL
NOV. 1968

FIG. VI · 9

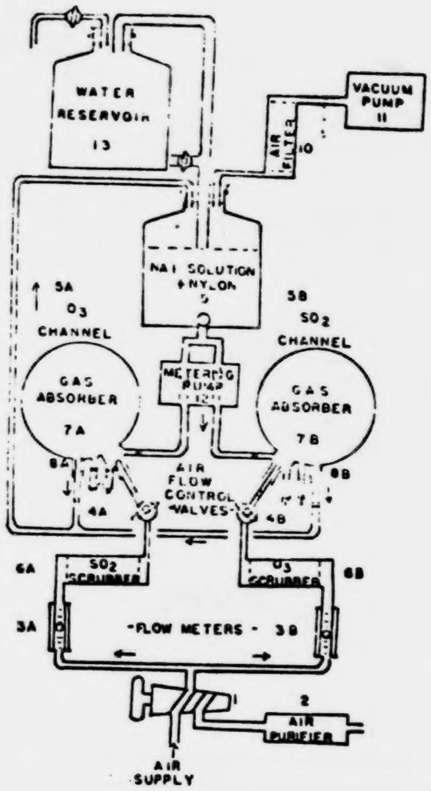
WATER RESERVOIR 13
VACUUM PUMP 11
AIR FILTER 10
NAI SOLUTION + NYLON 5
5A
O_3 CHANNEL
5B
SO_2 CHANNEL
GAS ABSORBER 7A
METERING PUMP 12
GAS ABSORBER 7B
8A
8B
AIR FLOW CONTROL VALVES
4A
4B
6A
SO_2 SCRUBBER
O_3 SCRUBBER
6B
3A
FLOW METERS
3B
1
2
AIR PURIFIER
AIR SUPPLY

Flow diagram of ozone–sulfur dioxide analyzer

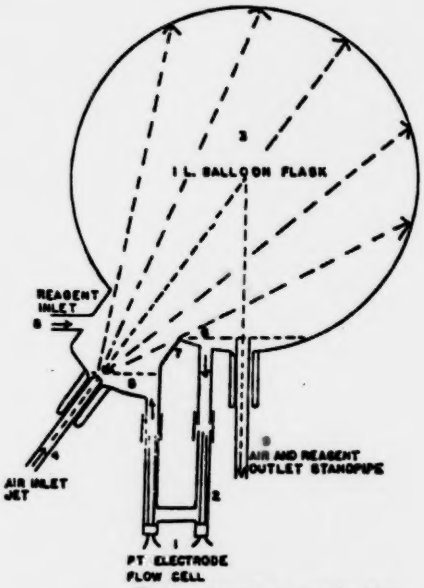
3
1 L. BALLOON FLASK
REAGENT INLET
8
7
6
4
AIR INLET JET
9
AIR AND REAGENT OUTLET STANDPIPE
2
1
PT ELECTRODE FLOW CELL

Gas absorber and electrode assembly

FIG VI-4

NITROGEN DIOXIDE ANALYZER-COLORIMETRIC

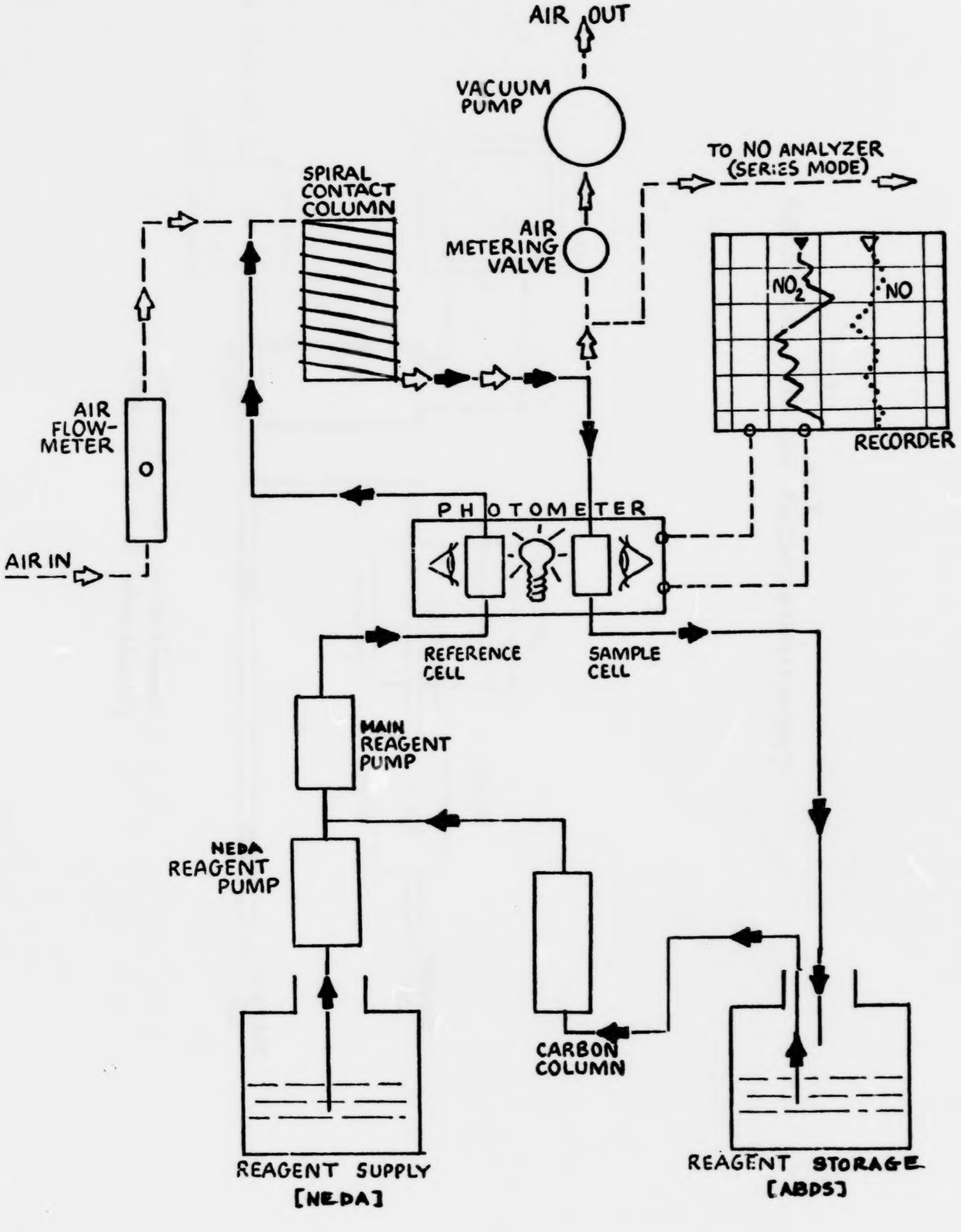
AIR OUT
VACUUM PUMP
TO NO ANALYZER (SERIES MODE)
SPIRAL CONTACT COLUMN
AIR METERING VALVE
NO_2
NO
RECORDER
AIR FLOW-METER
AIR IN
PHOTOMETER
REFERENCE CELL
SAMPLE CELL
MAIN REAGENT PUMP
NEDA REAGENT PUMP
CARBON COLUMN
REAGENT SUPPLY [NEDA]
REAGENT STORAGE [ABDS]

FIG VI-5
CHEMILUMINESCENT OZONE DETECTOR

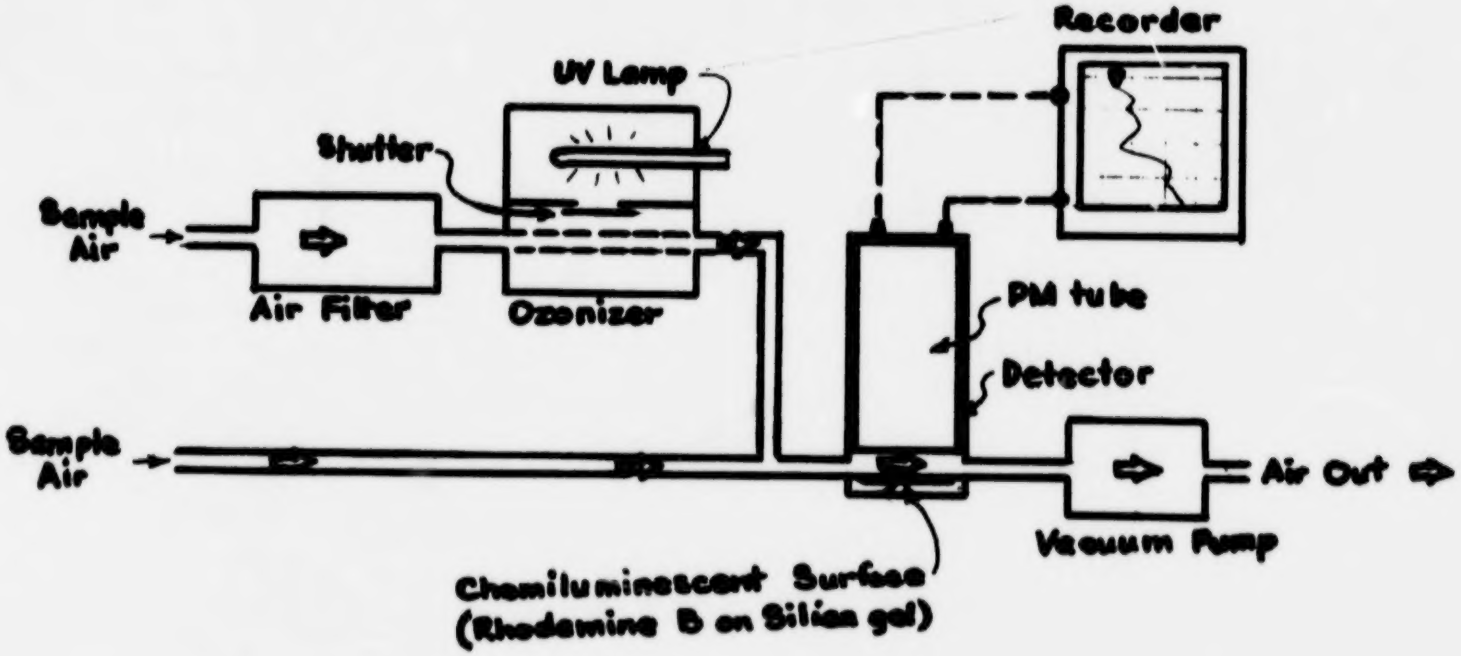
Recorder
UV Lamp
Shutter
Sample Air
Air Filter
Ozonizer
PM tube
Detector
Sample Air
Air Out
Vacuum Pump
Chemiluminescent Surface
(Rhodamine B on Silica gel)

Figure VI-6

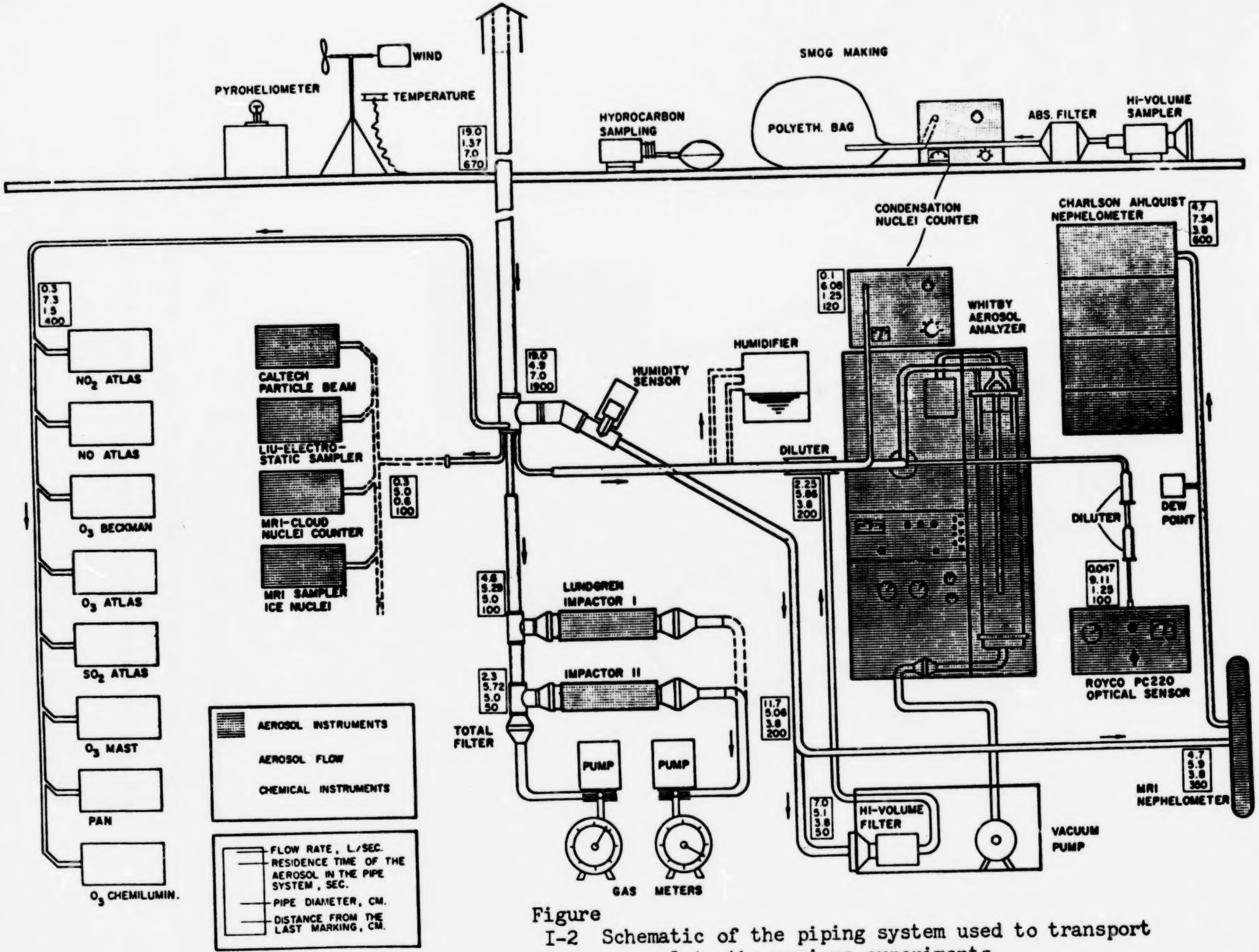

PYROHELIOMETER
WIND
TEMPERATURE
19.0
1.37
7.0
670
HYDROCARBON SAMPLING
SMOG MAKING
POLYETH. BAG
ABS. FILTER
HI-VOLUME SAMPLER
CONDENSATION NUCLEI COUNTER
CHARLSON AHLQUIST NEPHELOMETER
4.7
7.34
3.8
600
0.3
7.3
1.5
400
NO$_2$ ATLAS
NO ATLAS
O$_3$ BECKMAN
O$_3$ ATLAS
SO$_2$ ATLAS
O$_3$ MAST
PAN
O$_3$ CHEMILUMIN.
CALTECH PARTICLE BEAM
LIU-ELECTROSTATIC SAMPLER
MRI-CLOUD NUCLEI COUNTER
MRI SAMPLER ICE NUCLEI
0.3
5.0
0.6
100
19.0
4.9
7.0
1900
HUMIDITY SENSOR
HUMIDIFIER
0.1
6.08
1.25
120
WHITBY AEROSOL ANALYZER
DILUTER
2.25
5.86
3.8
200
DILUTER
DEW POINT
0.047
9.11
1.25
100
ROYCO PC220 OPTICAL SENSOR
4.8
5.29
5.0
100
LUNDGREN IMPACTOR I
IMPACTOR II
2.3
5.72
5.0
50
TOTAL FILTER
PUMP
PUMP
GAS METERS
11.7
5.06
3.8
200
7.0
5.1
3.8
50
HI-VOLUME FILTER
VACUUM PUMP
4.7
5.9
3.8
350
MRI NEPHELOMETER
AEROSOL INSTRUMENTS
AEROSOL FLOW
CHEMICAL INSTRUMENTS
FLOW RATE, L/SEC.
RESIDENCE TIME OF THE AEROSOL IN THE PIPE SYSTEM, SEC.
PIPE DIAMETER, CM.
DISTANCE FROM THE LAST MARKING, CM.

Figure
I-2 Schematic of the piping system used to transport aerosol to the various experiments

NOT REPRODUCIBLE

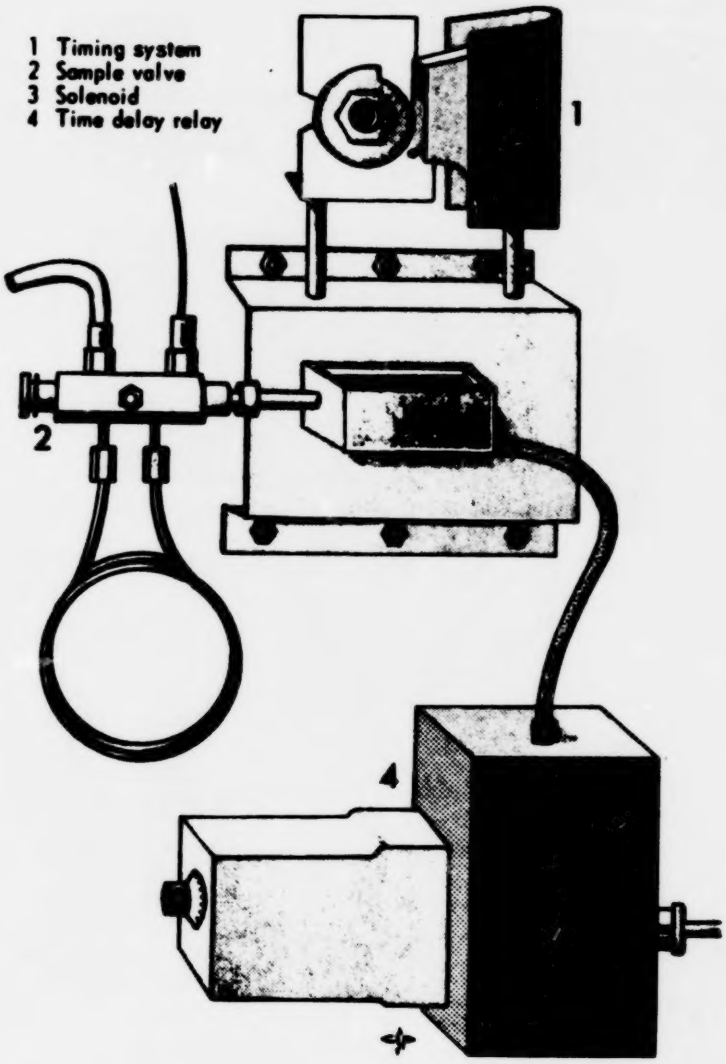
1 Timing system
2 Sample valve
3 Solenoid
4 Time delay relay
1
2
4

Figure VI-7 Automatic sampling system consisting of: 1) standard timing system; 2) hexaport valve and 2 ml sample loop; 3) solenoid to activate valve; and 4) time delay relay to control recorder chart drive motor.